The Development of a Biosensor for the Detection of Pathogenic Bacteria in Water

Dissertation submitted for the degree of

DOCTOR OF PHILOSOPHY

Department of Engineering Science

UNIVERSITY OF OXFORD

NAOMI VICTORIA JANE WISE

Supervisors: Professor Steve Sheard and Professor Ian Thompson

Trinity College
Hilary Term 2015

The development of a biosensor to detect viable pathogenic bacteria in water

Naomi Wise, Trinity College, University of Oxford
A thesis submitted for the degree of Doctor of Philosophy, Hilary term 2015

Abstract

Pathogenic bacteria are causative agents of epidemics and deaths worldwide; water is a vector for the transport of bacteria and their consequent consumption by humans. The accepted "gold standard" for assessing bacterial concentrations in water is by traditional plate counts. However, this globally accepted technique takes longer than 24 hours. An alternative method to rapidly detect and to continuously assess bacterial concentration is required. A biosensor that provides near real-time information on the bacterial loading of a waterbody is proposed. This thesis describes the development of a microfluidic-magnetophoretic device to detect bacteria in water.

Escherichia coli is a well-reported bacterium found in the intestinal tract of mammals. Particular strains of *E. coli* are pathogenic to humans. *E. coli* is used as an "indicator" for water contamination and was chosen as the target for the biosensor. Magnetic particles (MPs) were functionalised with an anti-*E. coli* antibody. The functionalised MPs were used to capture *E. coli* from drinking water by forming MP-bacterial complexes.

A microfluidic device was designed, incorporating magnetophoresis, to separate and concentrate MPs suspended within a sample. A separation efficiency of approximately 80% of the MPs from a sample flow was achieved. Using a magnetic gradient and video tracking of the MPs, the magnetic-drift velocities of unbound and bound MP-bacterial complexes was determined. It was found that viable and non-viable MP-bacterial complexes had different magnetically-induced drift velocities. A single viable *E. coli* bound to an MP travelled at 0.49 times the velocity of an unbound MP, and a single non-viable *E. coli* travelled at 0.75 that of an unbound MP. As such, this novel magnetophoretic separation technique can be used to determine the viability of bacteria. The developed biosensor provides the ability to concentrate, separate and enumerate viable *E. coli* from drinking water, with the potential for automation and sampling from continuous flow.

Acknowledgements

The support of my family has been incredible; they have contributed to this work through countless dinner table discussions. To my parents, for all they have done and for their patience; to my grandfather, Professor M.J. Wise, an inspiration; my sisters, who have maintained my sanity; and of course my Nan.

My supervisors; Professor S. Sheard and Professor I. Thompson, for their expert and unwavering supervision and support; it has been a joy to work with them. I am extremely grateful for all they have taught me.

Thanks go to the management of Coldharbour Marine for the "leg-up" onto this project and for the part-funding, I am very grateful.

Two DPhil colleagues, in particular, have helped make sense of the sometimes confusing outlook, thank you Tim G. and Cordelia R. for our enlightening discussions.

I would like thank the Oxford University Materials Department for the use of the Malvern Zetasizer Pro and Chemicell, Germany, for the supply of the long-linker biotinylated beads used within this study.

In addition, I am thankful of the financial assistance received from Trinity College, University of Oxford and Silver Star Society.

Table of Contents

Abstract 2

Acknowledgements 3

Table of Contents 4

List of Figures 11

List of Tables 15

Glossary 16

1. The continuous detection of pathogenic bacteria in waterbodies 19

1.1. Current detection methods for the presence of pathogenic bacteria 19

1.2. Physiological states of bacteria 20

1.3. Biosensors for bacterial detection 21

1.4. Objectives of the proposed biosensor and thesis overview 21

1.4.1. Exploration of microbiological techniques suitable for continuous assessment of bacterial populations 22

1.4.2. *Escherichia coli* as an indicator organism for the biosensor to target 22

1.4.3. Microfluidics as a sampling, separation and concentration device 23

1.4.4. Immuno-magnetic labelling of magnetic particles 23

1.4.5. Magnetophoretic mobilities of superparamagnetic particles 24

1.4.6. Magnetophoretic mobilities of captured *Escherichia coli* 24

1.5. Thesis summary 24

2. The continuous detection of pathogenic bacteria in water: A review of current technologies and areas for development 26

2.1. Water contamination by pathogenic bacteria 26

2.2. Contamination sources 28

2.3. Threat to human health 29

2.3.1. Seasonal fluctuations in microbial concentrations 29

2.4. Indicators of contamination 30

2.4.1. Species of bacteria suitable as indicators 30

2.5. Physiology of bacteria 33

2.6. Physiological states of bacteria 34
2.6.1. Environmental stressors 34
2.6.2. Resuscitation 35
2.6.3. Cell damage as viability analysis 35
2.7. Current methods and standards for detecting pathogens in waterbodies 36
2.7.1. Culture-based techniques 36
2.7.2. Biochemical tests 37
2.7.3. Need for improved, real-time, continuous sensing 37
2.8. Species specific sensing 38
2.8.1. Nucleic acids 38
2.8.2. Aptamers 39
2.8.3. Immunoassays for pathogen detection 40
2.8.4. Cell-based sensors 42
2.8.5. Secretions 43
2.8.6. Bacteriophage 44
2.8.7. Summary 45
2.9. Sensing technologies 46
2.9.1. Enzyme-linked immuno-sorbent assays 46
2.9.2. Polymerase-chain reaction 46
2.9.3. Optical sensors 47
2.9.4. Interferometric 50
2.9.5. Electrochemical 51
2.9.6. Quartz crystal microbalance 54
2.9.7. Vibrational spectroscopy 54
2.9.8. Magnetic 55
2.9.9. Summary 61
2.10. Capture mechanisms and cell labelling 62
2.10.1. Nanotechnologies 62

2.10.2. Microparticles 64
2.10.3. Liposomes 65
2.10.4. Summary 66
2.11. Separation strategies 66
2.11.1. Microfluidics 66
2.11.2. Ultrasonic separation 67
2.11.3. Separation by size 68
2.11.4. Separation using dispersed bubbles 68
2.11.5. Gradient separation 69
2.12. Proposed technologies 75
2.12.1. Immuno-magnetic labelling 75
2.12.2. Microfluidics 76
2.12.3. Summary 76
3. Methods to determine the physiological state of bacteria 77
3.1. Introduction 77
3.1.1. Electrophoresis 77
3.1.2. Flow cytometry 80
3.1.3. Fluorochromes for bacterial viability assessment in conjunction with flow cytometry 81
3.1.4. Traditional plate counts 83
3.1.5. Defining viability of bacteria 83
3.2. Materials and method 85
3.2.1. Bacterial cultures 85
3.2.2. Zeta potential 86
3.2.3. Flow cytometry 86
3.2.4. Fluorescent staining procedures 86
3.2.5. Plate counts 86
3.2.6. Solution preparation 87
3.2.7. Statistics 87

3.3. Results 88
3.3.1. Zeta potential 88
3.3.2. Development of flow cytometry protocol to assess bacteria in water 93
3.3.3. Comparative analysis 99
3.4. Discussion 101
3.5. Conclusions 102
4. Continuous separation using microfluidics and magnetophoresis 104
4.1. Introduction to microfluidics and magnetophoresis 104
4.1.1. Microfluidic devices for bacteria concentration 105
4.1.2. Hydrodynamic focussing 106
4.1.3. Magnetic microparticles 106
4.1.4. Microfluidics in conjunction with magnetophoresis as a continuous concentration and separation device 107
4.1.5. Reducing magnetic particles sedimentation 109
4.2. Theoretical considerations 109
4.2.1. Reynold's number 109
4.2.2. Two-dimensional hydrodynamic focussing 110
4.2.3. Theory of magnetism 111
4.2.4. Stokes's drag force 112
4.3. Method & materials 112
4.3.1. Microfluidic device 112
4.3.2. Magnet design 113
4.3.3. Separation experiments 113
4.4. Results of the magnetophoretic-microfluidic separation 115
4.4.1. Fluid dynamics and hydrodynamic focussing 115
4.4.2. Hydrodynamic focussing 115
4.4.3. Double magnet configuration 116
4.4.4. Separation of MPs using the double magnet configuration 119
4.4.5. Optimisation of the quadrupole magnet configuration 121

4.4.6. Separation using the quadrupole magnet configuration 123
4.4.7. Separation and concentration of MPs from a sample 124
4.5. Conclusions 126
5. Magnetophoretic velocities of superparamagnetic particles, agglomerates and complexes 128
5.1. Introduction to magnetophoretic separations 128
5.1.1. Superparamagnetic particles 129
5.1.2. Functionalised magnetic particles 130
5.1.3. Streptavidin-biotin binding 130
5.1.4. Zeta potential of magnetic particles 131
5.1.5. Continuous separation 132
5.2. Transport model 133
5.2.1. Magnetophoretic velocity 133
5.3. Materials and methods 133
5.3.1. Superparamagnetic particles 134
5.3.2. Mobility study 134
5.3.3. Binding observations 135
5.3.4. Observations 135
5.3.5. Zeta potential 136
5.3.6. Software packages 136
5.4. Results for the magnetophoretic mobilities of magnetic particles 137
5.4.1. Magnetophoretic mobility of magnetic particles 137
5.4.2. Magnetically induced velocity on magnetic particle chains 138
5.4.3. Zeta potential measurements 141
5.4.4. Bound particles 144
5.5. Conclusions 145
6. The separation and detection of single, viable *Escherichia* 147
6.1. Introduction 147
6.1.1. Superparamagnetic microparticles 147

6.1.2. *Escherichia coli* as a biosensor target 148
6.1.3. *Escherichia coli* carriers and vectors 148
6.1.4. Immuno-labelling of magnetic particles and magnetophoresis 149
6.2. Transport model 150
6.3. Materials & method 150
6.3.1. Immuno-labelling of magnetic particles 151
6.3.2. Binding calibration 151
6.3.3. *Escherichia coli* preparation 152
6.3.4. Antibody-MP-bacterial binding 153
6.3.5. Mobility study 153
6.3.6. Observations and software packages 153
6.3.7. Statistics 153
6.4. Results 154
6.4.1. Antibody Specificity 154
6.4.2. Antibody-magnetic particle functionalisation capture efficiencies 156
6.4.3. Magnetophoretic velocity of *Escherichia coli* 158
6.4.4. Magnetophoretic velocity of viable and non-viable *Escherichia coli* 160
6.5. Discussion 162
6.5.1. Antibody conjugation of magnetic particles 163
6.5.2. Magnetophoretic velocity of viable and non-viable *Escherichia coli* 165
6.6. Conclusions 165
7. Summary, conclusive remarks and future work 166
7.1. Summary of research and discussion 166
7.1.1. Microbiological viability analytical techniques 166
7.1.2. Microfluidics and magnetophoresis for the continuous separation and concentration of pathogenic bacteria 168
7.1.3. Magnetophoretic mobilities of magnetic particles 169
7.1.4. Separation and detection of *Escherichia coli* 170
7.2. Concluding remarks 171

7.2.1. Towards a “Lab-on-a-Chip” 171
7.2.2. Increasing separation efficiency and through-put 173
7.2.3. Viable and non-viable analysis 174
7.2.4. Scope of sensor – a broader perspective 175
8. References 177

List of Figures

Figure 2.1. The rates per 100,000 people, of laboratory confirmed *Escherichia coli* 33

Figure 2.2. The general structure of bacteria 34

Figure 2.3. A schematic of the Miltenyi batch magnetic separation device 57

Figure 2.4. Magnetic split flow fractionation of magnetic material 58

Figure 2.5. A schematic of the quadrupole flow sorter) 59

Figure 2.6. A schematic of the continuous and periodical trapping and releasing of the magnetic particles 60

Figure 2.7. A schematic of on-chip magnetophoresis for continuous separation) 60

Figure 2.8. A schematic displaying the electrical double layer 71

Figure 3.1. The electrical double layer that surrounds a particle.....78

Figure 3.2. The zeta potential of live bacteria 89

Figure 3.3. The zeta potential of four species of bacteria.....90

Figure 3.4. The zeta potential of *Escherichia coli*, *Bacillus megaterium*, *Enterococcus saccharolyticus* and *Vibrio harveyi* 91

Figure 3.5. The zeta potential of viable and $AgNO_3$ treated bacteria. 92

Figure 3.6. The correlation between flow cytometry analysis of the uptake of fluorochrome 2-NBDG.....94

Figure 3.7. Calibration curve of 2-NBDG with plates counts with $AgNO_3$ treatment of *Escherichia coli* 95

Figure 3.8. The percentage uptake of 2-NBDG by live *Escherichia coli*.....96

Figure 3.9. The uptake of the five fluorochromes by *Escherichia coli* cells when suspended in drinking water 96

Figure 3.10. Flow cytometry analysis of the uptake of SYBR green and propidium iodide by *Escherichia coli* with heat treatment 98

Figure 4.1. A schematic of the proposed microfluidic-magnetophoretic separation device using permanent magnets. 109
Figure 4.2. A schematic of the three inlet channels of the microfluidic device displaying hydrodynamic focussing of sample flow 111
Figure 4.3. A schematic of the microfluidic device, channel depths of 0.4 mm 113
Figure 4.4. A schematic of the magnet configurations mounted upon the microfluidic device in a. double magnet and b. quadrupole.....113
Figure 4.5. A schematic of the hydrodynamic focussing 116
Figure 4.7. The magnetic force acting upon a magnetic particle across the width of the microfluidic device as modelled in FEMM 118
Figure 4.8. The exit end of the microfluidic device, highly concentrated magnetic particles aligned in the region of equilibrium starting from the sample inlet,.....118
Figure 4.9. The separation of magnetic particles from a mixture of magnetic particles and blue non-magnetic beads 119
Figure 4.10. The correlation between flow rate and the percentage of the collected magnetic particles 120
Figure 4.11. The percentage of magnetic particles recovered from each exit channel at different flow rates.....120
Figure 4.12. The FEMM model of the magnetic flux lines of the quadrupole configuration.....122
Figure 4.13. The magnetic force acting upon a magnetic particle across the width of the microfluidic device as modelled in FEMM 122
Figure 4.14. A schematic of the hydrodynamic focussing used with the quadrupole configuration. 123
Figure 4.15. The separation efficiency of the quadrupole configuration in continuous and pulsed mode compared to the control of no-magnets 124

Figure 5.1. A schematic of the experimental setup used to determine the magnetically induced velocity of magnetic particles 135
Figure 5.2. A schematic of magnetic particles travelling towards a permanent magnet in configuration.....139
Figure 5.3. The normalised ratio of the magnetophoretically induced velocity per chain of magnetic particles to the magnetophoretically induced velocity of a single magnetic particle travelling towards a magnet.....141
Figure 5.4. The zeta potential of Chemicell i) streptavidin-ScreenMAG-G ii) short-linker biotinylated silica and iii) long-linker biotinylated silica beads, suspended in water adjusted to different pH values. 143
Figure 5.5. The velocities of single magnetic particles and single magnetic particles bound to a single biotinylated silica bead. 145
Figure 6.1. a) An M270-*Escherichia coli* complex and b) a Chemicell-*Escherichia coli* complex.....154
Figure 6.2. The capture efficiency of anti-*Escherichia coli*-MPs of *Escherichia coli, Staphylococcus warneri* and unfunctionalised MPs 155
Figure 6.3. The antibody absorbance calibration conducted at 280 nm 155
Figure 6.4. The binding efficiencies of the 2.8µm magnetic particles M270 (a) and M280 (b) functionalised with different concentrations of antibody 157
Figure 6.5. A comparison of the three types of magnetic particles functionalised with a) 20 µg/ ml and b) 40 µg/ ml of anti-*Escherichia coli* antibody 158
Figure 6.6. The scatter graphs of magnetophoretic velocity of a) Chemicell and b) MyOneC 159
Figure 6.7. The magnetically induced velocity of Dynabeads MyOneC as the beads traversed the observation chamber. 160

Figure 6.8. The magnetically induced drift velocities of magnetic particles attached to *Escherichia coli* 161

List of Tables

Table 2.1. Examples of pathogenic, waterborne bacteria 27

Table 2.2. The indicator bacteria used to determine drinking water quality in the United Kingdom 31

Table 3.1. The fluorescent stains discussed within this report and their characteristics .. 82

Table 3.2. The species of bacteria used within this study and their key characteristics ... 85

Table 3.3. A comparison of the three microbiological techniques of the viability of the four species of bacteria under starvation condition 100

Table 5.1. The six types of micro-particles used in the study and their individual physical and surface characteristics 132

Table 5.2. The magnetophoretic induced velocity obtained for the four different types of magnetic particles in water 137

Table 5.3. The surface properties of the magnetic particles and silica beads used within this study 144

Table 6.1. The magnetic particles used in the immunoassay to capture *Escherichia coli*, physical attributes and the amount of antibody applied and attached to the MPs with the calculated antibody surface area 156

Glossary

AC	Alternating current
ANOVA	Analysis of variance
ATP	Adenine triphosphate
ASW	Artificial seawater
B	Field induction
CA	Colonic acid
CCD	Charge-coupled device
Cd	Capacitance
CFU	Colony forming units
CNT	Carbon nanotube
CT	Cholera toxin
CTB	Cholera toxin B-unit
DC	Direct current
DI	Deionised water
$DiBAC_4$	Bis-(1,3-Dibutylbarbituric acid) trimethane oxonol
DNA	Deoxyribose nucleic acid
DW	Drinking water
ε	Permittivity
EB	Ethidium bromide
EDTA	Ethylenediaminetetraacetic Acid
f	Frequency
η	Dynamic viscosity
FOV	Field of view
FTIR	Fourier Transform Infrared Spectroscopy
GFP	Green fluorescent protein
GMR	Giant magnetoresistive sensor
h	Height
H	Field strength
HDF	Hydrodynamic focussing
L	Linear dimension of a channel
LB	Luria Bertani
LOD	Limit of detection

LPS	Lipopolysaccharide
M	Magnetisation of the medium
MFD	Microfluidic device
LLB	Long-linker biotinylated bead
μ	Magnetophoretic mobility
μ_e	Electrophoretic mobility
MNP	Magnetic nanoparticles
MP	Superparamagnetic particle
n	Number
NB	Non-magnetic bead
NP	Nanoparticle
PCR	Polymerase chain reaction
PI	Propidium iodide
QD	Quantum dots
Q_i	Volume flow rate of sample
Q_s	Volume flow rate of sheath
r	Radius
Re	Reynold's number
ρ	Density
Rs	Resistance
RNA	Ribonucleic acid
ROM	Region of minima
RPS	Resistive pulse sensor
RS	Raman spectroscopy
SB	SYBR green II
SERS	Surface-enhanced Raman spectroscopy
σ	Conductivity
SLB	Short-linker biotinylated bead
SPR	Surface plasmon resonance
SX	Sytox green
$\bar{u}$	Mean velocity
$\mathbf{u}_m$	Magnetic velocity ratio
V	Drift velocity
VBNC	Viable but non-culturable

V_0	Initial velocity
V_f	Final velocity
W_f	Width of the focussed sample stream
W_0	Width of the channel
χ	Susceptibility
Z	Impedance
ζ	Zeta potential
2-NBDG	2-(*N*-(7-nitrobenz-2-oxa-1,3-diazol-4-yl)amino)-2-deoxyglucose

1. The continuous detection of pathogenic bacteria in waterbodies

Pathogenic bacteria are the cause of infectious diseases throughout the world. Water is a common vector for the spread of bacterial contamination events. There are many species of pathogens that thrive, survive and persist in all water types such as *Escherichia coli* and *Vibrio cholerae*. The current method for detecting pathogenic bacteria in waterbodies takes longer than 24 hours and requires laboratory analysis. The objective of the work described in this thesis was to design and develop a biosensor that will detect bacteria in near-real time, at low-cost and from continuous flow.

1.1. Current detection methods for the presence of pathogenic bacteria

Current methods used to monitor the microbial content of water are culture-based techniques. A water sample is spread upon a plate of agar. The plate is incubated at an optimal temperature for 24 to 72 hours, after which the colonies are counted. The number of colonies on an agar plate is taken as the viable number of bacteria within a sample. This process is time consuming, requires laboratory facilities and trained users. As contamination of water supplies can be rapid and short-lasting, there is a demand to reduce the detection time for the presence of contaminants. Samples are often taken intermittently by means of "grab" samples. As contamination events are rapid and stochastic, they may be missed by this sampling method; samples are not representative of the whole waterbody [1]. The practicality and reproducibility of traditional plate counts has been debated rigorously in recent years. The total number of bacteria within an environmental sample can be hugely underestimated. As many as 99% of bacteria are thought to be un-culturable by the plating method [2]. The percentage of "unknown"

bacteria in the environment, poses a risk to human welfare. This method is no longer fit-for-purpose and replacements are being sought.

1.2. Physiological states of bacteria

A key attribute of new detection technologies, is the ability to determine between viable and non-viable bacteria. Bacteria can enter into a number of physiological states upon entering foreign environments, this phenomenon has not been well recognised until recently [3].

Human-pathogenic bacteria are not usually prevalent in the environment. Enteropathogens (such as *Enterococcus* sp. and *E. coli*) whose "natural" environment is in the intestines of mammals can be transported to waterbodies. Upon entering the "un-natural" waterbody environment the bacteria become stressed. Physiological and morphological changes are observed. Morphologically, the bacteria may change shape and reduce in size [4]. The physiology may be altered, metabolism may cease [5], and spore-like structures (endospores) are produced by some species of bacteria. Endospores provide a safety mechanism against harsh environmental conditions, safeguarding genetic material. Endospores can remain dormant in unfavourable conditions for many hundreds of years [6] and are unaffected by many disinfection techniques (e.g. ultra-violet irradiation).

In adverse environmental conditions, physiological changes can make pathogenic bacteria un-culturable upon agar plates yet the pathogenic bacteria may well continue to maintain their persistence and virulence. The term "viable-but-non-culturable" (VBNC) has been given to these organisms [7, 8]. VBNC will only return to a culturable i.e. reproducible, state when preferable conditions are re-encountered [9]. In at least some species, the VBNC state is distinct from the starvation response, where bacteria are still readily culturable when plated on suitable media [10]. Species with a true VBNC state, a resuscitating step is required before the cells can again reproduce. There are

environmental and chemical stimuli, which resuscitate VBNC cells; these are dependent upon the species of bacteria. Described resuscitation steps include temperature changes, co-culture, culture in preferential media [11] and the addition of resuscitating promoting factors (Rpf) [12]. VBNC bacteria can still be a danger to any person that consumes them; their detection is therefore important to preventing the spread of disease.

An early-detection system could provide authorities with the necessary information to implement treatment or closure of a waterbody. An infectious dose of pathogenic bacteria can be as little as 10 to 100 colony forming units (CFU) [13]. This is a small amount and difficult to detect. When developing a biosensor to detect pathogenic bacteria in near-real time, the sensor must be able to detect 10 CFU/ ml and determination of bacterial viability at the single cell level is necessary. The proposed biosensor should also enumerate the number of viable and non-viable bacteria.

1.3. Biosensors for bacterial detection

There has been a plethora of novel biosensor designs for the detection of bacteria. Scientific and engineering advancements have been made [13–17], and the detection of single cells has been accomplished [18, 19]. The technologies used to achieve this do not yet offer the advantage of sampling in continuous flow, in real-time with an automated response. These are the attributes, described above, that are required to monitor for bacterial contamination events.

1.4. Objectives of the proposed biosensor and thesis overview

There were three objectives when developing a continuous monitoring system, “a biosensor,” for pathogenic bacteria in aqueous environments. Firstly, it was necessary to assess available microbiological techniques that could be adaptable for the biosensor and could provide a viability assessment of bacteria. Secondly, a continuous method for extracting the target from water was required; this method must enable the concentration

of the target-pathogens for further analysis. Thirdly, the captured bacteria would be defined as being viable or non-viable, and enumerated at the single-cell level. To meet these objectives, the technologies employed were microfluidics, superparamagnetic micro-particles and immuno-labelling. An overview of the research and development that was conducted to design a biosensor for monitoring waterbodies is given here.

1.4.1. Exploration of microbiological techniques suitable for continuous assessment of bacterial populations

Flow cytometry and zeta potential measurements were explored as suitable rapid microbiological techniques. Flow cytometry is a well-established microbiological technique, for assessing cells. The use of fluorochromes in addition to flow cytometry allows a thorough analysis of a population and can provide information on the physiological state of bacteria. Flow cytometry is restricted by a detection limit of 10^3 cells/ ml, expensive instrumentation and the need for skilled users. Commercially available fluorochromes were used to assess bacterial populations in different physiological states. The aim was to identify a fluorochrome that could be used as a viability indicator and that had a good correlation using traditional plate counts.

When suspended in water, bacteria act as bio-colloids. The bacterial-cell surface and the transport of ions across the bacterial-cell membrane give the cell a charge. This charge can be measured by means of the zeta potential. Zeta potential measurements were compared to those obtained by flow cytometry and plate counts to establish whether a correlation between the three microbiological techniques could be found.

1.4.2. *Escherichia coli* as an indicator organism for the biosensor to target

E. coli is persistent in the environment as it is a facultative anaerobe and has the ability to maintain its virulence [20]. When in an extra-enteric environment, *E. coli* is unable to replicate until it is within a host enteric environment again [21].

E. coli has long been used as a model pathogenic bacterium and its physiology is well documented. The correlation between *E. coli* and other faecal contaminants such as *Enterococcus* sp. is well established [22] and the presence of *E. coli* in a waterbody is indicative of faecal contamination. As such, *E. coli* was determined as a suitable target bacterium for the proposed biosensor.

1.4.3. Microfluidics as a sampling, separation and concentration device

Microfluidic devices (MFD) offer the potential to monitor samples, and therefore waterbodies, in near real-time and from continuous flow. Microfluidics can be designed with almost any geometry to suit the application. Measurements can be conducted from small volumes of complex fluids with efficiency and speed [23]. The use of novel micro- and nano-technologies as additional detection mechanisms, in conjunction with an MFD, offers specificity, and separation and concentration of low-concentration cells, from large volumes of samples. A three-inlet, three-outlet MFD was designed. The MFD enabled a sample flow to be hydrodynamically focussed and permitted the separation of bacteria from continuous flow in conjunction with magnetophoresis, as described in the following sections.

1.4.4. Immuno-magnetic labelling of magnetic particles

Immuno-magnetic labelling of magnetic particles (MPs) using an anti-*Escherichia coli* antibody was used to isolate, separate and concentrate *E. coli* cells from water samples. The ligand-protein interaction of streptavidin to biotin was used to orientate the antibodies upon the MPs to obtain maximum capture efficiency. Incubation of MPs with the sample enabled the capture of *E. coli*. Upon binding of the MPs to *E. coli,* the bacteria inherit the magnetic properties of the MPs and can be manoeuvred by an external magnetic field. Using a permanent magnet and a magnetic gradient, captured *E.*

coli was separated from the sample flow using the designed microfluidic-magnetophoretic device.

1.4.5. Magnetophoretic mobilities of superparamagnetic particles

Magnetic separations are characterised by the magnetic properties of the MPs used in the assay. The response of an MP to a magnetic gradient is dependable upon the susceptibility of the magnetic material and therefore the magnetic moment, the "mobility". To maximise the separation efficiency of the described magnetophoretic-microfluidic device, a study of the magnetophoretic mobilities of commercially available MPs was conducted. The magnetic properties of the MPs were investigated by design of a magnetophoretic observation chamber. The uniformity, with regard to magnetic content, and the magnetically induced drift velocities of the MPs in a non-uniform magnetic field was determined. The self-assembly of the MPs into chains and the resultant magnetophoretic mobilities was predicted using a simple model. MPs were used to capture a mock biomarker, a silica non-magnetic bead (NMB) to confirm the applicability of the derived model.

1.4.6. Magnetophoretic mobilities of captured *Escherichia coli*

The MFD was used to concentrate the immuno-labelled MPs from drinking water (DW). Using a magnetophoretic chamber and a magnetic gradient with microscopic video tracking of the MPs and MPs-bacteria complexes, the magnetically induced drift velocities were determined. It was found that there was a significant difference in the magnetophoretic drift velocities of captured viable and non-viable *E. coli* cells.

1.5. Thesis summary

The aim of this thesis was to develop a biosensor that enabled the detection of pathogenic bacteria in water. To achieve this, an MFD was developed, encompassing magnetophoresis and the use of immuno-labelling of MPs, is described in this thesis. The

technology offers the potential for the continuous monitoring of species-specific pathogens from waterbodies. The low-cost sensor analyses captured bacteria at the single-cell level; the viability of the bacterial cells was determined by the magnetically induced drift velocity of captured bacteria. The biosensor offers the potential for automation and progression towards a total-analysis system as a “Lab-on-a-chip”.

2. The continuous detection of pathogenic bacteria in water: A review of current technologies and areas for development

The contamination of waterbodies by pathogenic bacteria is a cause for concern on a global scale. Current detection methods are time consuming and laborious. There is a requirement to reduce the detection time in sensing pathogens and to provide a continuous method for monitoring waterbodies. The development of a near real-time, continuous sensing system for the detection of pathogenic bacteria, a biosensor, is a sensible ambition for the discipline. The biosensor must be user-friendly, reasonably priced, portable and easily maintainable, for its users may not be scientifically trained. If the biosensor is to be commercially viable, the technologies employed must allow for automation and, eventually, a digital readout of the number of pathogens present.

Biosensing employs a wide range of scientific and engineering disciplines including chemistry, biology, physics and electronics [24]. This review sets out to discuss and highlight advances within these fields, and assess technologies and methods that are suitable for the rapid and continuous monitoring of waterbodies.

2.1. Water contamination by pathogenic bacteria

The microbiological contamination of waterbodies can have, and is demonstrated to have, serious adverse effects upon human health [25]. In developing nations, the leading cause of death is by bacterial infections, accounting for an estimated 40% of the 50 million deaths each year [14]. More than 2.6 billion people do not have access to clean DW, which alone has been attributed to 2.2 million deaths annually [22].

Pathogenic bacteria can occur in very low concentrations in environmental settings; but even at low concentrations they pose a risk to human health. Waterbodies that possess low purification capacities can episodically contain pathogenic bacteria [26]. Examples

of pathogenic bacteria found in waterbodies can be seen in Table 2.1; many strains of pathogenic bacteria have extended survival periods in water systems, regardless of the temperature [27].

DW has low mineral content and ideally only contains a few live non-pathogenic microbial cells per litre [28]. A key challenge in microbiological sampling of waterbodies, is obtaining representative sampling. Current monitoring methods of DW supplies utilise "grab" sampling, which may not be representative of the whole waterbody and could miss flash contamination events [29]. It is current practice to monitor waterbodies for contamination by detecting "indicator" species of bacteria. Indicator species include *Enterococcus* sp. and *E. coli* as examples. The presence of these species in water is indicative of recent faecal contamination. Lakes and coastal waters that are popular for recreational activities should be regularly assessed to determine the levels of indicator bacteria in the water to ensure that the area is safe for the public's use. A portable biosensor is required that is able rapidly, and accurately to detect in water samples the total number of indicator bacteria, along with their viable percentage.

Table 2.1. Examples of pathogenic, waterborne bacteria [30]

Species of bacteria	**Persistence in Water Supplies**	**Relative Infectivity**
Burkholderia pseudomallei	May multiply	Low
Campylobacter jejuni, C.coli	Moderate	Moderate
Escherichia coli – Pathogenic	Moderate	Low
E. coli – Enterohaemorrhagic	Moderate	High
Francisella tularensis	Long	High
Legionella spp.	May multiply	Moderate
Leptospira	Long	High
Salmonella Typhi	Moderate	Low
Other *salmonellae*	May multiply	Low
Shigella spp.	Short	High
Vibrio cholerae	Short to long	Low

The infective dose of a pathogen can be as low as 10 CFU/ ml [31]. The microbial communities of waterbodies can be expected to be temporally and spatially dynamic, with fluctuations and regular variations. Very few sensors have been documented to detect below 10 CFU/ ml [17], and those that do, tend to involve complex microbiological pre-enrichment steps [18].

2.2. Contamination sources

In developing countries, a major concern is that of waterbodies becoming polluted by receiving direct loading of pathogenic bacteria from open sewers, industry and farming. Whole communities are dependent upon untreated, contaminated waterbodies for drinking, washing and cooking [32]. These communities are at a high level of risk of becoming infected by a plethora of pathogenic bacteria. It has been reported that as many as 60% of households in Indian slums do not have any method for water purification [33].

In the developed world, the danger of contaminated waters reaching domestic water supplies is mitigated with care, legislation and extensive infrastructure. However, during winter months the level of ground water can increase dramatically and flooding frequently occurs. During periods of extreme rainfall, untreated sewage waters may overflow into water courses, contaminating the water supply; leaving the public at risk of infection [34].

Many of the species of bacteria that pose a risk to human health can be found living in mammals and birds. There is evidence to suggest the largest sink for pathogenic bacteria, in the developed world, is farmed livestock. Wilson *et al*., found that 96% of cases of Campylobacteriosis (the most commonly identified cause of gastro-enteritis) caused by the *Campylobacter jejuni* and *Campylobacter coli* could be associated to strains isolated from chicken and cattle [35].

A global increase in the intensive farming of poultry, cattle, sheep, pigs and fish will also increase the abundance of pathogenic bacteria harvesting sites. These potential contaminants will be brought closer to water resources where bacteria are readily transported and dispersed. A study into the presence of antimicrobial resistant *E. coli* in Canada, reported that the probability of contamination was higher in private wells if livestock were kept on the nearby land [36]. Farms store, and fertilise crops with manure, which again adds possibility of the leaching and seepage of contaminants into groundwater [34].

2.3. Threat to human health

It has been estimated that the number of children who die each day because of water-related disease is 4,000 [38]. As an example, *V. cholerae* is a Gram-negative, oxidase-positive bacillus [39] that can cause chronic diarrhoea. The species is autochthonous to coastal and freshwater environments [40]; coastal water is deemed as contaminated if 1 CFU/ 100 ml is present. The regulation is so constrained due to the epidemic nature of the bacterium [41]. The Haitian cholera epidemic in October 2012 infected 93,000 people of whom 2,100 people died in a matter of weeks; the outbreak was caused by a strain of *V. cholerae* from a distant geographic region [42].

2.3.1. Seasonal fluctuations in microbial concentrations

During winter months, and during the rainy seasons in the tropics, there is an increase in the transport of microbes into water supplies from sediments and surface water. This is attributed to the increased rainfall washing allochthonous bacteria from the land and being re-suspended from riverbeds, into ground waters [34]. After the occurrence of a major weather event or natural disaster, contaminated DW supplies is one of the major causes of rapidly spreading diseases [43].

2.4. Indicators of contamination

The presence of enteric bacteria in DW is considered by the US Environment Agency and the European Union as an indicator of faecal contamination (see Table 2.2). The presence of these organisms is monitored, and detection will result in a supply being confined until levels return to those permitted by the standard. Studies have found correlations between physico-chemical water conditions and the presence of pathogens [44]. Increased nutrient levels in water supplies often lead to the presence of increased counts of bacteria. For example, in groundwater increased phosphate levels > 0.05 mg l^{-1} are positively correlated to the number of *Cryptosporidium* sp. and *E. coli* [37]. In addition, the size of particulate matter, and its distribution within a waterbody has been reported to correlate with increased microbial loading in aquifer systems [45]. This technique may be used as early warning signals for water supply contamination. These methods do not provide quantifiable results of microbial contamination. It is proposed that an indicator species is often used as the biosensor target, as an indicator for contamination.

2.4.1. Species of bacteria suitable as indicators

There have been a number of species of bacteria that have been defined as indicators of contaminated waters. Examples of these bacteria are described here.

2.4.1.1. *Coliforms*

Coliform bacteria are Gram-negative, rod-shaped, non-spore forming bacteria that ferment lactose with the productions of acid and gas when incubated between 35 and 37 °C [46]. They are easily characterised as coliforms using membrane filtration techniques. Coliforms encompass a wide range of bacteria that are found in soils, water, human and animal waste [47]. They are widely used as an indicator of water contamination. Although many coliform bacteria are non-pathogenic, their presence in water is a sign of

the water being contaminated and as such with the potential presence of pathogenic agents from the intestinal tract of warm-blooded animals [48].

Table 2.2. The indicator bacteria used to determine drinking water quality in the United Kingdom [41]

Parameter	**Description**	**Standards (per 100 ml)**	
		Drinking Water	**Bathing Water**
E. coli	Their detection in water is an indication of faecal contamination.	0	2000
Enterococci species	Their detection in water is an indication of faecal contamination. They are readily killed by disinfection but the occasional detection in drinking water can occur.	0	330
Coliforms	Their presence in water may indicate faecal pollution has occurred. They are readily killed by disinfection but the occasional detection in drinking water can occur.	0	10000
Clostridium perfringens	Bacterium that can produce spores that can persist in the environment for long periods of time. Their presence in water can indicate historic contamination.	0	N/A
Colony counts measured	General measure of the bacterial population within drinking water.	No abnormal change	No abnormal change

2.4.1.2. ***Enterococci***

An example of a widely used group of bacteria, used as an indicator of contaminated watercourses, is *Enterococci* [49]. The bacteria in the genus *Enterococci* are Gram-positive, facultative anaerobic cocci and are prevalent in mammalian digestive tracts. They are known to cause a number of urinary tract diseases, meningitis and have increasing antibiotic resistance [50].

2.4.1.3. ***Bacteroid*** **spp.**

Bacteroid spp. have a short persistence in the environment due to the truly anaerobic nature of the organisms. In addition, the concentration of *Bacteroid* spp. in animal excrement is much lower than in human, it is therefore a good indicator of recent sewage contamination [1].

2.4.1.4. ***Escherichia coli***

E. coli is a Gram-negative, rod-shaped, facultative anaerobe of approximately 2 µm in length [51]. It is one of the most important species in biotechnology and microbiology [52]. There are only a small number of sero-groups, compared to the numerous strains of *E. coli,* that are enterohemorraghic [53]. Pathogenic *E. coli* O157:H7 is still a major cause of diarrhoea and can even lead to renal failure and meningitis [54]. The consumption of as little as 10-100 CFU/ ml can cause infection [55]. "*Escherichia coli provides conclusive evidence of recent faecal pollution and should not be present in DW*" [30].

Reported infections by *E. coli* are increasing (Figure 2.1). Urinary tract infections are widely caused by *E. coli*, as is bacteraemia (the presence of bacteria in the blood which is usually sterile) [56]. Furthermore there has been an increase in number of strains of *E. coli* that are resistant to anti-microbials.

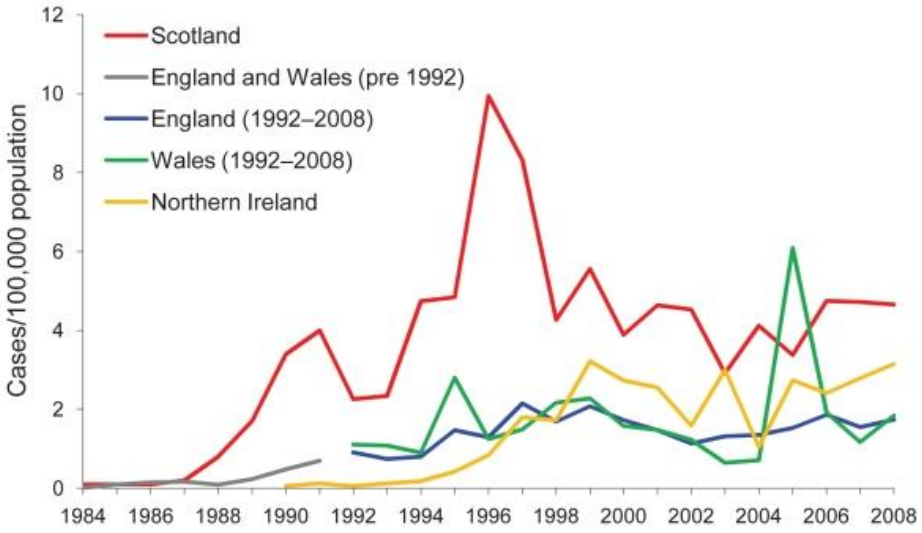

Figure 2.1. The rates per 100,000 people, of laboratory confirmed Escherichia coli O157 cases between 1984 and 2008 in the United Kingdom [57]

2.5. Physiology of bacteria

The identification of bacteria in water, in real-time, requires a method for detecting and identifying the particular species. The physiology of bacteria holds important markers that may be used as detection mechanisms.

A bacterial membrane consists of an outer membrane or capsule, a rigid peptidoglycan cell wall and a tightly controlled cytoplasmic membrane (Figure 2.2) which prevents cells from direct interactions with environmental macromolecules [58]. Many species of bacteria (e.g. *E. coli*) respond to changes in the environment in the search for nutrients via a process termed chemotaxis (i.e. swimming) [59]. Changes in the environment are responded to via a signal transduction, via chemotaxis-specific sensors, and the rotation either clockwise or anti-clockwise of the flagellum [60].

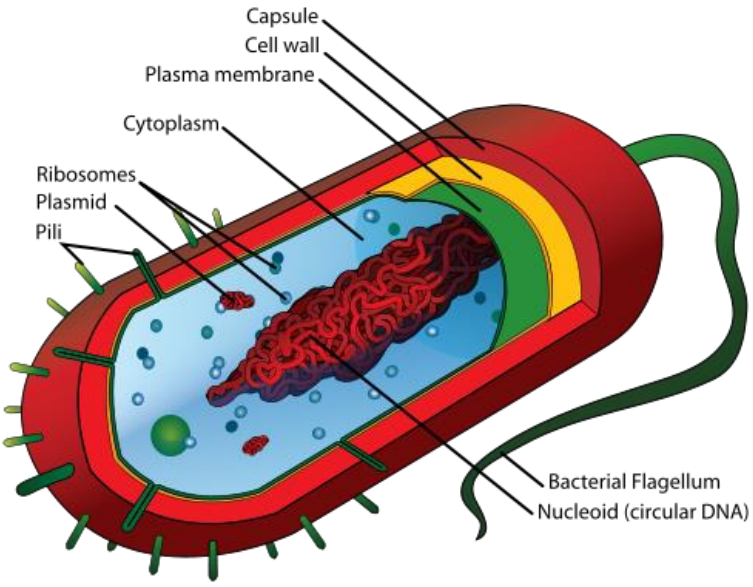

Figure 2.2. The general structure of bacteria [61]

2.6. Physiological states of bacteria

The death of a bacterial cell has long been defined as the inability to grow a visible colony on bacteriological media [62]. Parthuisot *et al*, [63] report that viability should be restricted to circumstances where evidence that a cell is able to divide is provided, therefore viability is demonstrated by an ability to culture the cell. However, much attention has been given to dormant or quiescent bacteria that when stressed become un-culturable on standard media and have been given the term VBNC (viable but not culturable). It has been reported that VBNC cells maintain their virulence [64], as such a method to detect VBNC cells is required.

2.6.1. Environmental stressors

The physiological state of a microbe is dependent upon the stressors encountered, such as pH, temperature, hyper- and hypo-salt concentrations, oxygen levels and other chemical stressors such as chlorine [65]. A gastrointestinal bacterium, upon exiting its preferred environment and entering a watebody, will be subjected to a number of these stressors. Whilst some cells will maintain their pathogenicity, their physiological state

will be altered. When a cell enters unfavourable conditions, the changes may be physiological with differences in cell size, the structure of cells walls and the permeability of cell membranes [66].

2.6.2. Resuscitation

VBNC cells can remain dormant for many years. A change in the chemical or physical environment is required to resuscitate the bacteria. There are a number of species which have been reported to recover from a VBNC state via a variety of resuscitation steps. *E. coli* can be resuscitated by changes in temperature, the addition of the supernatant of a growing culture of bacteria and the addition of amino acids [11]. Rpf (resuscitating promoting factor) are a group of secreted proteins which have been used to resuscitate VBNC actinobacteria [12]. The resuscitation step required is likely to be dependent upon the stressors encountered that induced the VBNC state. As an example, the addition of sodium pyruvate to a culture, has been reported to enable the resuscitation of hydrogen peroxide sensitive cells [67].

2.6.3. Cell damage as viability analysis

It is important, when designing a biosensor, that the viability of the target organism is reported by the sensor. Liao *et al*., [68] describe some of the characteristics that may be used to determine cell death: wrinkles/holes on bacterial cell surface, degree of hollowness, increased surface veins, condensation and loss of cytoplasm, disruption and aggregation of cytoplasmic membranes, fractures in the membranes and severe inner damage of the intracellular organisation. Viability is not easily defined in terms of a single physiological or morphological parameter [3]. *"Defining cell death and cell viability is philosophically and experimentally difficult"* [69].

When bacteria are subjected to a disinfection technique, Nebe-von-Caron *et al.,* [70] hypothesise that a stressed bacterial cell first loses the ability for active transport across

the cell membrane, the cytoplasmic membrane then becomes depolarised and finally permeabilisation of the cell membrane occurs. It is not clear when a cell loses its ability to replicate and when a pathogen loses its virulence.

Non-spore forming bacteria lose their culturability when subjected to stress. This results in the formation of VBNC cells which maintain their virulence but go undetected using traditional culture-based methods [71]. When favourable environments are re-encountered, the VBNC cells return to their "viable state."

2.7. Current methods and standards for detecting pathogens in waterbodies

DW supplies are generally monitored via low frequency, grab sampling [29]. Pathogenic bacteria may evade detection due to their presence in low numbers [72]. Common methods to determine microbial levels are most probably number and membrane filtration [58]. The most widely used tests are culture-based methods; a review of current methods is described below.

2.7.1. Culture-based techniques

Monitoring the number of microorganisms in DW using cultivation-dependent methods of heterotrophic plate counts was introduced at the turn of the 20th century [73]. It is common for culture-based enumeration of microbial content to take more than 24 hours. In this time a contaminated waterbody could cause a threat to public health [74]. In addition to the duration of the culture-based technique, the standard deviation in CFU can be as great as 20% [75]. There can be large discrepancies between the total number of microorganisms in a sample and the numbers determined by plate counts [76]. This adds uncertainty to the results obtained by traditional methods.

2.7.2. Biochemical tests

Adenosine triphosphate (ATP) is a product released during respiration. ATP detection has long been accomplished through bioluminescence and the enzyme luciferase. There are numerous commercially-available kits that analyse ATP by simply adding luciferin/luciferase to a sample and measuring the luminescence (e.g. StayBrite™, ENLITEN®). The measurement of ATP can be conducted using a handheld device, offering both portability and speed of response. These attributes offer the potential for near-real time and continuous monitoring of a waterbody. As ATP is only released by live cells, this technique can be used as an indication of viability [77]. However, free ATP must also be determined, as this is released by cells in the die-off phase. An estimation of the active proportion of the biomass within a sample can be found by: Microbial ATP = Total ATP – free ATP [29].

Quantitative measurements of ATP have been applied to biological and environmental systems for many years [78]. As an indicator for an estimation of biomass, ATP measurements provide useful data. However, at low biomass concentrations, the standard techniques are not sensitive enough.

2.7.3. Need for improved, real-time, continuous sensing

Point-of-need biosensing must make use of automatable technologies that are inexpensive and can be used by non-skilled personnel [79]. In addition, there is a demand to assess the physiological status of the detected organisms, not only the total number of cells in a sample [3]. With all current real/short-time technologies there is a detection limit [80]. The technologies that provide a platform for fast bacterial detection with a low detection limit (LOD) will be reviewed in the following sections.

2.8. Species specific sensing

A species specific bacterial sensor must be capable of sensing only the strain of bacteria which is of interest. To confirm the interaction or capture of a particular species, labels are used [81]. There are a number of methods that have been employed to enable this.

Bacteria have many attributes which may be used as sensor recognition sites or labels. Generally bacteria are negatively charged [82], many contain or excrete toxins [83], numerous species contain intrinsic fluorophores such as tryptophan [84], and have a mass of approximately 10^{-12} g [85]; all of which are detectable. Bacteria have a number of components that a biosensor can target. Examples include: ribonucleic acid (RNA), deoxyribonucleic acid (DNA), lipid, lipopolysaccharide (LPS), peptidoglycan, glycogen and polyamine [86]. The following sections will explore relevant detection labels and the target bacteria.

2.8.1. Nucleic acids

In vitro nucleic acid amplification is designed to amplify a target nucleic acid sequence that is unique to the pathogen of interest [87]. Nucleic acid based sensors involve the attachment of a capture oligonucleotide onto the sensor surface, the target nucleic acid is detected via hybridisation of the capturing probe [88]. Molecular fingerprints based upon environmental nucleic acids provide a tool for screening an array of bacteria, viruses and protozoan pathogens [89]. The different types of reported nucleic acid sensing methods are reported here.

2.8.1.1. *Deoxyribose nucleic acid*

DNA sequences can be only present as one copy per cell, this makes DNA a difficult target for a biosensor [74]. For this reason, DNA probe hybridisation assays are usually performed for culture confirmation [87]. The sensitivity of DNA sensors is critically dependent on the signal amplitude corresponding to a DNA hybridisation event [90].

2.8.1.2. *Deoxyribose nucleic acid microarrays*

The use of microarray technology in conjunction with DNA-based typing provides a valuable tool in pathogen detection. Using only one sensing platform, several species can be tested for. Oligonucleotides are printed directly onto a glass surface, incorporation of a fluorescence marker enables a colorimetric result which can be read by a scanner, quantified and analysed [91]. The detection limit is approximately 4 x 10^4 CFU/ g and requires improvement [92] to enable the detection of low concentrations of pathogenic species.

2.8.1.3. *Ribonucleic acid*

16s ribosomal RNA exists in high copy numbers in bacterial cells, and it is an essential component in ribosomes [93]. RNA is often selected as a target molecule in the identification of bacterial detection [94]. RNA detection can also be an indication of the viability of the cells sensed [87] as RNA rapidly degrades once a cell has died or is inactive. The use of 16s rRNA labelled onto capture and detector probes was described for the electrochemical detection of uropathogens with an LOD of 2.6×10^3 in only 45 minutes [93]. The rapid degradation of RNA makes this technique unsuitable for use in an environmental sensor.

2.8.2. Aptamers

Aptamers are artificial oligonucleotides (either DNA or RNA) that can bind to a variety of pre-determined entities [95] with high affinity and have a similar capacity for protein-protein interactions as antibodies do [96]. Aptamers are composed of nucleic acids, usually adenine, guanine, cytosine and thymine; their structural changes can therefore be designed [97]. The single stranded nucleic acid sequences used in aptamer development are acquired through the process of Systematic Evolution of Ligands by Exponential Enrichment [98]. The advantages of using aptamers over antibodies are: their size -

which results in higher density of immobilised binding sites, better stability and heat resistance, lower cost and due to their synthetic nature, endless possibility for design [99].

Aptamers and their production have been thoroughly reviewed by Fowler *et al.*, [100]. Due to the ability to generate aptamers *in vitro*, their low cost and the ability to develop without a host, aptamers are receiving increased attention in the medical industry [101]. Aptamers with a reversible configuration would be preferable [95] to use within a biosensor platform. When an aptamer is bound to the target, a conformational change occurs that can be measured [97]. This change may be "re-set" by the introduction of a buffer containing a DNA sequence with higher competiveness to the already bound target [102]; the reaction may then begin again.

2.8.2.1. *Aptamer beacons*

An aptamer beacon is an aptamer that is labelled with a fluorochrome. Upon interaction with an analyte, the fluorochrome is separated from its quencher and "lights up" [103]. One method of designing an aptamer beacon is by creating an antisense oligonucleotide that denatures the functional structure of an aptamer. A fluorescent reporter and quencher are located so that they are opposite to one another in the denatured structure and upon binding a change in fluorescence will occur [104].

2.8.3. Immunoassays for pathogen detection

The immune system has evolved clearance mechanisms to recognise surface markers on bacteria. Examples that are used in bacterial detection are described here.

2.8.3.1. *Peptides*

Anti-microbial peptides (AMPs) are found in nature as primary defence mechanisms against infection by bacteria and fungi. They are stable and can be continually exposed to harsh environments, making AMPs an attractive alternative to antibodies. AMPs bind to

a variety of pathogens [105]. Coating a sensor surface in AMPs will then enable the detection of multiple pathogenic species with a detection limit of 1 cell/ µl. However, this technique does not allow for species specificity; Mannoor *et al.,* reported that AMPs capture different pathogens with differing affinities [106]. AMPs offer a promising tool for pathogen detection; however, their use is still in its infancy and requires further development.

2.8.3.2. *Antibody-based immunoassays*

Immunoassay techniques are based upon the interaction between an antibody and an antigen. Bacterial isolates may be tested for their characteristic antigens, which interact with specific antibodies. The first concept of using an immunoassay as a sensing agent was reported by Yalow and Berson [107].

A bacterial cell may carry one or more of these antigens: somatic (O) antigens, which in Gram-negative bacteria are made of the O-polysaccharide. Flagella (H) antigens, which are heat labile proteins and capsular (K) antigens, are made of the carbohydrate of cell capsules [28]. High specificity antibodies have been developed [108] to utilise this recognition element. The region of the antibody that binds to the antigen is called the paratope, and the region of an antigen that binds with an antibody is called the epitope [109].

Antibodies only have one target-binding site; the orientation of an antibody when using antibodies as a bio-sensing platform is paramount to obtaining high specificity and detection levels [110]. There are methods of orientating bacteria on biosensor surfaces, to optimise the affinity of the sensor. These are described later in Chapter 5.

Although the use of antibodies to detect pathogenic bacteria offers a highly sensitive approach, they do not provide any information on the physiological state of the targeted pathogen [108]. In addition, a challenge for field diagnostics that employ antibodies is the need to maintain the antibody's structure and prevent thermal denaturation;

antibodies may not maintain specificity when used in harsh environments [106]. The sensitivity and reliability of a sensor utilising immuno-labelling via antibodies will depend upon the chemistry of labelling the sensor and storage of the sensing probe [111].

2.8.4. Cell-based sensors

Cell-based sensing uses living cells or tissue as an integral part of the sensor [112]. Whole cells, when used as a biosensing element, are capable of responding to threats in a physiologically relevant manner. Cell-based sensors make use of the electrical properties of cells to report on the changes in the cell's vicinity [24].

2.8.4.1. *Genes, proteins & enzymes*

Proteins and enzymes have been used as markers for individual species and groups of bacteria. The outer membrane of bacteria has characteristic proteins. For example, the enzyme β-D-glucuronidase is an accepted biomarker for *E.coli* detection in microbiological water quality analysis [113]. Protein targets include murein lipoprotein, of which there are ~7 × 10^5/ cell and porins which produce channels for small hydrophilic molecules to cross the cell membrane [86]. An example of a sensor that utilises an enzyme, is that of a tyrosinase biosensor used to determine the presence of *E. coli* with an LOD of 10 CFU/ ml [114].

2.8.4.2. *Polysaccharides*

On the cell surface of enteric bacteria, a number of polysaccharides are synthesised and displayed [115]. LPS, a glycolipid, is found exclusively in the external leaflet of the outer membrane. In Enterobacteriaceae, LPS is composed of three structural regions: the hydrophobic lipid A, the core oligosaccharide and the 'O' antigen polysaccharide side chain [116]. An example of an exopolysaccharide (defined as a saccharide that is loosely associated with the outer membrane) is that of colonic acid (CA). CA is produced by enteric bacteria when they are outside of the intestine [86] and when grown in sub-

optimal conditions [115]. CA may therefore be a target to test for enteric bacteria in aqueous environments.

2.8.5. Secretions

It is important to understand the virulence factors of pathogenic bacteria as these offer signals for the specific detection of the pathogenic microorganisms. Classical virulence factors include toxins, adherence molecules, invasion of the host cells and the evasion of the host's immune system [83].

There are a number of volatile metabolites produced by bacterial strains that may provide identifying fingerprints for a sensor to detect [117]. In order to replicate, bacteria require iron. Once invasion of the host cell has occurred, iron is limited. The pathogenic bacteria release siderophores to chelate iron [83]. A biosensor may use the concentration of siderophores in a sample as an indicator for the presence of pathogens. However, this technique would not allow for species specific identification, and a further detection technique would be required.

2.8.5.1. *Toxins*

There are two major groups of toxins, endo- and exo-toxins. The former are part of the integral structure of a bacterium, the latter are secreted molecules [83]. A large number of toxins target carbohydrates on cell surfaces to which they attach and gain entry into the cell [118]. The presence of bacterial toxins in the blood is an important indicator of the presence of virulent activity. Toxins can be present and detectable before an infestation by the microbes [119].

Radio-immunoassays, enzyme-linked immuno-sorbent assay (ELISA) and latex agglutination assays have all been developed for the detection of the cholera toxin (CT). However, these assays take several hours to complete. [120].

Bunyakul *et al.,* [121] describe the electrochemical and fluorescent detection of the CT B-unit (CTB) via liposome amplification in under an hour. Schofield *et al.,* [122] developed a gold nanoparticle-based colorimetric bioassay for the detection of the CTB. The theoretical LOD was determined as 54 nM (3µg/ ml) within ten minutes. These reports show the improvement upon culture-based techniques and potential for near-real-time bacterial sensing.

2.8.6. Bacteriophage

Bacteriophages are viruses which infect bacteria using their tail spike proteins [123]. They are particularly useful in identifying pathogenic bacteria from complex samples [27]. The interaction between a phage and a bacterium generates a quantifiable impedimetric behaviour [124]. Given recent advances in genetic engineering, it is possible to label phages with a fluorescent marker, for example a green fluorescent protein (GFP). The use of a fluorescently labelled phage has been used to identify *E. coli* in sewage water in only a few hours [125]. An additional advantage to this system is the ability to regenerate the sensor simply by treating with 20 mM sodium hydroxide. This allows the sensor to be reused for multiple cycles. In addition, a phage will only "infect" a viable bacterium [126].

As bacteriophage only infect live cells, it is possible to detect the number of viable cells in a sample. Using electrochemical impedance spectroscopy, Mejri *et al.,* [124] captured *E. coli* using magnetic nanoparticles (MNPs). Immobilising the *E.coli* onto the sensor surface, using a goat polyclonal IgG antibody, T4 bacteriophage was injected. The impedimetric behaviour was recorded over a 15 minute period and a strong decrease in, and the absolute value for, the number of live bacteria was determined.

The availability of bacteriophage is broad, however there is a concern about the specificity of culture techniques and given the infancy of bacteriophage development, antibodies provide a well-tested alternative [85]. Bacteriophage provide an estimation of

the number of live bacteria, a secondary technique would be required to enumerate non-viable bacteria.

2.8.7. Summary

There are several potential targets on, or within bacteria, for a bacteria sensor to exploit. Aptamers can be designed specifically to the target required; they are inexpensive and reversible, and as such seem useful for sensor design. However, aptamers are not readily available. Bacteriophages allow for the determination of viable cells in a sample, unlike nucleic acid-based techniques which are, on the whole, non-specific to viable/non-viable cells. Antibodies are expensive and laborious to produce [127] but there are many commercially available antibodies for key bacterial species, including those mentioned in this thesis. Given the extensive research surrounding the use of antibodies to detect pathogenic bacteria, and their commercial availability, antibodies will be used as the basis of the species-specific sensor described in this thesis.

2.9. Sensing technologies

Biosensor technologies have emerged as powerful and versatile alternatives to culture-based techniques. Many of the shortcomings of traditional methods are overcome, primarily due to speed of analysis and simplicity of operation [128]. *"The function of a pathogenic biosensor is to transduce receptor recognition towards the target pathogen into a detectable signal"* [129]. Biosensors usually incorporate a biologically active layer as a recognition element. The bio-recognition event is translated by a transducer into a signal that is proportional to the analyte concentration [88].

The many variations of biosensors have been reviewed previously [128–133]. Very few sensors have been documented to detect below 10 CFU/ ml [17]. Those that do, tend to involve complex pre-enrichment steps [18]. This review will explore recent advances in microbial sensing and identify technologies which may be suited to the proposed biosensor.

2.9.1. Enzyme-linked immuno-sorbent assays

Enzyme-linked immuno-sorbent assays (ELISA) are often used to detect pathogenic bacteria [134]. The principle of an ELISA is the detection of an antibody-antigen interaction. Typically ELISAs are conducted in a 96 well plate; require substantial reagents, labour and precision. This ultimately makes the technique expensive. The reported detection limits are not sensitive enough (10^6 CFU/ ml) and there is a lengthy procedure between sample preparation to final analysis. As such, this technique will not be suitable for the biosensor proposed here [135].

2.9.2. Polymerase-chain reaction

Polymerase chain reaction (PCR) is an *in vitro* technique used to amplify enzymatically specific fragments of nucleic acids through a series of repetitive reaction cycles. Ultra-fast PCR methods can detect as low as 5 CFU in a single assay with a 20 minute

detection time. In contrast to the short detection time, the process is lengthy as several pre-treatment steps are required in order to establish suitably conditioned samples suitable for the extraction of target DNA [18]. Ultra-fast PCR has been reported to be able to detect as few as 1 CFU/ ml of *V. cholera*e in seawater samples; however, the enrichment step took four hours [41]. The technique also offers possibility for part-automation [136], but requires highly-trained users as the enrichment step is complex.

2.9.3. Optical sensors

The selectivity and sensitivity achievable by using optical biosensors has made this sensing technique amongst the most popular in bacterial sensing [24]. Light absorption is a physical parameter which can be used to observe eukaryotic cells. The size of bacteria, being close to the resolution of optical microscopes, make optical measurements more challenging [137]. Individual species are not identifiable by optical measurement alone. Optical sensors, in conjunction with additional techniques do allow for sensitive bacterial analysis, these are described here.

2.9.3.1. *Fluorescence-based techniques*

A direct and efficient method that does not require pre-enrichment of samples, is that of fluorescence labelling of cells [138]. For a molecule to emit fluorescence, it must absorb light at a wavelength shorter, or equal to, the wavelength of emitted light, raising an electron to a higher energy level, known as an excited state. Fluorescence occurs when some, or all, of the energy is lost via light emission from the electron [137]. Fluorescence emitted from cells can be detected by devices such as photodetectors and intensified cameras [79].

2.9.3.1.1. Organic fluorochromes

A significant number of biosensors report the detection of pathogenic bacteria using organic fluorochromes. Whilst organic fluorochromes are extremely useful in providing

detailed information on the physiological states of microorganisms, there are some inherent flaws in their use, for example, the poor photo-stability and low intensity fluorescence [17]. Use of fluorochromes in samples that are complex and unfiltered may result in fluorescent quenching [94]. Environmental samples may have organisms that have fluorescent properties such as algal cells containing phycoethyrin and chlorophyll. Furthermore, the presence of fluorescent background material may produce false positive and negatives results when used in an environmental biosensor.

2.9.3.2. *Flow cytometry*

"*Flow cytometry is the registration and measurement of optical phenomenon (fluorescence, scattering, absorption etc.) occurring when particles flow past a laser beam*" [139]. Flow cytometry offers fast and detailed analysis of cells and microorganisms. The presence of cells can be measured in real time by employing organic fluorochromes targeting biological components and structures. There is presently a lower size limit of detection of flow cytometers; being approximately the size of bacteria 1 µm. Analysis of environmental samples often provides a great deal of background noise and false positive and negative results.

2.9.3.3. *Time resolved fluorescence*

Time-resolved fluorescence (TRF) utilises chelate labels which produce intense fluorescence signals with a long half-life and a large Stokes's shift with narrow emission peak. Therefore, the chelate label can be read after the non-specific background noise has decayed [140]. This technique, coupled with immuno-labelled MPs, has been used to detect *E. coli* in apple cider (10 CFU/ ml), ground beef (1 CFU/ ml) and alfalfa (4 CFU/ ml) [141].

2.9.3.4. *Surface plasmon resonance*

Surface plasmon resonance (SPR) based sensors can be used to detect bacterial cells by direct detection, sandwich assay, or inhibition assay [80]. They have a rapid detection time [142]. SPR is an optical method that measures the refractive index of thin layers of a material on a metal surface [143]. SPR sensors have been developed for the measurement of antigens which bind to antibody molecules immobilised on the SPR sensor surface. SPR sensors are capable of detecting analytes in complex biological media with high specificity and sensitivity. Jyoung *et al.*, [39] describe the detection of *V. cholerae* O1 using SPR but the detection limits were between 10^5 and 10^9 CFU/ ml. Also using SPR, Oh *et al.*, [134] developed a sensor with a minimum detection limit of 10^2 CFU/ ml suitable to monitor *E. coli* O157:H7 in wastewater. However, it also proved difficult to stabilise the instrument for a period of more than eight weeks.

2.9.3.5. *Optical waveguides*

Planar surfaces offer the possibility of creating patterns of immobilised capture molecules on the surface of the waveguide allowing a single surface to be used in screening of multiple samples and multiple target analytes [144]. The use of an evanescent wave to provide a real-time assessment of a binding assay has been reported [145, 146]. The planar waveguide has an evanescent field which extends above and below the waveguide. When a target adsorbs to the sensor surface, the evanescent field is perturbed allowing optical detection. The US Naval Research Laboratory use a fully portable planar based biosensor (RAPTOR) to simultaneously detect bacterial cells and toxins on a single surface [147] with an assay time of between 10 and 15 minutes [145]. A complex optical system is required making development expensive and difficult to manufacture. Due to the large size of bacteria compared to viruses, for example, the evanescent field only penetrates the bacterial structure to a small degree. It is suggested

that the evanescent field needs to be enhanced to increase the sensitivity and selectivity of the technique for use in detecting bacteria [148].

2.9.4. Interferometric

Several sensors have been reported which utilise waveguides as their sensing technique. There are two commonly used interferometric sensors: the Mach Zehnder and Young designs [149]. Briefly, a light source is coupled to an optical channel waveguide, the light is guided parallel along the optical channels of the sensor and is emitted forming two cones at the end of the planar device. The cones superimpose and form characteristic interference "fringes" [150]. Small displacements in the waves that travel along the waveguide are measured [151]. Bio-recognition molecules with binding sites are immobilised onto a sensing surface, the sample passes over the surface and the target is bound [152]. The binding causes light to be refracted and this change is detectable by the lateral movement of the fringe pattern [15]. The nature of optical chips that incorporate waveguides permits the analysis of a number of analytes in parallel. Different analytes may be utilised in separate channels, the number of channels incorporated on chip will determine the number of analytes for analysis. In addition, if multiple wavelengths are used to probe a change in the refractive index, at different distances from the sensor surface, a sensor may discriminate particles of different size as described by [153]. Interferometric sensors can be affected by background interference due to background binding or auto-fluorescent molecules. They are generally better suited to nanometre-sized targets due to the limited penetration depth of the evanescent field.

2.9.4.1. *Fibre optics*

The use of fibre optics in biosensing offers several advantages; they are electrically isolated and are immune to electro-magnetic interference. Fibre optics can have a high degree of sensitivity, are lightweight, compact and biocompatible [154]. The difficulty in

using fibre optics is the precision in which the alignment of the fibre that is required [155].

2.9.5. Electrochemical

In electrochemical sensing, the cell membrane functions as the capacitor whilst the suspending medium acts as the resistance element [24]. A capture probe, such as a nucleic acid sequence, is anchored to a sensor surface. The target is captured onto the sensor surface; the detector probe recognises the target. Electrochemical sensors can be sensitive enough to directly sense nucleic acid hybridisation, this removes the requirement for nucleic acid amplification, as in PCR, and therefore reduces the problems associated with deploying this additional technique [93]. The different types of electrochemical sensors are described here.

2.9.5.1. *Impedance*

Impedance measurements are of the resistance, capacitance and/or inductance of a sample and are obtained by the use of electrodes suspended in a sample [156]. When an alternating, sinusoidal current is applied, the impedance (Z) of a system is a function of its resistance (R_S), capacitance (C_d) and the applied frequency (f) as shown in equation 2.1 [156].

$$|Z| = \sqrt{R_s^2 + \left(\frac{1}{\pi f C_d}\right)^2} \tag{2.1}$$

The bacterial cell membrane is highly insulating, presenting a conductivity of 10^{-7} S/m, whereas the inside of the cell, containing *inter alia*: DNA, nutrient storage granules, ribosomes and many more dissolved charged molecules, is more conductive (1 S/m) [157]. When cells are exposed to alternating electric fields within the range of radiofrequencies, interfacial polarisation across the cell membrane causes cells to become polarised [158]. At low frequencies, there is more time for ions to encounter the

cell membrane, thus polarising the cell. At higher frequencies, the change in electric field direction is so rapid that only a few ions have time to reach the cell membrane, making the contribution to capacitance negligible [159]. The frequency used in impedance measurements is therefore important. At low frequencies, cells are polarisable, the cell membrane acts as an insulator and the cells therefore store charge, acting as small capacitors [160]. At high frequencies the charge passes through the cells, the cells are more conductive [161].

2.9.5.1.1. *Multi-frequency Impedance Spectroscopy*

Multi-frequency electrical impedance spectroscopy measures the bulk capacitance of a suspension at different frequencies. The change in the bulk capacitance of a cell suspension changes with frequency, which is proportional to the number of membrane-enclosed cells present [162]. The range of frequencies within which cells lose their polarisabilities between about 0.5 and 3MHz and is termed the β-dispersion [163]. The Biomass Monitor (Aber-Instruments, Aberystwyth, UK) is a commercially available instrument that utilises this technique.

2.9.5.1.2. *Impedance Biosensors*

A change in impedance can also be observed when cells adhere to the surface of the electrodes, causing a reduction in the surface area, increasing the impedance across the electrodes, as interfacial capacitance [164]. Antibodies may be used in conjunction with an impedance biosensor to enable species selectivity and improve adherence of the cells. The number of bacteria present is directly proportional to an increase in impedance [165]. In a two electrode impedance system, the reference electrode also works as a counter electrode. The use of multiple electrode systems enables better reproducibility by using a reference electrode, a counter electrode and a working electrode [166]. Microfabrication has enabled the development of microelectrode array impedance

detection systems [156]. Furthermore, incorporating impedance measurements with microfluidics enables a non-invasive and label-free device with the potential to monitor single-cells.

2.9.5.1.3. Impedance Microbiology

Impedance microbiology is a common approach that enables bacterial growth to be monitored. When bacteria are cultured in a nutrient medium, the medium will change in composition as the nutrients are used up and metabolic end products are produced. As this occurs, the resistance to the flow of the current passing through the medium will change, and is therefore measureable [167]. The detectable range of impedance-microbiology measurements is usually between ~10^4 and 10^8 cells/ ml [168] and is therefore not sensitive enough to be used in the proposed sensor.

2.9.5.2. *Amperometric*

Amperometric methods measure the current across a sample. The amperometric detection of *E. coli* cells was described by Laczka and *et al*., [169] by first coupling the bacteria to MPs using immuno-labelling and trapping the cells downstream of a gold micro-band electrode; the lower limit of detection was 55 cells/ ml with a detection range of 10^2 to 10^8 cells/ ml. Whilst this biosensor can detect bacteria in milk, there is no current means of determining the physiological state of the bacteria that are captured.

2.9.5.3. *Potentiometric*

Potentiometry is a simple method to measure the voltage of a sample, that is portable and suitable to environmental sensing [170]. An aptasensor, using potentiometric measurements, has recently been described that can selectively detect 1 CFU/ ml of *Staphylococcus aureus* in only 1 to 2 minutes [171] and which is reversible, given the nature of the utilised aptamers. A potentiometric biosensor coupled with carbon nanotubes (CNT) was described that provided data close to real-time, with an immediate

response ranging from 0.2 to 10^6 CFU/ ml [18], however the precision required for the use of CNTs does not lend itself to field-based activities.

2.9.6. Quartz crystal microbalance

A quartz crystal microbalance (QCM) is composed of a quartz crystal detector that is used as a transducer. A piezoelectric standing wave is used to oscillate the surface. A metal coated plate is layered with self-assembled carboxyl-terminated alkanethiol and an antibody is attached to this coating. A detection limit of 10^3 to 10^7 CFU/ ml of the fish pathogen *Vibrio harveyi* was reported using a 5MHz QCM [172]. Increasing the voltage and hence amplitude of the oscillation of a QCM causes the rupturing of the bonds attaching bacteria to the surface resulting in a detectable acoustic noise. The quantitation of bacteria using this method is termed rupture event scanning [173] and is quantitative over a range of six orders of magnitude and with as few as 20-30 bacteria; greatly improving the sensitivity of standard QCM methods. Immuno-labelling of gold nanoparticles as enhancers and amplifiers of the signal enabled the detection of *E. coli* at the single cell level. The process was completed in 24 hours, which is a limitation of this technique [174]. The detection limits of QCM are promising and recent advances indicate single cell detection of bacteria. The methods are presently only suitable to batch processes; further advances need to be made before this technique can be incorporated into a continuous sensing system.

2.9.7. Vibrational spectroscopy

Fourier Transform Infrared Spectroscopy (FTIR) and Raman spectroscopy (RS) techniques are based upon vibrational energy levels of chemical bonds [175]. Vibrational spectroscopy is a powerful tool for bacterial analysis. It enables the mapping of a bacterium with such detail that a “fingerprint” can be established [176] which is unique to each species, and potentially each strain.

2.9.7.1. *Fourier transform infrared spectroscopy (FTIR)*

Veiseh *et al.,* [177] combined a microarray of a single macrophage cell with FTIR spectro-microscopy. The infrared shift of the macrophage cell was observed when exposed to LPS (a major component of gram negative bacterial cell walls [178]). The spectrum shift as observed by FTIR was dependent upon time, several hours allowed for a clear shift.

2.9.7.2. *Raman spectroscopy*

RS is a spectroscopic technique which is used to study the vibrational, rotational and other low frequency modes in a system [179]. A major advantage of RS is the ability to analyse specimens without fixation or being sectioned. Vibrational spectroscopic techniques provides specific chemical information about the bio-analyte and is a potential detection technique for species identification [180] and a viability assessment. Water molecules have small Raman scattering and RS is suited to applications in an aqueous medium [181]. The weakness of the inelastic scattering (~1 in 10^8 incident photons) results in analysis time taking several minutes and is a potential drawback of this method [176]. Surface enhanced RS (SERS) can overcome this to some degree. The enhanced signal is due to the local optical fields from resonance of the applied field with surface plasmon oscillation of metallic nanostructures [181, 182]. The use of expensive metal colloids is required, e.g. silver and gold nanoparticles, which also have a toxic effect upon microorganisms. In addition, due to the polishing preparation between measurements, there is irreproducibility of SERS intensity and irreproducibility of Raman spectrum at the single cell level [183, 184].

2.9.8. Magnetic

A magnetic field may be used to collect samples with magnetic properties. The introduction of functionalised-MPs, that capture target organisms, can be manoeuvred by

a magnet field. Environmental samples generally do not contain much in the way of magnetic materials. As such, background signals are low, and noise interference of measurements is minimal [17]. There are two types of magnetic-microfluidic separation devices: batch and continuous [185].

2.9.8.1. *Batch magnetic separations*

Batch separation involves the trapping of MPs by an external magnet, the removal of the supernatant and the removal of the trapped particles, once the magnetic field has been removed. Miltenyi Biotech (Bergisch Gladbach, Germany) produces a wide variety of magnetic-activated cell sorting columns and MPs (Figure 2.3). The Miltenyi system utilises functionalised MPs, coated in antibodies, to capture cells by binding to the corresponding antigenic site. The sample and the MPs, is passed through a separation column, with an internal separation matrix that is magnetised by an external permanent magnet. The unbound cells pass through the column and internal matrix freely. Bound MP-cell complexes are captured in the magnetised-matrix of the separation column. Removal of the external magnetic field will enable the flushing of the column and removal of the MP-cell complexes for further analysis [186]. A batch method was described by Beyor *et al*., that had a detection limit of 2 CFU/ µl and the separation of *E. coli* from a mixed population with *S. aureus*; the reported capture efficiency is approximately 70% [187]. A limitation of batch magnetic separations is the restricted volume that can be used in one separation. Processing of large volumes would be time-consuming due to the saturation of the separation surface and subsequent flushing requirements.

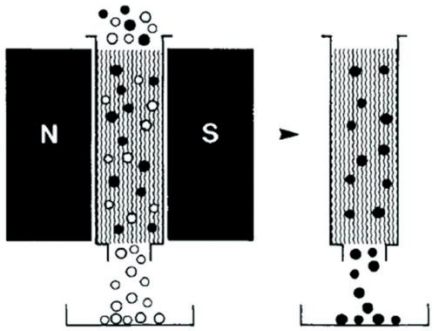

Figure 2.3. A schematic of the Miltenyi batch magnetic separation device. The magnetic particles are trapped in the separation matrix when it is magnetised by two external permanent magnets. The magnets are later removed which enables separation of the magnetic particles [188].

Electromagnets have the ability to be switched into active and inactive mode and with an adjustable magnetic field which can exceed 1 Tesla [189] and offer a versatility in design. However, electromagnets are bulky and an expensive method for magnetic separation of samples. Permanent magnets, although providing a weaker magnetic field are easy to use and provide an immediate magnetic field and are often preferred when designing a magnetic separation device [190]. Rotating permanent magnets have been described that allow the control of the magnetic field from on to off. The removal of the magnetic field in this manner allows cleaning and flushing of the magnetisable collection matrix from semi-continuous flows. An advantage to this device is enabling the flexibility to the separation as an electromagnet would, but without the additional costs and bulky electromagnets [190]. The semi-continuous approach to separating magnetic material from non-magnetic material and has been described by other authors [191] in more complex systems that incorporate automation of sampling filling, flushing and collection.

2.9.8.2. *Continuous magnetic separations*

Continuous magnetic separations of micrometer-sized particles are achievable when used in combination with fluidic devices. In clinical settings, continuous separation of red and white blood cells has been demonstrated with a 94% and 89% efficiency of separating

red and white blood cells, respectively. A lateral flow magnetic separation was achieved using a ferromagnetic wire array in a glass chip, separating the red blood cells using their inherent magnetic properties [192].

Magnetic split-flow fractionation has been described [193] and can be seen in Figure 2.4. A two inlet and two outlet device is used to direct the flow of a sample stream and a buffer stream around two 90 degree turns in a fluidic device. The centre of the device directs the two streams to merge to allow for the separation of non-magnetic material into the outer stream flow. This technique was successful at separating 94% of magnetic material from non-magnetic material, after two passes of the magnet.

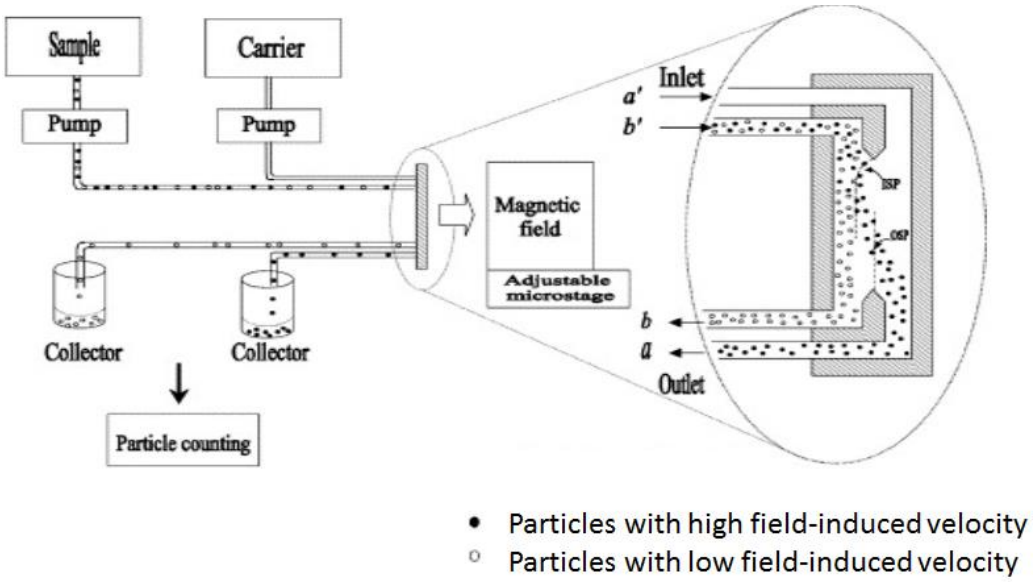

Figure 2.4. Magnetic split flow fractionation of magnetic material from non-magnetic material [193]

Obtaining a high gradient magnetic field that enables the deflection of magnetic material into a separation flow, from continuous flow is difficult given the limited strength of permanent magnets. To overcome this, multiple magnets may be used [194] in a quadrupole configuration displayed in Figure 2.5. A sample flow and sheath flow are introduced to the device using hydrodynamic focussing; the magnetic material is deflected from the inner sample flow, to the outer flow and separated by use of two

channels after the magnets. High flow rates (4 ml /s) were used enabling large sample volumes to be separated.

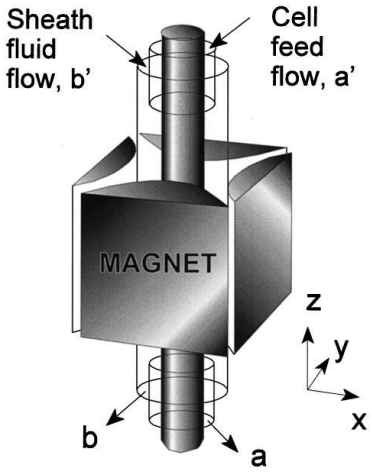

Figure 2.5. A schematic of the quadrupole flow sorter with arrows to describe the direction of the flows [194]

Using an axial rotating glass tube and computerised-electromagnets, separation of magnetic material from non-magnetic was achieved without use of a buffer flow by alternating the on-off mode of the electromagnets. The on-off cycle deflected magnetic material into a different region of the sample flow than the non-magnetic material; a 60% separation was achieved per phase switch [195]. A microfluidic device using rotation of permanent magnets has also been described [196]. The sample with functionalised MPs to capture waterborne pathogens is passed through a microfluidic device. External permanent magnets rotate, trapping MPs at various positions along the microfluidic device. Whilst the magnets are engaged, non-magnetic material flows through the device. After several trapping cycles, it is hypothesised that all non-magnetic material has exited the device and only MPs remain (Figure 2.6).

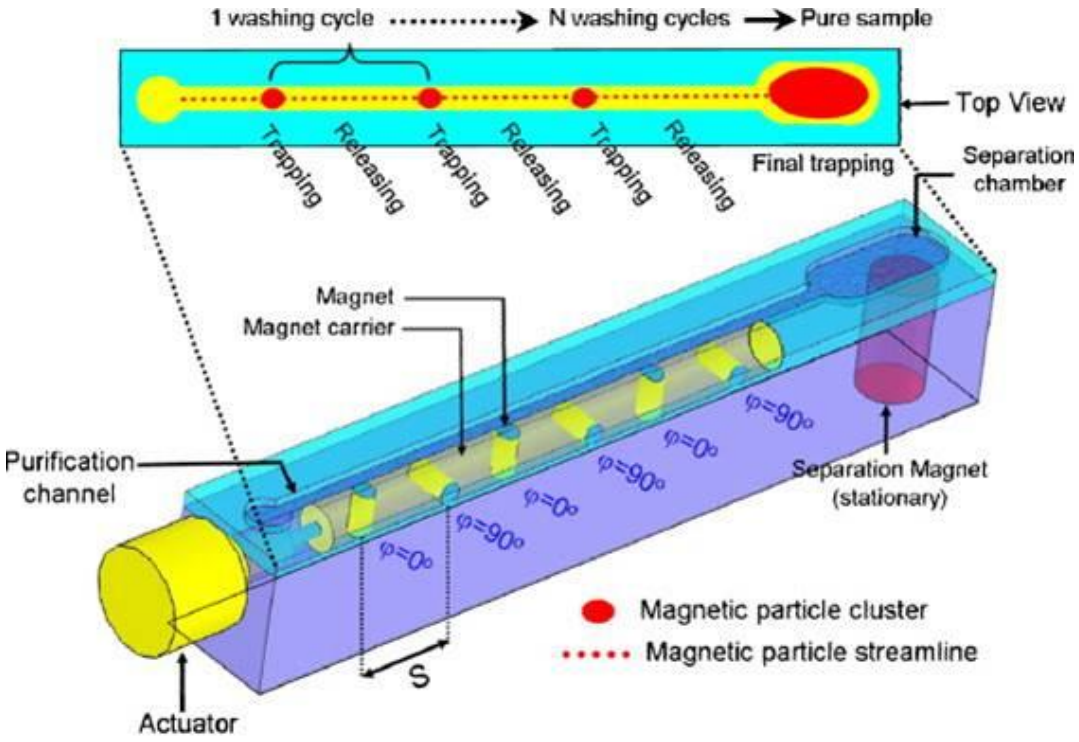

Figure 2.6. A schematic of the continuous and periodical trapping and releasing of the magnetic particles through the channel creates a path-phase shift between the magnetic and non-magnetic particles. Finally, the purified sample is collected in the collection reservoir using a stationary permanent magnet [196]

On-chip magnetic separation incorporating microfluidics has been demonstrated that enable the separation of magnetic material with differing magnetic mobilities [197]. A permanent magnetic is placed above the microfluidic chip, a sample flow is introduced in a channel furthest from the magnet, as the flow passes through the chip, magnetic material is deflected towards the magnet, with the particles with highest magnetic moments travelling the furthest along the magnetic gradient (Figure 2.7).

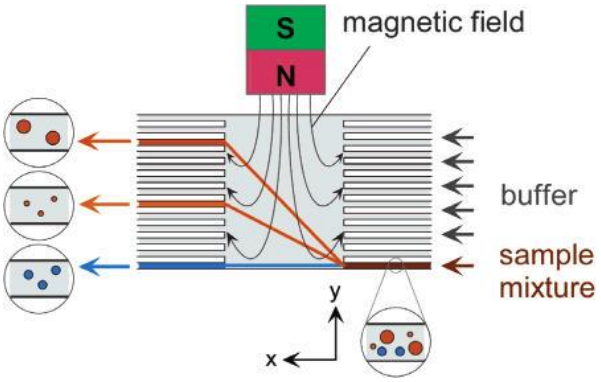

Figure 2.7. A schematic of on-chip magnetophoresis for continuous separation of magnetic particles with different magnetic mobilities [197]

2.9.8.3. *Giant magneto-resistive sensors*

Giant magneto-resistive (GMR) sensors are paradoxically small and easily incorporated with other technologies e.g. microfluidics. In conjunction with immuno-labelled MPs, GMR sensors offer high sensitivity sensing devices. Briefly, a coil at the base of the sensor is magnetised, MPs are pulled down by the external magnetic force (which may be a permanent- or an electro-magnet) onto the antibody-labelled sensing surface. Those MPs carrying the target organism become immobilised, creating a sandwich assay. Unbound MPs may be removed using a secondary magnet or via washing. Bound particles "*perturb the magnetic field of a resonant coil detector*" [198]. Cyclic voltammetry is conducted before and after a sample has passed through a sensor. The difference in this measurement can be correlated with the number of organisms in a sample [124]. The sensitivity of the device is dependent upon many features. The magnetic flux decreases rapidly with distance from the magnet surface [199]; the sensor surface must be carefully designed in order to maximise the magnetic attraction upon the MPs.

2.9.9. Summary

Due to their sensitivity and selectivity, optical and electrochemical based sensors are the most popular sensors used to detect pathogens [23]. Interferometric sensors allow the immobilisation of several different capture molecules onto a planar surface, allowing for the screening of multiple target analytes [200]. However, evanescent field-based sensors suffer from the field which is limited to approximately 110 nm above and below the waveguide. Due to the larger size of bacteria (1 μm) the evanescent field minimally penetrates the cell structure which limits the LOD [201]. RS is a highly powerful technology and should be explored further. As water molecules exhibit small Raman scattering, this technique has been shown to work well in an aqueous medium [181]. Raman technologies are not as yet broadly available; magnetic and fluorescence-based

technologies are and, as such, will be used in this project.

2.10. Capture mechanisms and cell labelling

There are a number of methods for capturing target bacteria from a sample. The different technologies available for cell labelling and capture are described within this section.

2.10.1. Nanotechnologies

The use of nanoparticles (NPs) as labels in conjunction with novel detection technologies has led to improvements in sensitivity and to multiplexing sensing systems. Many technological advances have focused on the development of nano-structured biosensors to enhance surface-to-volume ratios and reduce cross section, thus enabling a more effective bio-target immobilisation onto the nanostructure [202]. The localised surface-plasmon resonance (SPR) of metal NPs is characterised by the presence of intense adsorption and scattering peaks, which greatly improves the sensitivity of biosensors that incorporate this technology [203].

NPs have many favourable attributes for microorganism detection; they have a large surface area to volume ratio and compositional-dependent properties such as fluorescence and magnetism [204]. A micro-fabricated device coupled with NPs was reported as being 100,000 times more specific and 10 times more sensitive for DNA detection than modern genomic detection systems [205], although genome analysis has greatly advanced in sensitivity since Devadhasan's study. NPs offer signal enhancement to traditional optical and electrochemical transductions which enables the ultrasensitive detection of microorganisms [17]. Some of the most commonly reported nano-structures are discussed here.

2.10.1.1. *Carbon-nanotubes*

The exceptional properties of carbon-nanotubes (CNT) include: small size, great strength and high electrical and thermal conductivity [17]. These offer substantial improvements

as electrochemical transducers compared to traditional electrodes. An aptamer-based, highly selective *Salmonella* Typhi potentiometric biosensor was reported by Zelada-Guilén *et al*., that can detect a single CFU, without cross-reaction with any other types of bacteria [18]. Whilst CNT offer an extremely sensitive method for the detection of bacteria, it is reported that CNT have a toxic effect upon bacteria (dependent upon the CNT structure) [206]. As such, CNT use in a biosensor which determines the physiological state of the microorganism, in addition to total number, may produce false-negative results with regard to viability.

2.10.1.2. *Gold nanoparticles*

Gold-NPs and fluorescent polymer constructs have been used for the fluorescent identification of microorganisms without the need for antibodies [207]. Using thiolated lactose derivatives and gold-NPs, researchers were able to detect the cholera toxin using a spectrophotometer to detect the change in colour of the NP suspension [122]. However, gold-NPs are an expensive means of targeting bacteria and more cost-effective technologies are required.

2.10.1.3. *Quantum dots*

Luminescent semiconductor nanocrystals, also known as quantum dots (QDs), are ideal labels for use in detecting multiple binding events [208]. Traditionally QDs are chalcogenides (selenides or sulphides) of metals such as cadmium or zinc which range from 2 to 10 nm in diameter [209]. QDs have size-dependent fluorescence with a narrow-bandwidth [208]. This fluorescence is stabilised by the presence of an outer shell e.g. zinc sulphide, which provides photo-stable properties [210] above that of organic dyes [211].

A flow-through system using antibody-coated QDs to detect *E. coli* O157:H7 in 20 minutes with a LOD of 2.3 CFU/ ml [212] has been reported. This demonstrates the

potential that QDs have for use in sensing techniques. However, little has been published so far on this topic [17].

QDs are potentially toxic to bacteria given their nanoscale properties and chemical composition [213]. The concentration of QDs used has been reported to have inhibitory effects upon the growth of *E. coli* cells [214]. The use of QDs as a detection system in a biosensor should be carefully considered in terms of size and material in order to avoid the occurrence of false-negative readings. In addition, given the structure of bacteria, the cell membrane prevents macromolecules entering the cell. The QD label must attach to the cell via immuno-labelling, or enter the cell after it has been permeabilised [58]. There is no direct method of determining cellular pathways or mechanisms with quantum dots; QDs will therefore have limited use in viability studies.

2.10.2. Microparticles

Colloidal microparticle suspensions provide a binding mechanism that is mobile, easily dispersed throughout a sample, with a large surface area for binding a target organism, resulting in highly efficient capture [215].

2.10.2.1. *Magnetic particles*

Magnetic particles (MPs) can be coated with capture molecules specific for desired targets [216]. In a batch, sandwich assay, utilizing MPs and immuno-labelling, a sensor surface is coated with an antibody. The sample flows through; target antigens bind to the antibody sites. When exposed to a heterogeneous sample, the MPs attach to the surface of desired cells via antibody–antigen interaction [217] creating a sandwich assay. An external magnetic field is applied and the response can be measured [109].

Recent molecular advances now enable aptamers to be immobilized onto an MP [218] which could provide a more versatile technology. The use of MPs allows for the detection of microorganisms in complex media with high throughput and a LOD of 10^3

CFU/ ml using magnetic NPs [124] and as low as 15.5 to 38.75 CFU/ ml [219]. Tu *et al*., [141] describe a streptavidin-coated, immuno-magnetic bead assay to detect *E. coli* O157:H7 with the associated cost being just 0.50 USD/ assay. Immuno-labelling of MPs was used in conjunction with a magneto-resistive sensor, to detect *E. coli* O157:H7 at a concentration of 10 CFU/ ml in a handheld microfluidics (MFD) [109]. Although promising, there is still a need to improve the capture efficiency of MPs, and although low limits of detection and short assay times are reported (less than two hours), capture efficiencies can range between 40% and 90% of target cells [182, 196, 220, 221].

The growth and replication of a single bacterium was monitored through the attachment of a single bacterial cell to an immuno-MP of 2.8 µm. Using a rotating asynchronous magnetic field, the bead rotated with the field and the growth was recorded [222]. This method is a powerful means of observing bacteria at the single cell level and controlling the position of the bacteria within a viewing location.

2.10.3. Liposomes

Liposomes are synthetic structures composed of a phospholipid bilayer. The first form of liposome was reported in 1978 by Day and Ringsford [223]. Diacetylenes, consisting of a long-chain alkane hydrophobic end and a hydrophilic end would self-assemble at the water-gas interface to form polymerisable monolayers. The hydrophilic end; a carboxylic group could be linked to a guest substrate or "lectin". Assembling the diacetylenes into vesicles and photopolymerising the structures, liposomes were formed [224]. Fluorochromes can be encapsulated to act as signal amplifiers [225] and detection of a target is reported via a change in colour of the liposome. The use of liposomes as colorimetric indicators in biosensor applications has been reported for the detection of the influenza virus [226] and bacteria [227]. Detection ranges were in the order of of 6×10^3 to 6×10^7 cells, and the total assay time was less than 45 minutes [13]. The electrochemical detection of haemolytic bacteria was reported by Kim *et al.,* [228].

When a redox-active bacterium comes into contact with the liposome, an entrapped mediator is released by the breakdown of the liposome bilayer, allowing for electrochemical detection. A drawback of using liposomes is that the breakdown can be triggered by a number of physical conditions (such as pH and mechanical agitation), and not only by the presence of the target molecule [224].

2.10.4. Summary

The ready availability of commercially produced MPs and QDs, their reported low LODs, and their low associated costs, make the use of micro- and nanoparticles an attractive technology for cost-effectively targeting and sensing pathogenic bacteria. However, the potential toxicity of QDs needs to be investigated further before pursuing their use within a bacterial sensor. Given this finding, MPs are the preferred choice, and will be used as the basis of the proposed bacterial sensor.

2.11. Separation strategies

The identification of viable bacteria from DW will involve several stages. The preliminary step will be to extract the organisms of interest from a heterogeneous sample. Physical isolation methods, including centrifugation and filtration, are unsuitable due to their high power demands and are time-consuming. In addition it has been reported that physical damage may be caused to intact-viable cells by these techniques [229]. Potential separation techniques will be discussed in the following section.

2.11.1. Microfluidics

MFDs offer a high throughput of samples, are cheap to fabricate and allow versatility when being designed [121]. The micro-scale geometry of MFDs ensures fluid flow is laminar compared to that of macro-scale devices [230]. This allows for predictable and repeatable cell movements [217]. Microfluidic systems are able to conduct measurements with efficiency and speed from small volumes of complex fluids; they can

be engineered such that they do not require skilled users [23]. The nature of microfluidics allows the incorporation of micro-fabricated structures, magnetophoresis or dielectrophoresis, within the chip to enable concentration [129] or sorting of a sample. Inclusion of a resistive pulse sensor in an MFD would allow for individual cells to be counted [231], which would be a useful attribute.

Microfluidics also offer the ability to run multiple channels in parallel. Such an approach can increase sample throughput and monitor samples for a number of target molecules, without compromising purity and efficiency [217]. A drawback of using narrow channels in microfluidics is the tendency for particles to clog the channels and for pressure drops across the device [232], as such careful design of the geometry is necessary.

2.11.2. Ultrasonic separation

The generation of nodal planes by ultrasonic standing waves can be used to collect and separate micron-sized particles. Cells within an ultrasonic standing wave will typically be driven to pressure nodal planes within the standing wave [233]. Cells agglomerate, depending on their density, at either the node or the anti-node; the primary force on a particle is proportional to the ultrasonic frequency.

Acoustic radiation forces have been used for non-intrusive manipulation of microscopic objects [234] and for harvesting microalgae and bacteria on a large scale [235]. An ultrasonic standing wave may be used to move cells in a solution into the standing wave where the cells amalgamate at the nodal planes [236]. Incorporating microfluidics, balancing the flow rate, and acoustic force, particles can be organised to travel along a fluid channel through acoustophoresis as described by Petersson *et al.,* [237]. This collection of cells can then be directed to exit into a sampling chamber [238].

Acoustophoresis requires high powered devices with high frequencies (1MHz) in order to avoid cavitation and consequent damage to bacterial cells [235]. A primary

requirement for the proposed sensor is that cost is minimal and therefore this technique is not considered to be appropriate.

2.11.3. Separation by size

MFDs may be designed to separate a heterogeneous sample into groups as a function of the size of the particle. An input channel will guide the sample into a matrix of channels of decreasing size or with obstacles of varying sizes [217, 239]. Particles with dimensions smaller than the width of the obstructions will pass through. Particles of a size larger than the obstruction will collide with the obstruction and will be displaced in a direction towards wider channels by an additional flow [217]. Size-based cell sorting enables the capture of target cells without any attachment to the cell surface which is advantageous for the study of the cells after separation. However, to achieve this, the target cells must be significantly different in size from the rest of their surroundings [240], which is not the case for bacteria.

2.11.4. Separation using dispersed bubbles

The nature of suspended solids in seawater are of hydrophilic molecules [241]. In order to remove bacteria from seawater, rather than suspended matter, a technique using bubbling has been reported [242]. The hydrophilic nature of suspended solids means they tend not to stick to bubbles. Bacteria, however, with surface active substances such as polysaccharides and proteins and with the addition of a cationic surfactant, adsorb onto bubbles when foam is generated. Proteins and polysaccharides appear to change the interface of solids from hydrophilic to hydrophobic. The bacteria attach to the bubbles and rise to the surface of the water where they can be removed. A continuous flow through system has been described where as much as 86% of the bacterial community of seawater was removed in this manner [243].

Dissolved air flotation (DAF) as a method for DW treatment has also been described [244]. To achieve DAF of flocculants in DW, divalent cations (e.g. Ca^{2+} and Mg^{2+}) are required and added in an optimised manner that is dependent upon the water constituents [245]. The flocculation process will bind the bacteria in large masses, and although separation from the main waterbody can be achieved, the flocculants would then need to be broken up in order to detect individual bacterial cells, adding an unnecessary additional process when compared to other separation techniques.

2.11.5. Gradient separation

The use of different types of gradients to separate particles of different size, shape and charge has been widely reported. Gravitational, hydro-, electro- and magneto-phoresis will be discussed further. Further examples of gradient separations including diffusion, which are not described in detail in this work, can be found [246].

2.11.5.1. *Gravity*

Incorporating gravitational pull and microfluidics, Huh *et al.,* [247] designed a device that operated perpendicular to gravity. Using sedimentation velocities, particles of different sizes were separated into two collection chambers. The use of gravity greatly simplifies the system and minimises the volume/ power requirements.

2.11.5.2. *Hydrophoresis*

Hydrophoresis is the movement of suspended particles under the influence of a micro-structure induced pressure field which enables a flow-rate independent separation [248]. Many techniques offer continuous flow separation e.g. field-flow fractionation [249], pinched flow-fractionation [250] and size-exclusion chromatography [251]. Existing separation technologies have a high power demand [247].

2.11.5.3. *Electrophoresis and dielectrophoresis*

Electrophoresis is the term used to describe the motion of charged particles arising from an electrostatic force within an electric field [252, 253]. In electrophoresis, an analyte has a constant migration velocity which is a result of the balance between the hydrodynamic drag and the driving force exerted upon the particle from the applied potential difference [254]. Electrophoresis is different from dielectrophoresis which describes the translational motion of non-charged dielectrically polarised particles in a non-uniform electric field [255]. Dielectrophoresis is an electrokinetic method that allows the intrinsic dielectric properties of suspended cells to be exploited for separation [256]. When an external electric field is applied, there is a lowering of the internal electric-field energy density within a cell. The cell will experience a force in the direction of the steepest gradient in energy density, to reduce the overall energy in the system [257]. The electrical properties of a cell must be different to the suspending solution in order for a dielectric force to be induced [258].

2.11.5.4. *Electrophoresis*

The use of gels in electrophoresis, act as a molecular sieve for the macromolecular analytes, restricting their diffusion along the electrolyte buffer [254]. Denaturing gradient gel-electrophoresis has been extensively used in the study of microbial populations e.g. [259]. Used in conjunction with PCR, an increasing amount of denaturing chemicals is used to unwind DNA molecules. DNA is negatively charged and is attracted by positive electrodes. The DNA is forced to migrate through the pores of the gel. The hydrogen bonds between the base pairs are broken down by the increasing chemical gradient. The variation in the DNA sequence results in different sequences migrating different distances, providing the ability to determine between species of bacteria and to detect mutations [260]. However, the technique suffers from irreproducibility in analyte migration times and low detection sensitivity [261].

2.11.5.4.1. *Capillary Electrophoresis*

The use of electrophoresis with capillaries, to separate whole cells, has been widely reported and extensive reviews may be found [262, 263]. As an example, acospores and diploid cells of the yeast *Saccharomyces cerevisae* were successfully separated using electrophoresis with such purity that the acospores could be used in genetic analysis [264]. Capillary zone electrophoresis has been demonstrated successfully to separate mixtures of five species of bacteria: *Enterococcus faecalis, Streptococcus pyogenes, Streptococcus agalactiae, Streptococcus pneumoniae*, and *Staphylococcus aureus* into discrete regions [265]. As such, electrophoresis is a powerful tool for separating heterogeneous populations of micro-organisms.

2.11.5.4.1.1. Particle charge

In an electric field, charged particles experience a motion dependent upon the particles' net charge. Aqueous solutions contain positive and negative ions (cations and anions respectively). The adsorption of ions onto the particle surface is caused by the partial charge of a particles surface, termed the "stern layer."

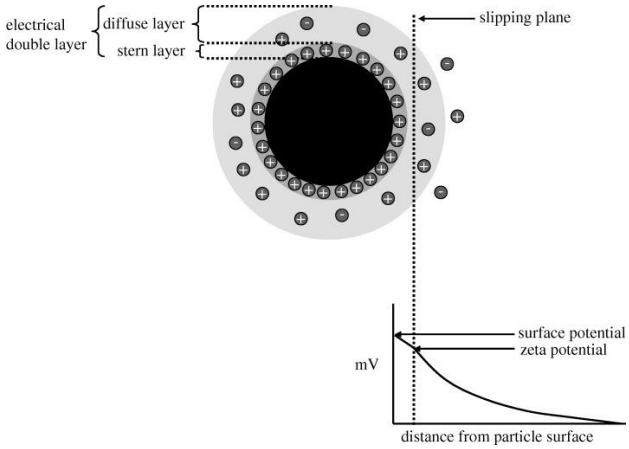

Figure 2.8. A schematic displaying the electrical double layer that surrounds a particle in an aqueous medium, the zeta potential is the electrical potential measured at the slipping plane [266]

The absorption results in the "net charge" of the particle. Counter-ions surround this layer in a cloud formation and extend from the surface into the solution, termed the

"diffuse layer" [267]. The zeta potential is defined as the electrostatic potential at the colloidal surface, or the slipping plane as displayed in Figure 2.8. The zeta potential provides an estimate of the magnitude of the electric field between particles that results from the combined effect of ionized charged groups on the particle surface, counter-ions released into the surrounding solution and salt ions [268]

2.11.5.1. *Dielectrophoresis*

In contrast to electrophoresis, where the electrophoretic force is linearly proportional to the applied field, dielectrophoresis refers to the effect of an electric field gradient on a polarisable particle [269]. "*The motion of suspensoid particles relative to that of the solvent resulting from polarisation forces produced by an inhomogeneous electric field*" as first described by Pohl [270]. The dielectrophoretic force acting upon a particle is dependent upon the magnitude and non-uniformity of an externally applied electric field. The physical and electrical properties of the surrounding medium, conductivity and permeability, and the particle radius also influence this force [271]. The movement of a dielectric particle can be a propulsive force towards a region of high field strength when the particles are more polarisable than the media (positive dielectrophoresis). When the particles are less polarisable than the media, a movement towards a region of low field strength is witnessed (negative dielectrophoresis) [271, 272]. The use of direct current (DC) in conventional dielectrophoretic applications enables the separation of particles through their migration to the electrode with the opposite charge. This technique has been demonstrated to separate successfully symmetrical particles [272] such as beads, viruses and bacteria. A large voltage is required in DC-dielectrophoresis which is costly in device fabrication and also causes joule heating within the device. When used in biological applications this can cause denaturing and deactivation of the biological matter [273]. In addition, the heating causes electro-thermal gradients to develop within

the device which can counteract the direct motion of the particles, decreasing device performance [273].

An alternative to DC is to use alternating current (AC) in dielectrophoretic applications. The use of AC permits high field strength without water electrolysis and development of electrothermal and thermal-osmotic gradients [272]. Flexibility in experiment design can be achieved by changing the wave shape, phase, symmetry and the magnitude and frequency. AC dielectrophoresis has proved an important mechanisms for trapping particles [274].

Dielectrophoretic methods have been reported to be capable of distinguishing between physiological states. Bacteria in different physiological states may have distinct morphological features including differences in cell size, structure of cell walls and permeability [66]. These characteristics can lead to a change in cell electrical polarisabilities and hence particle conductivity [66]. Li & Bashir [275] describe the dielectrophoretic separation of live and dead *Listeria innocua* with 90% efficiency.

Dielectrophoretic concentrations of biomarkers can be actuated in short sample times; a toxin immuno-sandwich concentration assay was described incorporating microfluidics that produced results in only five minutes [276] with detection limits as low as 0.1 pg/ml. A major drawback of micro-scale dielectrophoretic methods is the bubble formation caused by the internal electrodes. Bubbles can distort both the fluid stream and the electric field, disrupting separation trajectories [277]. In addition, the separations must be conducted on samples with low cell numbers and in a non-complex matrix.

2.11.5.2. *Magnetophoresis*

The presence of magnetic dipoles is generated by the spin of some of the particle's electrons when situated within a magnetic field. The electrons can be aligned parallel or anti-parallel to neighbouring electrons [203]. The interaction of the polarised electrons with one another, gives rise to the categorisation of the magnetic material. In micron-

sized materials paramagnetism and diamagnetism are relevant. Paramagnetism is a term that describes the attraction of a particle when an external magnetic field is applied. The magnetic dipoles in paramagnetic materials are orientated randomly. When an external magnetic field is applied, the dipoles align with the magnetic flux lines [278]. A paramagnetic particle will move to a region of maxima in a magnetic field. Diamagnetism describes the characteristic of a particle with movement that is directed against the applied magnetic field; the diamagnetic particle is forced to regions of minima in the magnetic field [199]. Diamagnetism is a weak force compared to paramagnetism [279].

Magnetophoresis is a term which describes the motion resulting from the influence of a magnetic field gradient on magnetic materials relative to a fluid [280]. Magnetophoresis is separable from electrophoresis where no induced magnetic dipoles exist. A major advantage of separations using magnetophoresis is that target cells can be extracted *in situ* without any sample enrichment and minimal preparation. "*Magnetophoresis is not significantly affected by many physical parameters such as pH, temperature or salinity*" [281].

High gradient magnetophoresis has limitations when used to separate MPs. MPs interact with each other over distance; forming chains and agglomerates which result in unpredictable behaviour and clumping at surfaces [280]. In order to separate continuously and effectively using a magnetophoretic gradient, these unpredictable behaviours need to be resolved or correctly managed [282]. The magnetic moment of different sized MPs was used to develop a magnetophoretic separation device, in conjunction with fluorescent biological labels, to separate particles into 25 different categories [283]. This is an example of how versatile magnetophoresis is for separating at the micro-scale.

2.12. Proposed technologies

An affinity sensor determines the binding between the receptor molecules on the biosensor (probes) and the analyte molecules under detection (target) [81]. To enable the separation of *E. coli* from water samples, as a continuous process, and the subsequent concentration and detection of viable- and nonviable-cells, a combination of technologies will be employed. Environmental biosensors must operate in non-ideal operating conditions, within complex matrices, including particulate and organic matter. An extreme range of temperatures (from zero to 30 °C or more) will be experienced by the biosensor. The biosensor must therefore show little background interference and perform to a similar standard to those operating in ideal buffer solutions [284].

2.12.1. Immuno-magnetic labelling

The development of mono- and poly-clonal antibodies, targeting bacteria, has been on-going for many years. As an established and well-documented technique for capturing bacteria with high specificity and affinity, antibodies will be used in the proposed biosensor developed in this study. Many manufacturers offer MPs readily coated with covalent or non-covalent bonds to attach antibodies to the MPs surface. An example of a non-covalent binding is that of streptavidin coating of MPs and biotinylated antibodies. Streptavidin binds to biotin with high affinity. Both are also commercially available and given the reported success of using this conjugation chemistry [141] it will be used in this study.

When immuno-labelled MPs are placed in a magnetic field gradient, they experience a force that is proportional to their magnetic moment [285]. This relationship enables a separation device to be modelled and the movements of MPs, once bound to the target bacteria, predicted.

2.12.2. Microfluidics

Microfluidics provide advantageous characteristics for environmental sampling, including small sample throughputs, low manufacturing costs [286] and they do not require vast quantities of costly reagents [287]. Microfluidics can greatly reduce analysis time from days to minutes, thereby creating the potential for monitoring in real, or close to real-time and with portability at a hand-held level [17]. Multiple assay steps can be incorporated into the design of an MFD; sample mixing, sorting, separating and enumeration [169]. Sensing pathogens in water requires the concentration of the pathogens from large samples at low concentrations [187]. Microfluidics offer a platform that enables this process and will therefore be used in the proposed biosensor.

2.12.3. Summary

Immuno-labelling of MPs with an antibody specific to the target bacteria will be used to extract and concentrate the target bacteria. The sample with conjugated particle-bacteria complexes will then be passed through a microfluidic device. Using magnetophoresis the MPs (both bound and unbound) will be separated from the sample and suspended in a solution suitable for sensing. A tertiary step will employ magnetophoresis to separate bound from unbound particles and to explore the physiological status of the cells bacteria, whether they are viable or non-viable.

3. Methods to determine the physiological state of bacteria

As part of the development of a biosensor to monitor pathogenic bacteria in water, a method is required to characterise captured bacteria as posing a risk to human health, i.e. viable or non-viable. The research described in this chapter explores the available microbiological techniques that offer the potential to assess rapidly bacterial-viability and as such could be used in the development of a continuous flow biosensor.

3.1. Introduction

The viability of bacteria has previously been defined as the ability of a bacterium to form a colony on an agar plate [288]. "*Viability should be restricted to circumstances where evidence that a cell is able to divide is provided, therefore viability is demonstrated by culture*" [289]. Identifying viable bacteria using culture-based approaches requires days rather than hours [290] and no-longer meets the requirements for detecting bacterial contamination. Pathogenic bacteria are ubiquitous; they can be found in soil, river, seawater and drinking water.

A new method is necessary to differentiate between viable and non-viable cells, and to further explore the physiological status of cells, whether they are in a VBNC state, or stressed cells that are able to recover, or dormant. This study explored methods that may be employed as part of a biosensor recognition element that would assess bacterial populations in water and the physiological state of the cells.

3.1.1. Electrophoresis

The electrophoretic mobility of a particle, and therefore a bacterium, is dependent upon the ratio of the conductivity of the particle to that of the environment [291]. Aqueous solutions contain positive and negative ions (cations and anions respectively). The adsorption of ions onto the particle surface is caused by the partial charge of a particle's surface, termed the "stern layer." This adsorption results in the "net charge" of the

particle. Counter-ions surround this layer in a cloud formation and extend from the surface into the solution, termed the "diffuse layer" [267]. The electrophoretic mobility of particles in solution can be measured with commercially available instruments, such as the Malvern ZetaSizer (Malvern, UK). Such instruments enable rapid analysis of suspended particles, and could be utilised to measure the electrophoretic mobility and the "net-charge" of bacteria from environmental samples.

3.1.1.1. *Zeta potential*

The zeta potential is defined as the electrostatic potential at the colloidal surface, or the slipping plane as displayed in Figure 3.1. The zeta potential provides an estimate of the magnitude of the electric field between particles that results from the combined effect of ionized charged groups on the particle surface, counter-ions released into the surrounding solution and salt ions [268].

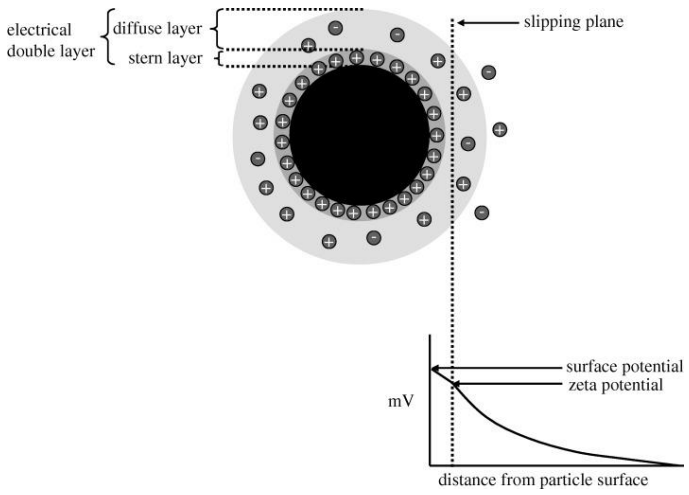

Figure 3.1. A schematic displaying the electrical double layer that surrounds a particle in an aqueous medium, the zeta potential is the electrical potential measured at the slipping plane [266]

The zeta potential may be measured using a combination of electrophoresis and Laser Doppler Velocimetry. An electric field is applied and the velocity of the suspended

particles measured, the term electrophoretic mobility is also used to describe the particle's velocity. The Henry equation may be used to derive the zeta potential:

$$\mu_E = \frac{\varepsilon\,\zeta}{\eta}\left(\frac{1}{1 + \sigma_2/2\sigma_1}\right) \quad (3.1)$$

where μ_E is the electrophoretic mobility, ε the permittivity, ζ the zeta potential, η the viscosity and σ_1 and $\sigma_2$the conductivity of the particle and solution respectively [291].

3.1.1.2. *Electrical properties of bacteria*

Bacteria can be simply described using three structures: the cytoplasm, surrounded by the cell membrane and the cell wall which provides a boundary between the cell and the surrounding medium [161]. Each species of bacteria has a complex and unique composition of cell wall [292]. The components of the cell wall (e.g. proteins, teichoic acid, peptidoglycan), contribute to the surface charge of bacterial cells through ionisation of proton-active functional groups [293]. An intact cell membrane, found in viable bacteria, is almost non-conducting due to the high regulation of ion transport through the transmembrane channel proteins [161]. The absorption of ions through the cell membrane from a solution affects the electrical potential [294] of a bacterium. The interior of a bacterial cell, containing many dissolved charged molecules may have conductivity as high as 1 S/ m. However, a viable cell has an intact cell membrane, which is highly insulating [162]; the membrane may have a conductivity as small as 10^{-7} S/ m [157]. If the cell membrane becomes permeabilised, the exchange of material between the inside of the cell and the suspending medium will increase as the cell membrane is no longer regulated. As the cell membrane is compromised, it no longer acts as an insulator and the conductivity of the membrane will increase [158].

3.1.1.3. *Zeta potential as a viability indicator*

It has been reported that bacteria treated with different antibiotic compounds increase in conductivity with duration of treatment [295]. As shown in Equation 3.1, the

conductivity of a bacterial cell affects its electrophoretic mobility and therefore the zeta potential. It is hypothesised, that given the reported change in conductivity of a bacteria cell when treated with membrane permeabilising agents, it should be possible to distinguish between live and dead cells by measuring their zeta potential.

3.1.2. Flow cytometry

Flow cytometry is a process that utilises hydrodynamic focussing to align a sample, so that particles are in single file as they pass a laser. The laser excites the sample and information is collected as particles cross the laser beam. Generally, flow cytometers can collect five or six parameters at a single pass of a cell. Morphological characteristics determined by flow cytometry are determined by the amount of light scattered by a cell, and this is dependent upon the size of the cell, its surface roughness, membrane, nucleus and its internal granular material [290]. The forward scatter measurement provides information on the amount of light that is blocked as a cell passes the laser and is correlated with the size of the particles. The side scatter parameter is collected from an angled detector and provides information on the integrity of a cell and the intracellular structure. There are usually three or four fluorescence channels in mainstream flow cytometers in which emitted fluorescence can be collected, although analytical machines can have as many as eight. Each channel has a photomultiplier which enhances the signal in order for it to be computed. Some organisms have natural fluorescence, for example cyanobacteria and fluorescent bacteria including Pseudomonads [296]. Non-fluorescent bacteria require the addition of a fluorochrome to label the cell with a fluorescent marker. There are a number of fluorochromes available for the analysis of bacteria; these are described in Section 3.1.3.

Flow cytometry has been shown to have marked advantages over other microbiological methods [73]. It allows the "*rapid and simultaneous*" analysis of differing cell parameters with high precision [69]. Flow cytometry is most widely carried out as a

batch process; however, it does allow for adaptation into a continuous monitoring system. The software for analysing flow cytometric measurements is advanced. These benefits make flow cytometry an attractive method for analysing environmental samples, without the requirement for pre-enrichment, and with only a short (approximately 20 minute) incubation phase.

3.1.3. Fluorochromes for bacterial viability assessment in conjunction with flow cytometry

A number of fluorescent stains (fluorochromes) are commercially available that enable the labelling of bacterial cells and that provide evidence of the physiological state of bacterial populations such as cell integrity, glucose uptake or membrane potential [297–299]. Commercially-available fluorochromes that are excited by 488 and 640 nm lasers of the BD Accuri C6 flow cytometer used within this study, will only be discussed (Table 3.1).

3.1.3.1. *Nucleic acid stains*

In order for a bacterium to generate electrochemical gradients which enable transport of essential molecules across its membrane, the membrane must be intact [298]. It is suggested that if a cell has a permeabilised membrane, it is no longer viable as essential transport cannot occur [300]. There are a variety of fluorochromes that are membrane impermeable. These fluorochromes can only enter a cell when the membrane is compromised. All bacterial cells contain nucleic acid; dyes which target this region are common. Membrane impermeable dyes that mark nucleic acids are often used as indicators of non-viable cells, for example propidium iodide (PI) [300–302] and sytox green (SG). PI has been widely used in conjunction with Syto 9 [66, 303, 304], a nucleic acid stain that is membrane permeable. Syto 9 (Molecular Probes) can be used to obtain the total number of bacterial cells. When used as a double stain with PI, PI quashes the

Syto 9 fluorescence of dead cells and a percentage of live and dead cells can be obtained. However, the efficacy of Syto 9 has been questioned [305]. Syto 9 is suspended in DMSO which has antibacterial properties [306] and may therefore produce false-negative results, in addition Syto 9 exhibits high background fluorescence [307]. SYBR Green I (SB) has been suggested as an alternative stain to use alongside PI [300, 301] given its enhanced quantum fluorescence compared to Syto 9. SYBR Green in combination with PI was therefore used in this study.

Table 3.1. *The fluorescent stains discussed within this report and their characteristics (adapted from* [298]*)*

Fluorochrome	Characteristic	Absorption (nm)	Emission (nm)	Molecular weight
Propidium iodide	Membrane integrity	535	647	668
Sytox green	Membrane integrity	502	523	600
Ethidium Bromide	Efflux activity	518	605	394
$DiBAC_4$	Membrane potential	493	516	517
Syto 9	Nucleic acid	488	510	*
SYBR green I	Nucleic acid	497	520	510
2-NBDG	Glucose uptake	475	550	342

*Not specified by manufacturer

SG is another membrane impermeable stain used for the assessment of dead bacterial cells [308]. Roth *et al*., [309] found SG to have much less background fluorescence (5%) compared to PI (50%) and markedly improved flow cytometric results were reported.

The use of nucleic acid stains in viability studies has been widely reported. However, cells with compromised membranes have been seen to recover and reproduce [302]. Yoshioka *et al.*, [310] suggest that membrane permeability may not always be related to viability.

3.1.3.2. *Membrane potential*

Metabolising bacteria have an electrochemical potential across their plasma membrane, generated by respiration. The anionic lipophilic oxonol Bis-(1,3-Dibutylbarbituric Acid) Trimethine Oxonol ($DiBAC_4$) has been widely used to explore the membrane potential

of bacteria [311, 312]. A reduction in the membrane potential allows for the stains to collect within the cells. $DiBAC_4$ is suspended in ethylenediaminetetraacetic acid (EDTA) which increases membrane permeability. This step enables the measurement of the membrane potential, it would otherwise be a measurement of membrane integrity [69].

3.1.3.3. *Metabolic activity*

Metabolic activity cannot be determined by use of traditional plating techniques [313]. A fluorescent derivative of D-glucose, 2-(*N*-(7-Nitrobenz-2-oxa-1,3-diazol-4-yl)Amino)-2-Deoxyglucose (2-NBDG) has been used as a marker for metabolising cells [314]. As glucose is required for vital cell functions such as ATP synthesis, it is a good candidate as a marker for active cellular metabolism. It is taken up by the cell via the glucose-specific phosphoenolpyruvate-phosphotransferase system (PEP-PT) [315] by competing with D-glucose. The uptake of 2-NBDG can therefore be used as a mechanism for detecting active metabolism and therefore cell viability.

3.1.4. Traditional plate counts

The growth of bacteria on agar plates has been, and is still, a widely used technique to explore the species in the colonies that form. The agar acts as a nutrient supply for the bacteria. Using different "recipes" of agar, it is possible to create a culturing platform that is selective and differentiative for identifying microorganisms. Environmental bacteria are notoriously hard to culture on agar plates. It is thought that only 1% of the total species of bacteria have been successfully cultured [316]. As the industry standard for detecting pathogenic bacteria, plate counts will be used in this investigation as a comparative analysis to zeta potential and flow cytometry analysis.

3.1.5. Defining viability of bacteria

There is no single physiological or morphological parameter that defines viability [3]. It is widely reported that different disinfection techniques have different impacts upon

bacteria. For example, chlorination of bacteria is reported to damage the DNA of the cells to such an extent that nucleic acid dyes cannot bind [317].

In this study flow cytometry and fluorochromes were used to identify the signs of inactivation of bacterial cells. To add a further dimension, the zeta potential of bacterial cells, was measured in order to determine whether variations in zeta potential were correlated with differing physiological states. A comparison of the viability measurements made using zeta potential, flow cytometry and traditional plate counts was conducted.

Bacteria were induced into different physiological states. The cells were: heat treated, starved of nutrients, and incubated overnight with silver nitrate ($AgNO_3$). The aim was to investigate these effects upon the bacteria, through assessment of the populations of the bacteria using the different microbiological techniques. Heat treatment of bacteria causes drastic changes in the outer membrane of Gram-negative bacteria, with the loss of LPS which is indicative of membrane permeabilisation. LPS contribute to the exclusion of hydrophobic compounds from the cell [318]. Starvation of bacterial cells has been reported to alter the size and shape of the bacteria [319], although starved cells may maintain viability they become unculturable [320]. Bacterial populations treated with silver ions have been shown to release potassium ions, an intracellular component, suggesting a loss of membrane potential. Silver ions are reported to interact with thiol groups in enzymes and proteins contributing to bacterial inactivity. In addition, the silver may bind to key functional groups of enzymes [321]

Four species of bacteria were used in the investigation as model organisms. The species used in this study were: *Bacillus megaterium, Enterococcus saccharolyticus, Escherichia coli,* and *Vibrio harveyi* (see Table 1). The strains and species of bacteria were selected as human-pathogen model organisms, but nonetheless are non-pathogenic, for safe working in the laboratory.

Table 3.2. The species of bacteria used within this study and their key characteristics

Species	Gram	Origin	Vector	Size (μm)	Shape
Bacillus megaterium	+ve	Soil	Soil	4	rod
Enterococcus saccharolyticus	+ve	Birds	Water/Soil	1	cocci
Escherichia coli	-ve	Mammals	Water/Soil	2	rod
Vibrio harveyi	-ve	Marine	Seawater	2	rod

3.2. Materials and method

The materials and methods used to conduct microbial analytical techniques upon four species of bacteria under different conditions and physiological states are described.

3.2.1. Bacterial cultures

Escherichia coli (NCTC 4001) was obtained from Environmental Scientifics Group, Derbyshire. *Vibrio harveyi* (1280), *Enterococcus saccharolyticus* (702594) *Bacillus megaterium* (4821) were obtained from National Collection of Industrial Food and Marine Bacteria (Aberdeen, Scotland).

Bacterial cultures were prepared in 20 ml of: Luria-Bertani (LB) broth for *E. coli*, nutrient broth for *B. megaterium* and *E. saccharolyticus* cultures and marine broth for *V. harveyi*. Cultures were grown overnight in an orbital incubator at 150 rpm at 30 °C.

Due to the antimicrobial effect of silver nitrate [322], dead samples were prepared by treating cells with 1 ml $AgNO_3$ overnight. Before analysis, cells were centrifuged and washed three times in the appropriate solution to remove $AgNO_3$ from the sample.

In order to create samples of stressed cells - with a number of cells having permeabilised membranes but not the entire population - cells were prepared by heating at 50 °C in a water-bath and samples were taken for analysis at different time intervals up to 30 minutes.

To explore the effect of starvation upon bacteria, cultures were washed in the required solution three times and stored at 4 °C until examination.

3.2.2. Zeta potential

Zeta potential measurements were obtained using a ZetaSizer (Malvern Instruments, UK). Samples were measured at a temperature of 25 °C. The instrument was allowed to equilibrate for two minutes before a set of three measurements was taken. Consumable capillary cells were used for all samples and were thoroughly washed with ethanol and three subsequent flushes of the respective solution before a new sample was measured.

3.2.3. Flow cytometry

Flow cytometric measurements were obtained employing an Accuri C6 Flow Cytometer (BD Biosciences Europe, Oxford, UK) equipped with two lasers which excite at 488 and 640 nm. Samples were prepared so that the concentration of cells did not exceed 10^6 CFU/ ml. Samples were run through a core size of 4 µm and for a volume of 30 µl. Data was analysed using Flowing Software (http://www.flowingsoftware.com/).

3.2.4. Fluorescent staining procedures

Samples of 1 ml were incubated at 25 °C with either SYBR Green I (SB) $1:10^4$ dilution and propidium iodide (PI) 10 µg/ ml [73] for 15 minutes, ethidium bromide (EB) 12 µg/ ml $DiBAC_4$ 15 µg/ ml for 10 minutes [116] or 2 µg/ ml of 2-NBDG for 25 minutes. PI and EB fluorescence were collected above 585 nm; the remaining fluorochromes were measured using the 530 nm filter. All stains were purchased from Invitrogen, UK.

3.2.5. Plate counts

To calculate the concentration of viable cells in a sample, serial 1:10 dilutions were made by adding 100 µl of a sample to 900 µl of the relevant suspending solution. The dilution was vortexed and 100 µl was removed and then added to 900 µl of the relevant suspending solution. This was repeated until a dilution of 10^{-9} was achieved. The serial dilutions were then drop plated using the Miles & Misra technique [323]. Three 20 µl drops of each dilution were spotted onto a divided, numbered agar plate, each making

three separate pools of approximately 1.5 to 2.0 cm diameter. The dilution which enabled individual colonies to be counted, with a statistically viable total number, was enumerated. The average of the three replicates was taken.

LB agar was used to culture *E. coli*, nutrient agar for *B. megaterium, E. saccharolyticus* and marine agar for *V. harveyi*. The numbers of colonies after incubation at 30 °C for 48 hours were counted from the highest countable dilution. The average number of colonies was calculated, and the CFU/ ml established.

3.2.6. Solution preparation

DW, deionised water (DI) and artificial saltwater (ASW) of salinity 33.3 ppt were sterilised by autoclaving. A range of pH values, from 3 to 10, was investigated due to the assumption that the more $[H]^+$ in the solution, the greater the charge of the suspended particles [324]. The pH was adjusted using HCL and NaOH to the value required.

3.2.7. Statistics

The statistical methods used were analysis of variance (ANOVA), T-Test (*denotes $P<0.05$) and linear regression.

3.3. Results

The results obtained from the investigation into the viability and the effect of disinfection treatments on the zeta potential of the four species of bacteria is described. An investigation into suitable fluorochromes that could be used as an alternative to plate counts was conducted with the bacterium *E. coli*. A comparison of the analysis on bacterial viability as obtained by measuring the zeta potential, flow cytometry and plate counts was conducted to establish whether a relationship existed between the microbiological techniques.

3.3.1. Zeta potential

The bacteria were selected to represent a broad taxonomic spread, being both Gram positive and Gram negative, and related to environmental pathogens. The zeta potential of each species was measured to explore whether the zeta potential was dependent upon species, physiological state and the suspending solution.

To avoid fluctuations of the momentary number of particles in the scattering volume of the ZetaSizer, and the bias this would produce, results were only accepted as good quality if the count rate was between 150 and 10,000 kilo-counts per second (kcps) [325]. In addition, results were classed as acceptable if the phase data met the criteria of the Dispersion Technology Software (provided as standard with the ZetaSizer Nano).

3.3.1.1. *Drinking water as a suspending solution*

The range of zeta potentials for the four species of viable bacteria suspended in DW at different pH values was -3.12 to -31.03 mV.

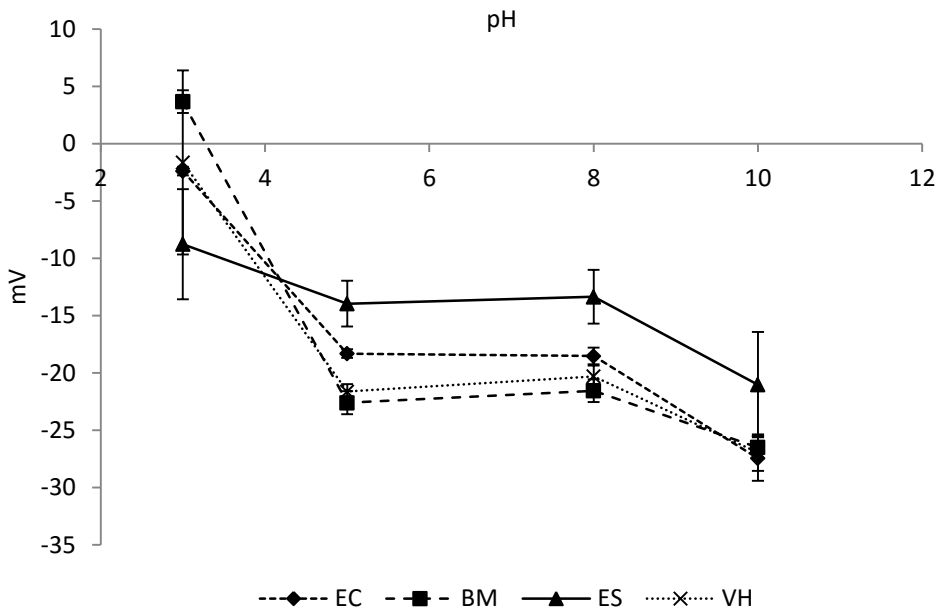

Figure 3.2. The zeta potential of live bacteria Escherichia coli (EC), Bacillus megaterium (BM), Enterococcus saccharolyticus (ES) and Vibrio harveyi (VH) at different values of pH (Error = 1 SD; n =3)

It may be seen from Figure 3.2 that, as the pH increases, the zeta potential of the bacteria becomes more negative, and above a pH of 3.5, bacteria were negatively charged when suspended in DW. The charge represents the electrical potential at the shear plane between a cell wall and its suspending solution [324]. *B. megaterium* was the only species of bacteria to display a positive zeta potential, when suspended at pH 3. The zeta potential of all the species of bacteria became more negative with increasing pH, this observation being a result of an increase in hydrogen ions in the solution from the addition of HCl and an increase of the negative charge of suspended particles [326].

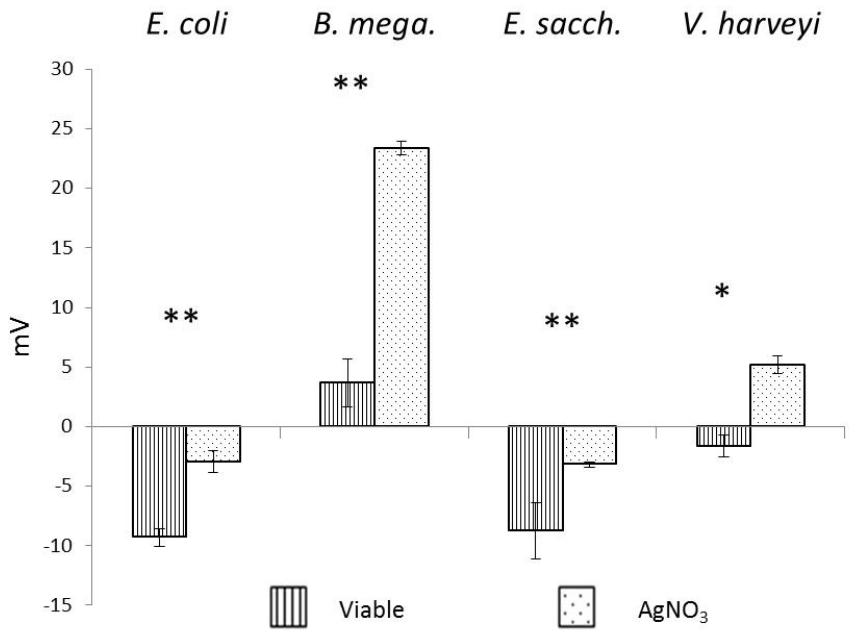

Figure 3.3. The zeta potential of four species of bacteria suspended in drinking water at pH 3. (Error = 1 SD; n = 6; P<0.05 **P<0.01; T-test)*

The zeta potentials of viable and $AgNO_3$ treated bacteria were significantly (P<0.05) different for each species of bacteria when suspended in DW at pH 3 (Figure 3.3). *E. coli* was the only organism that displayed significant difference between viable and treated cells across the range of pH values. $AgNO_3$ treated cells had more positive zeta potential than live cells. This may have been due to the breakdown of the cell membrane and the unregulated transport of ions across the boundary [327].

The pH of the suspending solution and the species of bacteria were all statistically significant in terms of the zeta potential when DW was used as the supending solution (ANOVA; Two factor $p < 0.05$).

3.3.1.1.1. Drinking water stress experiment

Figure 3.4 represents the zeta potentials measured after bacterial species were subjected to thermal stress in a water bath. The zeta potential became less negative after 30 minutes of thermal stress for all bacteria apart from *E. saccharolyticus*, where the zeta potential remained at approximately -13 mV. The zeta potential of viable and heat

treated *E. saccharolyticus* varied by only 0.74 mV at pH 8; this result was therefore expected.

Similar observations were made when exploring viable bacteria and $AgNO_3$ treated bacteria in experiments in DW; damaged cells were found to have a less negative zeta potential.

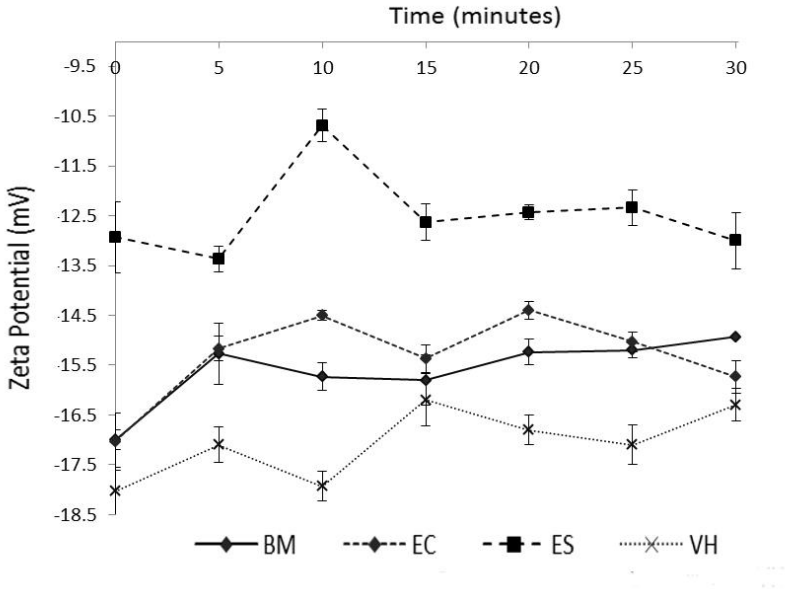

Figure 3.4. The zeta potential (mV) of Escherichia coli (EC), Bacillus megaterium (BM), Enterococcus saccharolyticus (ES) and Vibrio harveyi (VH) after being subjected to thermal stress when suspended in drinking water (Error = 1 SD; n=6)

3.3.1.2. *Suspending solutions*

The zeta potential of the four species of bacteria, both viable and $AgNO_3$ treated, is dependent upon the suspending solution. Figure 3.5 represents a comparison of the zeta potential at pH 8 of the three solutions; cells were suspended in DW, ASW and DI. Variances in the zeta potential were observed and they were dependent upon the constitution of the suspending solution and its pH. It can be seen that with increasing water composition and ion content, the zeta potential becomes less negative.

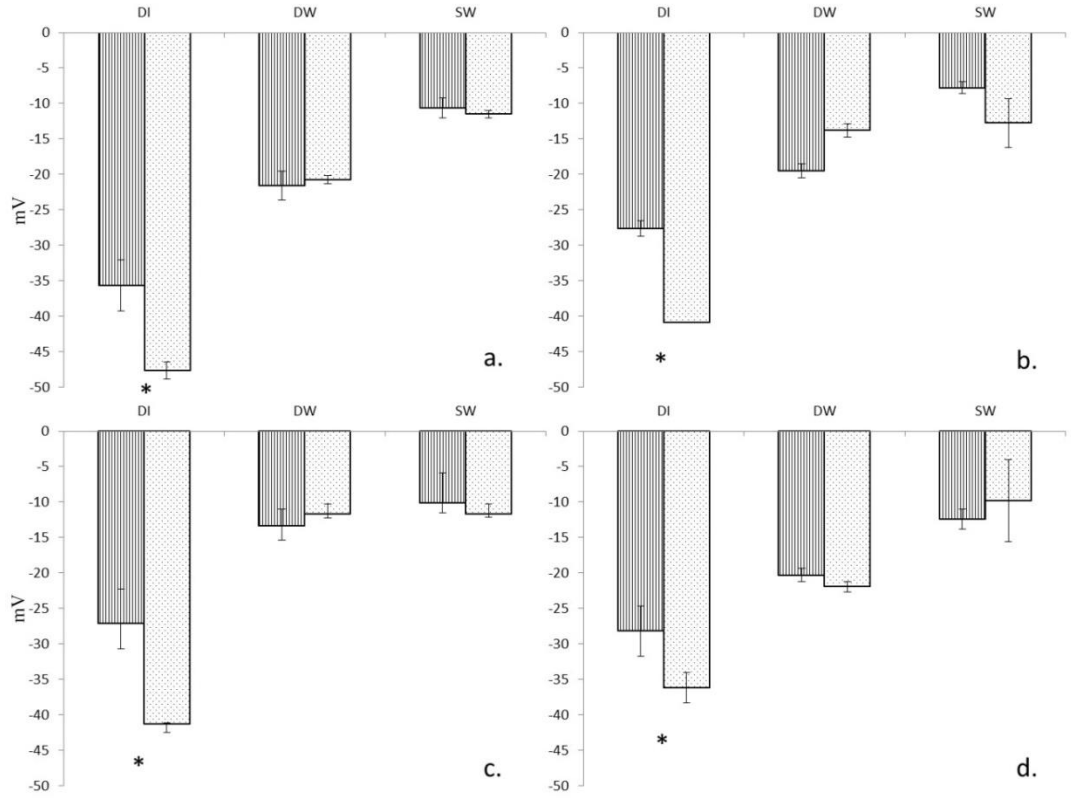

*Figure 3.5. The zeta potential of viable (striped) and $AgNO_3$ (dotted) treated a) Bacillus megaterium, b) Escherichia coli c) Enterococcus saccharolyticus and d) Vibrio harveyi when suspended in three water types at pH 8 (Error = 1SD; n=3 *denote T-Test P<0.05).*

Soni *et al*., [328] reported a zeta potential of viable *E. coli* (strain DH5α) cells suspended in DW of pH 8.4 of -47.8 ± 0.7 mV, compared to the value found in these experiments of -19.95 ± 0.32 mV at pH 8. The difference may be due to a combination of factors such as different concentrations of bacteria used in the study (zeta potential is dependent upon concentration [266], the strains of *E. coli* investigated and the slight difference in pH. The zeta potential of different species of bacteria was found to be significantly different (P<0.05) in this study when the bacteria were suspended in DW and DI, this may be attributed to the fact that each species of bacteria has a complex and unique composition of its cell wall [292]. Contrary to DW and ASW as suspending solutions, the zeta potential of $AgNO_3$ treated bacteria was more negative than viable bacteria when suspended in DI.

The use of ASW as a suspending solution made it difficult to obtain reliable zeta measurements for the ASW caused premature corrosion of the electrodes of the capillary cell.

Using ANOVA (Two factor with replication, $P<0.05$) no significant difference was detected between the zeta potential of the species of bacteria and the pH of the suspending solution when suspended in ASW. This trend may be explained by the increased number of cations in the solution and their potential to shield the surface charge within the proximity of the negatively charged cell surface [324]. In addition, the pH of the ASW suspending solution did not have a significant effect on the zeta potential; variance in zeta potential with differing salinities has not been well documented [329]. It is concluded that these species of bacteria, when suspended in ASW, have their intrinsic charged masked by suspended cations. The pH of the suspending solution of bacteria has previously been reported to affect the zeta potential [328]; in this study the pH was found to be a significant factor also.

The zeta potential was dependent upon the pH of the suspending solution, which is well understood and reported. The zeta potential can provide information on the physiological state of bacteria i.e. viable or non-viable. To be used in the proposed biosensor, the zeta potential measurement would be required at the single cell level. Measurements at the single cell level would remove the concentration dependency and complexity of heterogeneous samples of bacteria that may have different physiological states or stages in the bacterial life cycle.

3.3.2. Development of flow cytometry protocol to assess bacteria in water

It is not possible to differentiate between different species of bacteria using flow cytometry without using a fluorescent-antibody. For this reason, only *E. coli* was used in the development of a flow cytometry protocol using commercially available fluorochromes.

In order to remove background interference from cells debris, dead controls were prepared by subjecting cells to 20 minutes at 90 °C and fluorochromes subsequently added.

The fluorochromes utilised to assess the viability of cells whilst in starvation were SB and PI, in combination, as indicators of membrane integrity and total cell count. EB which is an indicator of cells that had lost efflux pump potential and SX was used as an additional indicator of membrane integrity. The collection of $DiBAC_4$ in cells indicated a loss of membrane potential and 2-NBDG uptake indicated an inability of cells to metabolise.

3.3.2.1. *Fluorochrome calibrations with plate counts*

To explore the use of fluorochromes as viability indicators that might replace the use of plate counts, *E. coli* was heat treated, and different concentrations of viable and heat-treated cells were analysed using the five fluorochromes and were then compared to plate count analysis. The only significant correlation with plate counts was found to be with the fluorochrome 2-NBDG (Figure 3.6); a correlation was observed ($R^2 = 0.88$).

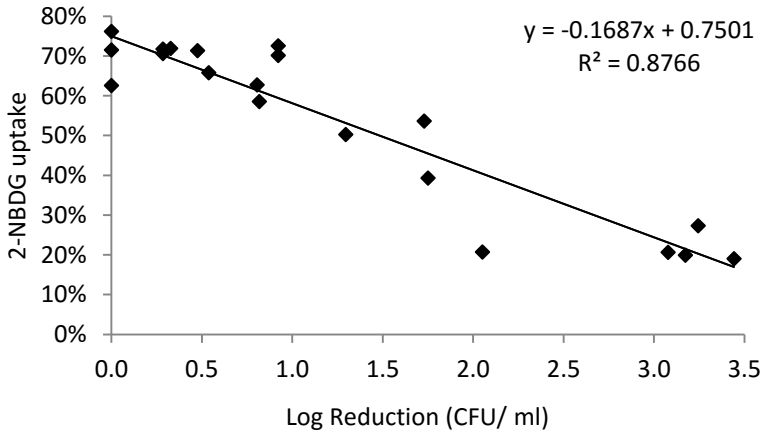

Figure 3.6. The correlation between flow cytometry analysis of the uptake of fluorochrome 2-NBDG in Escherichia coli cells treated using heat with the log reduction in plate counts

To investigate further the use of 2-NBDG as a viability indicator, different concentrations of $AgNO_3$ treated *E. coli* were assessed for viability using 2-NBDG and plates counts. A weak positive correlation was detected (Figure 3.7). This is in contrast to the reports in the literature, which suggest that live cells allow the uptake of 2-NBDG through the PEP-PT transport system, via glucose uptake (as seen in Figure 3.6).

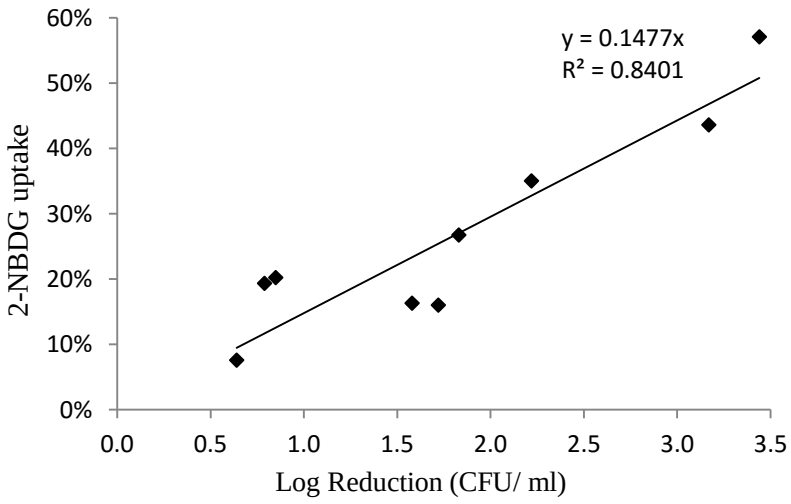

Figure 3.7. Calibration curve of 2-NBDG with plates counts with $AgNO_3$ treatment of Escherichia coli

It has been reported that when incorporated into living cells, the 2-NBDG metabolite can be further decomposed into a non-fluorescent derivative [310]. To explore this further a calibration of 2-NBDG uptake was conducted with respect to time and temperature. Figure 3.8 displays the uptake of live *E. coli* of 2-NBDG. The uptake is dependent upon time and temperature and at 15 °C the uptake is much slower than at 25 and 30 °C by 20 minutes; the uptake is reduced by as much as 20%. The results provide evidence that the incubation was not long enough to allow for the decomposition of the metabolite into its non-fluorescing stage.

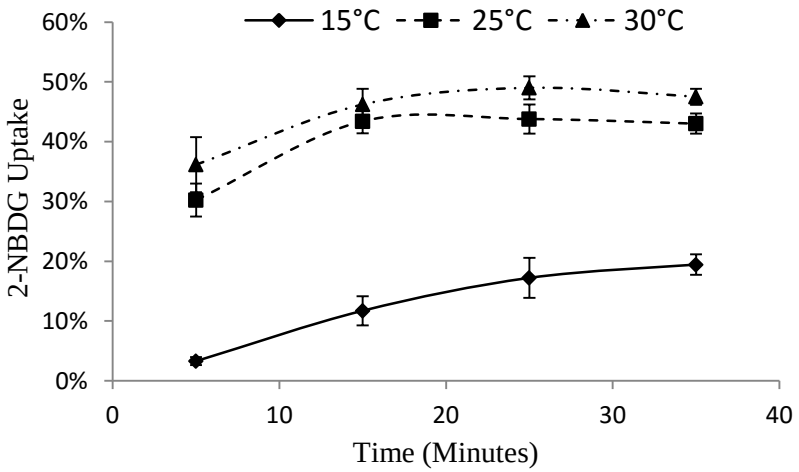

Figure 3.8. The percentage uptake of 2-NBDG by live Escherichia coli with respect to time and at different incubating temperatures (Error = 1SD; n=3)

E.coli was cultured at 30 °C, it can be expected that the cells metabolise more efficiently at the warmer temperatures and therefore metabolise the 2-NBDG into its fluorescent derivative more quickly. The contradicting effects of disinfection techniques, make the use of 2-NBDG in microbial analysis unreliable.

3.3.2.2. *Starvation and stress experiment*

Five fluorochromes were employed to assess the bacteria that had been entered into starvation states, in order to examine their physiological response.

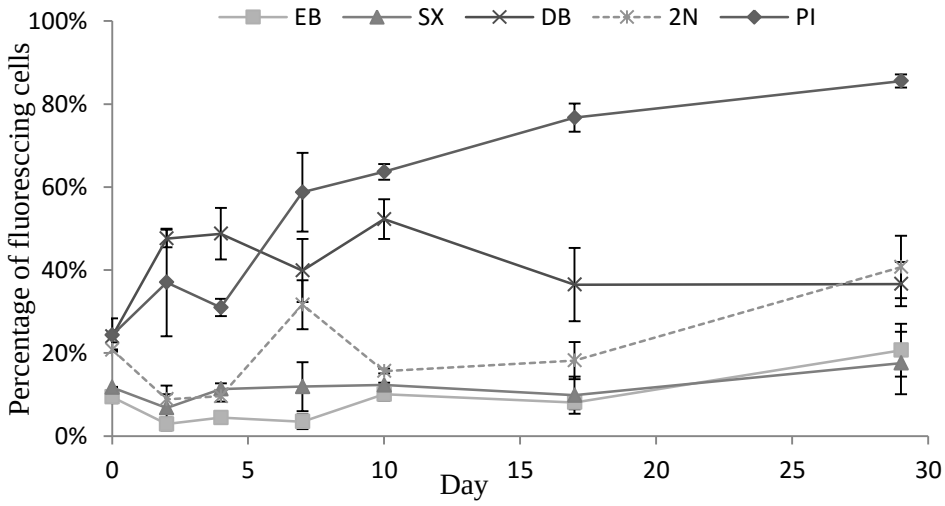

Figure 3.9. The uptake of the five fluorochromes by Escherichia coli cells when suspended in drinking water (Error = 1SD; n=3)

Of all the stains used, the combination of PI and SB produced the anticipated response; as the duration of starvation increased more cells lost membrane integrity. However, no correlation was observed between PI and SB staining, and plate counts (data not shown). Very little increase in uptake by the other stains was detected; the data presented in (Figure 3.9) are stochastic revealing no trends.

It has been previously reported that bacterial cells that are stressed, first lose their ability to metabolise, their membrane potential is then lost before the efflux pumping stops, finally the cells become permeabilised [70]. This trend was not observed in this study when cells entered into the starvation phase. There was very little, or no increase, in EB and $DiBAC_4$ staining. Previous studies using $DiBAC_4$ as a viability indicator have employed the stain in conjunction with EDTA in order to facilitate active transport across the cell membrane. EDTA was used to suspend $DiBAC_4$ before use in the assays, an increase in the concentration of EDTA may have enhanced uptake. However, EDTA is a well-known toxicity agent as it depletes the lipopolysaccharide layer of the bacteria; its use has the potential of providing false-positive results when used to assess viability of bacteria [330].

Figure 3.10 represents the uptake of PI by heat treated cells, which shows as the duration of heat treatment increased, so did the uptake of PI and therefore the number of cells that had permeabilised membranes.

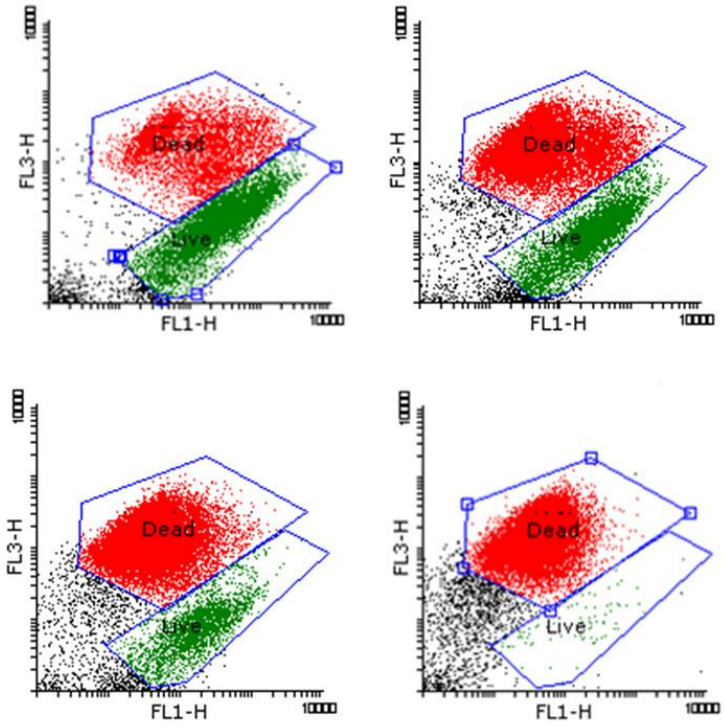

Figure 3.10. Flow cytometry analysis of the uptake of SYBR green (green FL-1) and propidium iodide (red FL-3) by Escherichia coli with heat treatment a. 0s b. 180s c. 270s d. 360s when suspended in drinking water.

No correlation was found between cell permeability, as indicated by PI and SB dual-staining, and viability plate counts. This result suggests that the short heat treatment (waterbath 60 °C) temporarily permeabilised the cell membrane, but the cells were able to recover and replicate when presented with optimal growth conditions.

3.3.2.3. *Flow cytometry summary*

PI and SX are both indicators of permeabilised membranes, it would therefore be expected that similar trends are observed when using these two fluorochromes as a viability indicator. This was not the case; there was little detectable uptake of SX, but 85% of cells after 19 days' starvation were found to be PI positive. The difference may have been in-part, attributed to the double-staining used with PI and SB; however, this does not provide an explanation for the total difference in uptake between the two

staining techniques. It has been reported that labelling with SX is markedly improved compared to that with PI [309]; the opposite was found in this experiment.

Much information may be derived from using multiple fluorochromes to assess a bacterial population and the changes to the physiology when subjected to different stressors. The data detailed in this study is non-conclusive and disparities exist between the data described and that reported in the literature.

Live bacteria, 50 /50 live /dead bacteria, and dead controls were all conducted to ensure the staining protocol worked reliably. It was also anticipated that, due to the SX, $DiBAC_4$, 2-NBDG and EB protocols being reliant upon only one fluorescence, that moribund (a physiological state between viable and non-viable) cells were included in the analysis as they were not easily discriminated.

The uptake of all fluorochromes was directly dependent upon incubation time and temperature. The development of a standard protocol is necessary for each fluorochrome. Use of an on-line monitoring system for water samples would require the sensor to be temperature controlled, thereby adding a complex dimension to the proposed sensor.

3.3.3. Comparative analysis

In order to compare the three microbiological techniques described in this Chapter, the four species of bacteria as detailed in Table 3.2 were routed into a starvation state. Plate counts were obtained at different time intervals into the starvation, as were zeta potential measurements and flow cytometry values using PI and SB. Table 3.3 summaries the differences obtained by the three analytical techniques.

Table 3.3. A comparison of the three microbiological techniques of the viability of the four species of bacteria under starvation condition after 16 days

Species	PI Uptake %	Change in Zeta (mV)	Plate Counts Log Reduction
Deionised Water pH 7			
E. coli	+ 37.62	+ 9.40	7.47
E. saccharolyticus	+ 37.9	+ 8.91	2.92
B. megaterium	+ 34.69	+ 4.57	4.24
V. harveyi	+ 73.39	+ 8.38	-0.60
Artificial Seawater pH 7.6			
E. coli	+ 17.37	+4.39	4.47
E. saccharolyticus	+52.36	-10.81	6.22
B. megaterium	+52.29	-0.60	7.65
V. harveyi	+35.48	+2.23	-1.11

All species of bacteria showed an increase in PI staining after 19 days of exposure to starvation conditions. PI & SB staining of *V. harveyi* cells in ASW at day zero also indicated 55% of the population had permeabilised membranes. The CFU/ ml as determined by plate counts, of *V. harveyi* increased by 0.60 log units over the course of the experiment. This suggests that bacterial cells, or at least a proportion of the cells, may have recovered from having permeabilised membranes. *V. harveyi* was cultured in marine broth (made with ASW). The species should not therefore have been affected by changes in osmotic pressures and the subsequent damage to the cell membrane this may have caused [331].

The zeta potential became less negative in six out of the eight tests. A slightly more negative zeta potential was observed in the case of *B. megaterium*, starved in ASW. *E. saccharolyticus* had a more negative zeta potential with a -10.81 mV difference in zeta potential. The log CFU decreased in *E. coli*, *E. saccharolyticus* and *B. megaterium*. *V. harveyi* did not show a reduction in CFU in either DI or ASW during the starvation phase.

E. saccharolyticus and *B. megaterium* had more negative zeta potentials after the starvation period in ASW. No correlation was found between flow cytometry

measurements and the reduction in CFU, as determined by plate counts, which is contrary to some previous reports [332].

V. harveyi revealed no detectable decrease in counts as assessed by viable plating. PI staining suggested that 73% of cells suspended in DI had permeabilised membranes and would be categorised as “non-viable”. The plate counts suggest that given optimal growth conditions, the bacteria could recover even with damaged cell membranes. Cells with an intact membrane may be dead or alive [333] and those that have a damaged membrane can recover.

3.4. Discussion

Three microbiological techniques were used to analyse the physiological states of four species of bacteria. Bacterial cell surfaces possess acidic and basic functional groups, such as carboxylic, phosphoric, hydroxyl and amine groups [334]. These properties all lead to independent surface charges, which were observed in this investigation. The bacterial cell surface is dynamic and responds to environmental changes [335] and this may be seen by the change in zeta potential when suspended in different solutions.

The use of fluorochromes as a viability indicator of bacteria, together with flow cytometry, offer a thorough process for investigating the physiological states of bacterial communities exposed to stressors. Discrepancies exist between the data obtained for total viable cell count, as determined by fluorescence-based methods, and those obtained employing viability plating, which may be attributed to the existence of VBNC cells [316], culture-based methods are argued to under evaluate the total number of microbes present in a sample. Fluorescent-based approaches have the additional benefit of allowing a more detailed analysis of the physiological state of microbes [62]. However, the associated technology is expensive, and there is a requirement for strict temperature control and incubation times for the staining procedures. Furthermore, the proper storage of the organic fluorochromes used in an on-line sensor would be challenging for

commercially-available fluorochromes have poor photo-stability and low-intensity. Incorporation into an automated biosensor would require correction for background fluorescence, and might also require a washing step in order to remove unbound-dye. QDs offer photo-stability and an alternative means of fluorescently-labelling cells. However, because the QDs are inorganic, labelling requires immuno-functionalisation of the QDs.. The QDs cannot enter viable cells via pathways. The cell membrane must be permeabilised and the cell envelope removed to allow collection of QDs within the cells [58]. QDs will therefore offer less physiological information when used as a labelling technique as compared to organic fluorochromes.

To understand better how the cells are inactivated, a technique such as RS could prove valuable. RS allows the chemical profiling of cells; a chemical "fingerprint" may be mapped and abnormalities between viable and treated cells may be detected [336]. A disadvantage of RS is the significant up-front cost and the relatively unestablished use of this technology in microbiological applications.

In order to decide upon a technique to assess the viability of a sample in a continuous flow measuring system, the nature of the sample must first be considered. Not all techniques are suitable, nor do they provide accurate assessments of the populations when compared to plate counts. Plate counts have been used to assess microbial contamination for many years. It is necessary, when finding an alternative method, to correlate the new assessment method of bacterial viability with the plate count method in order to determine the reliability and consistency of new methods. This was not achieved in this study.

3.5. Conclusions

The suspending solution, pH, physiological state and type of species all have a significant effect upon the zeta potential of bacteria when suspended in DW and DI. No correlation was detected between fluorescent staining and plate counts of starved cells.

Cells that appeared to have a permeabilised membrane could recover and go onto reproduce, as demonstrated by *E. coli* when subjected to heat stress and *V. cholerae* when subjected to starvation conditions. In order to measure the zeta potential of bacteria, the recommendation of this study is that the bacteria are suspended in a buffer that is optimised for zeta potential measurement. A buffer of pH 3 provided the greatest difference in zeta potential between viable bacterial cells and $AgNO_3$ treated bacterial cells.

Flow cytometry is a valuable technique that enables the study in near real-time of physiological states of bacteria. However, the dependency upon the staining protocols of temperature control is a major drawback of using this technique in an automated, on-line monitoring system. In addition, the cost of flow cytometers requires significant investment and the data is arbitrary and open to interpretation. The microbiological techniques described in this Chapter need adaptation before their use as viability indicators in the proposed sensor, or a suitable alternative should be found.

4. Continuous separation using microfluidics and magnetophoresis

To enable the isolation of pathogenic bacteria from water samples, a method to continuously capture, separate and concentrate the organisms from complex samples is required. A novel microfluidic-separation device is described that incorporates hydrodynamic focussing and magnetophoresis to achieve these requirements.

4.1. Introduction to microfluidics and magnetophoresis

As transient environments, waterbodies need to be continuously monitored for chemical and biological contaminants. Environmental applications include the detection of toxic metal contaminants (e.g. Cr^{3+}, Ni^{2+}, Co^{2+}) [326], viruses [337, 338], pathogenic bacteria [339] and protozoa [340]. An all-encompassing, real-time continuous system is required which determines the levels of designated pollutants in a waterbody. As an example, an online water toxicity monitor has been reported that utilises genetically and chemically modified *E. coli* reporter strains, that in the presence of metal contaminants, emit fluorescence [341]. The levels of naturally occurring fluorescent organic matter has shown to be an early warning signal for contamination of water reservoirs [342]. While there has been progress in the development of real-time chemical monitoring systems, biological contaminants e.g. pathogenic bacteria, are still difficult to detect in real-time, and even close to real-time. Further progress needs to be made.

Contamination incidents of waterbodies are characterized as being stochastic, short-termed and difficult to detect [342]. Pathogenic bacteria are approximately 1-2 μm in size and occur in low concentrations in the environment. Current micro-scale isolation methods involve various centrifugation techniques [343] and fluorescence active cell sorting [344]. Experienced users are required and both methods suffer from poor purity, they are expensive [345] and can cause damage to cells [229]. Improvements are needed

that enable a cost-effective, highly-efficient device that achieves the separation, concentration and isolation of micro-particles continuously. Due to the low infectious dose and toxicity level of many contaminants, it is highly desirable for the sampling procedure to increase the concentration of the targeted contaminant and to reduce limiting factors that will inhibit detection [346].

The research, as detailed in this Chapter, describes the design and optimisation of a microfluidic-manetophoretic device that will be used to concentrate the targeted pathogens and remove these cells from the environmental sample, suspending the cells in a solution that is optimal for further analysis. This is achieved through the use of MPs, microfluidics devices (MFD), hydrodynamic focussing (HDF) and the principles of magnetophoresis.

4.1.1. Microfluidic devices for bacteria concentration

Microfluidic devices, i.e. fluid handling systems with channel dimensions on the micrometer scale, have become widely used within the clinical and environmental sectors. Advantages include small sample throughputs, they are inexpensive to manufacture [286] and do not require vast quantities of costly reagents [287]. MFD can greatly reduce analysis time from days, to minutes or even seconds. This creates the potential for monitoring in real, or close to real-time [347].

There are three main types of label-free separations that are conducted using MFD. Firstly, kinetic separation, which is dependent upon the rate of cell deflection perpendicular to primary channel flow. Secondly, continuous equilibrium separations which are dependent upon the migration of cells from, or to, equilibrium positions. Thirdly elution methods, which are dependent upon forces antiparallel to primary flow to create differential retention [348]. Whilst these methods are useful for sorting and filtering a sample, they do not allow the separation of species-specific organisms. Pathogenic bacteria are difficult to discriminate between naturally occurring detritus and

non-harmful bacteria given their physical size and shape. In order to remove selectively a target cell from a complex, heterogeneous sample with particulates of a similar size, a marker must first be used to target the cells of interest. The incorporation of labelling cells within an MFD is achievable and has been widely reported [286, 349, 350].

4.1.2. Hydrodynamic focussing

Typical dimensions of microfluidic devices are on the milli- to nano-scale. At these dimensions, laminar flows are achieved which are advantageous due to their steady and predictable characteristics. The low Reynold's number of the flow within an MFD is dependent upon the size of the microchannels. These conditions allow for what is termed HDF of sample flows. Buffer fluids are used to focus a sample stream within a region of an MFD. Most widely reported HDF occurs in a two-dimensional plane (2D), however more complicated HDF in three-dimensions (3D) have recently been described [139]. The fluidic systems required to permit 3D focussing are complicated and many additional problems are introduced in design and function. This report describes a 2D HDF to enable a simplistic concept for an MFD.

4.1.3. Magnetic microparticles

Functional MPs are used in a variety of applications for the capture, transport and detection of magnetically labelled cells [185]. A specific capture molecule may be immobilised upon an MP [220]. When an MP comes into contact with a target cell, a binding event occurs. The target cell inherits the magnetic properties of the MP [350] and will thus be influenced by a magnetic field. The use of MPs allows for precise and repeatable binding events to be introduced into a separation experiment [349].

Paramagnetic and ferromagnetic materials have a magnetic susceptibility, greater than zero, whereas diamagnetic materials have a magnetic susceptibility less than zero. Ferromagnetic materials have a much larger susceptibility and therefore experience

greater forces. However, the residual magnetisation within the beads leads to hysteresis in the particles. The principles underlying detection using MPs that are superparamagnetic, is the ability to switch between a dispersed and assembled state [219]. The single superparamagnetic domain fluctuates rapidly due to thermal excitation, leading to no magnetic moment for macroscopic timescales [351]. Superparamagnetism is determined by the size of the nanoparticles of iron oxide (normally maghemite or magnetite) being less than 20 nm. The electrons inside the nanoparticle always have dipoles along the magnetic field lines. The commercially available superparamagnetic MPs used in this study were formed by incorporating several superparamagnetic maghemite nanoparticles in a micro-sized silica or polymer sphere. The sphere becomes a magnetisable particle with a mobility determined by an induced motion of an applied magnetic field [352].

4.1.4. Microfluidics in conjunction with magnetophoresis as a continuous concentration and separation device

Magnetic separation permits the targeted cells to be isolated directly from crude environmental samples [282]. The term magnetophoresis describes the influence of a magnetic field upon a particle in a viscous medium [353]. Incubating a sample with functionalised-MPs will render the targeted cells magnetic. There are two types of magnetophoretic-microfluidic separation device: batch and continuous. Batch separation involves the trapping of MPs by an external magnet, the removal of the supernatant and the capture of the trapped particles once the magnetic field has been removed. A magnetophoretic-microfluidic separation device has been reported to separate between 78 and 90% of the total MPs from the sample flow into a buffer flow and were analysed after exciting the chip [354]. However, the flow rates used were very low (25 – 40 µl/hr) which significantly limits the volume of sample that can be analysed. Alternative continuous methods e.g. [194, 355] have been described; however, these methods present

certain difficulties. The agglomeration of MPs is a particular problem. The greater the number of particles within close proximity of each other, the greater the magnetic force acting upon them due to their induced magnetic dipoles. This encourages particle agglomeration [356] which results in differing mobilities and velocities in the gradient magnetic field [357]. Even at low concentrations of MPs, variations in their physical properties cause undesirable differing mobilities, that can lead to poor separation efficiencies. The microchip designed by Pamme and Manz [197] uses magnetophoresis to separate MPs from a sample flow into one of nine separation channels; the reported separation of MPs in excess of 75%. The microchip design which incorporates multiple exit channels enables the separation of MPs with different mobilities. MPs with higher mobilities are deflected further and separate through an exit channel located at a greater distance away from the sample flow. The analysis of the separation efficiency is conducted on-chip and does not report the total throughput of the MPs. The permanent magnet is positioned above the chip, which is considered to be problematic by encouraging surface collisions, although this has not been discussed by the authors. It is well documented that the flow-profile within a rectangular microfluidic device is parabolic [358]. The velocity at the surfaces of the device is zero; MPs that collide with the surfaces are difficult to recover, especially at low flow rates.

To enable the continuous separation of MPs as single entities or agglomerates, and to allow higher volumes of samples to be processed, two novel magnet configurations were devised. The aim of the designs is to enable use of MPs of any size, susceptibility and concentration, to be continuously separated from a sample using microfluidics (Figure 4.1). The MPs are encouraged into a "region of minima" (ROM) where no magnetic force is experienced by the MPs; subsequently the MPs are separated by a continuous, hydrodynamically-focussed buffer flow. The ROM is located in the centre of the *z* axis thereby avoiding MP-surface collisions and subsequent loss of MPs within the device.

4.1.5. Reducing magnetic particles sedimentation

As stated, a common problem of using MPs in separation is their tendency to form agglomerates and sediment out of suspension. To reduce single MPs self-assembling into agglomerates, attractive forces must be counteracted by repulsive forces.

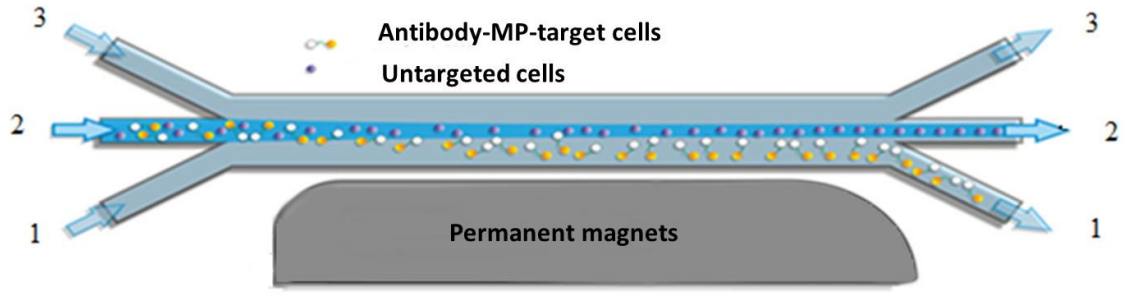

Figure 4.1. A schematic of the proposed microfluidic-magnetophoretic separation device using permanent magnets. A heterogeneous sample enters through channel 2; immuno-labelled MPs migrate towards the magnet and exit the device from exit channel 1 in the hydrodynamically focussed buffer flow.

A surfactant can prove useful. A surfactant consists of micelles that have hydrophobic tails which attach to the MPs, while the hydrophilic heads of the surfactant face into the water [359]. This acts as a buoyancy aid, reducing particle collision and sedimentation [360].

4.2. Theoretical considerations

When designing an MFD for the separation of pathogenic bacteria from waterbodies, there are certain physical conditions that first need to be understood and calculated.

4.2.1. Reynold's number

The Reynold's number is used to predict the flow patterns in fluid conditions:

$$Re = \frac{\rho \bar{u} L}{\eta} = \frac{\bar{u} L}{\nu_k} \tag{4.2}$$

It is a dimensionless quantity where ρ is the density of the fluid, $\bar{u}$ is the mean velocity, L is the characteristic length, η is the dynamic viscosity and υ_k is the kinematic viscosity of the fluid.

4.2.2. Two-dimensional hydrodynamic focussing

The parameters that are important to consider when using HDF are described in more detail by Kunstmann [361] but are summarised here. Based on the mass conservation principle for incompressible fluids, the volume flow passing through the central inlet channel must equal the volume of fluid passing through the focused sample stream, and the volume flow passing through all three inlets must be the same as the total fluid passing through the main channel.

$$Q_s = W_f h V_f \tag{4.3}$$

$$Q_s + 2Q_i = W_0 h V_0 \tag{4.4}$$

where W_0 is the width of the channel, W_f is the width of the focussed sample stream and h is the channel height; Q_i and Q_s are the volume flow rates of the sample and the sheath respectively and V_0, is the initial velocity along a channel and V_f the final sample stream velocity (Figure 4.2). By rearranging the two equations above the following expression for the width ratio can be found.

$$f = \frac{W_f}{W_0} = \frac{1}{y_r} \cdot \frac{\mathrm{Q}_i}{Q_i + Q_s + Q_s} \tag{4.5}$$

In order to predict the width of the hydrodynamically focused stream, the unknown velocity ratio $y_r = \frac{V_f}{V_0}$.

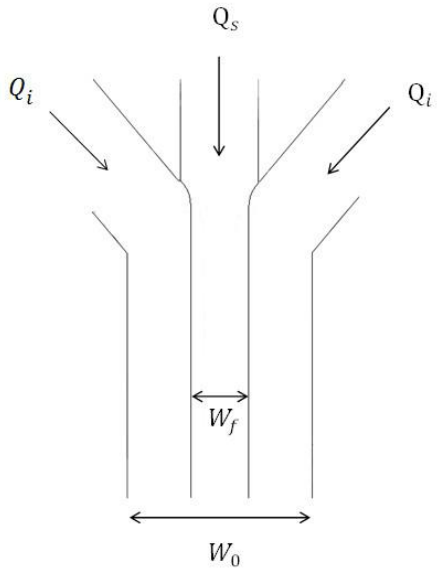

Figure 4.2. A schematic of the three inlet channels of the microfluidic device displaying hydrodynamic focussing of sample flow

Assumptions are made that the liquids are Newtonian and have a density (ρ) and viscosity (η), and all channels are the same height (h).

4.2.3. Theory of magnetism

Three vectors describe a magnetic field: **B**, the field induction, **H**, the field strength and **M**, the magnetisation of the medium. The detailed theory of magnetism is given by Zborowski [362]. Magnetism describes the interaction of materials in a magnetic field; this is dependent upon the material property, namely the magnetic susceptibility χ. Susceptibility is dependent upon the magnetisation **M** of atoms or molecules with the field **H**, which is equal to the relative permeability of the material in a vacuum (μ_r = 1).

$$\chi = \frac{|\mathbf{M}|}{|\mathbf{H}|} = (\mu_r - 1) \tag{4.6}$$

The magnetic field **H** is defined as:

$$\mathbf{B} = \mu_0 (\mathbf{H} + \mathbf{M}) \tag{4.7}$$

μ_0 is the magnetic permeability in a vacuum and **B** is the magnetic flux density.

The magnitude of the magnetic force acting on an MP in the direction of greatest change in energy density may be expressed as:

$$\mathbf{F}_p = \Delta\chi V \frac{\nabla|\mathbf{B}|^2}{2\mu_0} \tag{4.8}$$

$\Delta\chi$ the difference in magnetic susceptibility of the MP and the surrounding solution, and V the volume of the magnetic body [36].

4.2.4. Stokes's drag force

The magnitude drag force (F_d), defined by Stokes's law, acting upon a spherical object is given by:

$$\mathbf{F}_d = 6\,\pi r \eta \mathbf{u} \tag{4.9}$$

where r is the radius of the sphere, η is the viscosity of the suspending medium and **u** is the magnitude velocity of the spherical object [363, 364].

4.3. Method & materials

The materials and methods used to design a separation device using HDF, MFD and magnetophoresis are described in this section.

4.3.1. Microfluidic device

A custom designed MFD was manufactured (iBidi, Germany) in polydimethylsiloxane (PDMS), a schematic of the MFD is shown in Figure 4.3, the channel depth was 0.4mm, length 23.73mm and width of 3mm. The three inlets and three outlets allow for HDF at the inlet, and collection of the three separate fluid streams at the output.

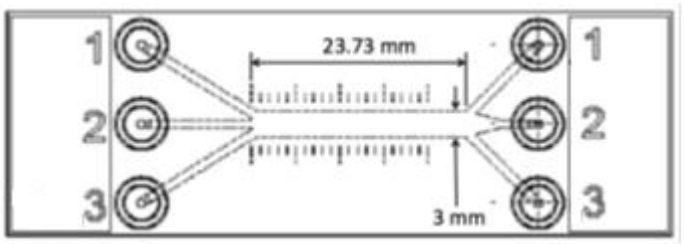

Figure 4.3. A schematic of the microfluidic device, channel depths of 0.4 mm

4.3.2. Magnet design

The primary step was to design novel magnet configurations that would reduce MP interaction with the side walls of the MFD and to enable the separation of MPs of any susceptibility. The software package FEMM was used to model the B-fields of two magnet configurations for use in the continuous-separation experiments. Magnets of dimensions 20 x 6 x 1.5 mm N42 Neodymium with a 1.2 kg pull (First4MagnetsTM, UK) were used in two configurations: a) a double magnet- and b) a quadrupole-configuration (Figure 4.4).

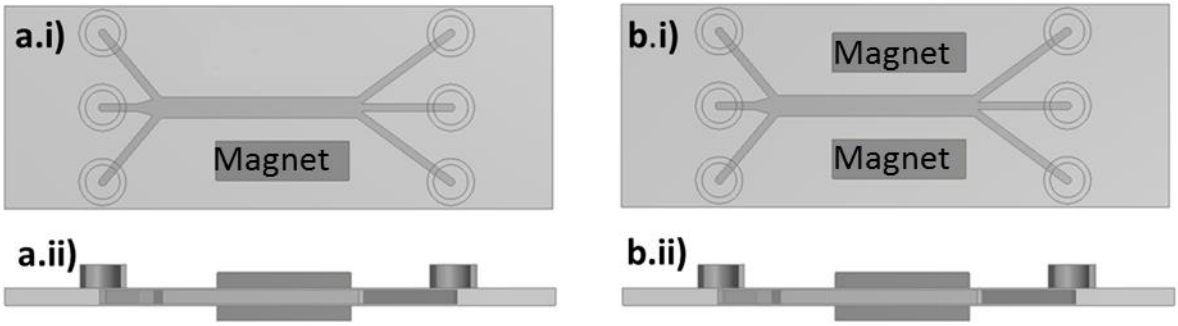

Figure 4.4. A schematic of the magnet configurations mounted upon the microfluidic device in a. double magnet and b. quadrupole and how the magnets are positioned on the microfluidic device from the i) top- and ii) side-views

4.3.3. Separation experiments

Fluorescent 1 µm MPs (superparamagnetic, fluorescent excitation 502 nm, emission 525 nm), were obtained from Chemicell (Germany). MPs (concentration of 10^6 particles/ ml) were suspended in blue ink to enable the HDF to be viewed clearly. The surfactant Pluronic F127 (Sigma-Aldrich) at 0.01% w/ v was added to the particle mixture to

prevent adhesion of MPs to the MFD surfaces. To demonstrate the separation of MPs from the sample inlet, a mixture of MPs and blue non-magnetic beads of 0.4 μm in size was used.

Prior to each experiment the MFD was flushed with DI and 0.1% F-127 surfactant for five minutes. Two hydrodynamic flows of DI and 0.1% F-127 Pluronic, were used to focus a sample flow containing the MP sample.

The MFD was connected to three 1.0 ml glass syringes (BD Biosciences, UK) mounted on Harvard syringe pumps using 0.5 mm inner diameter flexible tubing to introduce the flows to the device. The channels of the MFD were visualised and data recorded using a charge-couple device (CCD) camera mounted on a stereomicroscope and an inverted microscope. The outlet channels were connected by the same tubing to three 0.5 ml collection pots (Microfluidic Chip Shop, Germany) mounted on the MFD, which were capped after each experiment and removed for further analysis.

Samples were analysed using a BD Accuri C6 flow cytometer. A volume of 30 μl was analysed, core size 10 μm, on a fluidics setting of 8 μl/ min. Data was collected triggering with the FL-1 (510 nm) channel, with threshold setting of 8000 on forward scatter.

4.4. Results of the magnetophoretic-microfluidic separation

Simple computer models were used to determine the physical conditions of the magnetophoretic-MFD. The magnetic field was modelled using FEMM, and the velocity profile was determined using Matlab and fitted a parabolic flow regime.

4.4.1. Fluid dynamics and hydrodynamic focussing

It was important to understand the characteristics of the fluid as it travels through the MFD. The MPs experience forces from the magnetic field and a force from the fluid. In order to establish high separation efficiencies, these forces must equate to a greater pull towards the magnet, so that the MPs can be separated from the main sample flow and into a buffer flow for separation.

The Reynold's number (for total flow rates between 30 and 600 μl/ min) was calculated to be between 1 and 12; laminar flow is experienced within the MFD. This is distinctive of microfluidic channels [365]. An important characteristic of the fluidic dynamics is the parabolic flow through a rectangular channel and the resultant zero velocity at the internal surfaces of the channel. This flow regime is well documented in rectangular fluid channels [366]. When MPs hit a surface of the device, there will be zero velocity to drive the MPs along and out of the MFD. MPs will be deemed as "lost" if they arrive at an internal surface, as they are difficult to recover using continuous flow at low flow rates. In order for surface collisions to be minimised, and therefore the number of lost MPs, careful design of the magnetic field is necessary.

4.4.2. Hydrodynamic focussing

Lateral 2D HDF was achieved by focussing the central sample flow with two buffer flows channels 1 and 3 (Figure 4.5).

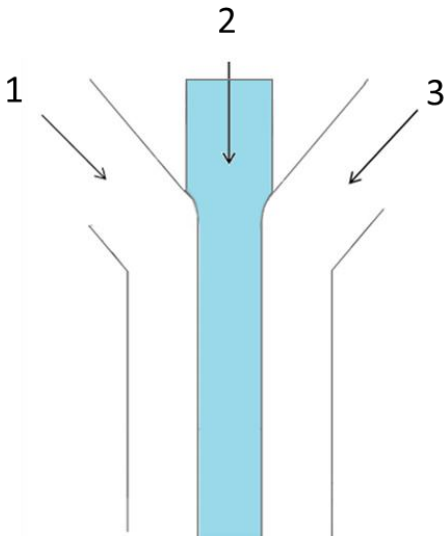

Figure 4.5. A schematic of the hydrodynamic focussing achieved by two buffer flows introduced in channels 1 and 3, and the coloured sample flow entering through channel 2.

In order to achieve steady state, the experiment was allowed to run for five minutes. It was found that a higher flow ratio produced a more narrowly focussed sample stream. Efficient HDF can only be achieved when the side-channel flows are equal or greater than the sample flow [361]. HDF was easily achieved over a wide range of flow rates (30 to 600 µl/ min). When conducting the separation experiments, the HDF was adjusted in each of the three inlet flows in order to fill, but not overspill, their respective exit channel.

4.4.3. Double magnet configuration

A novel configuration utilising two magnets was designed. Positioning the magnets in a double magnet configuration, one on top of the other (Figure 4.6), an ROM is observed in the horizontal plane. The magnetic gradient, which is both positive and negative within the device, results in the MPs traveling in the direction of the magnetic gradient (positive and negative) towards higher magnetic energy as displayed in Figure 4.7. The MPs then gather at the area of minimum magnetic-force, the ROM.

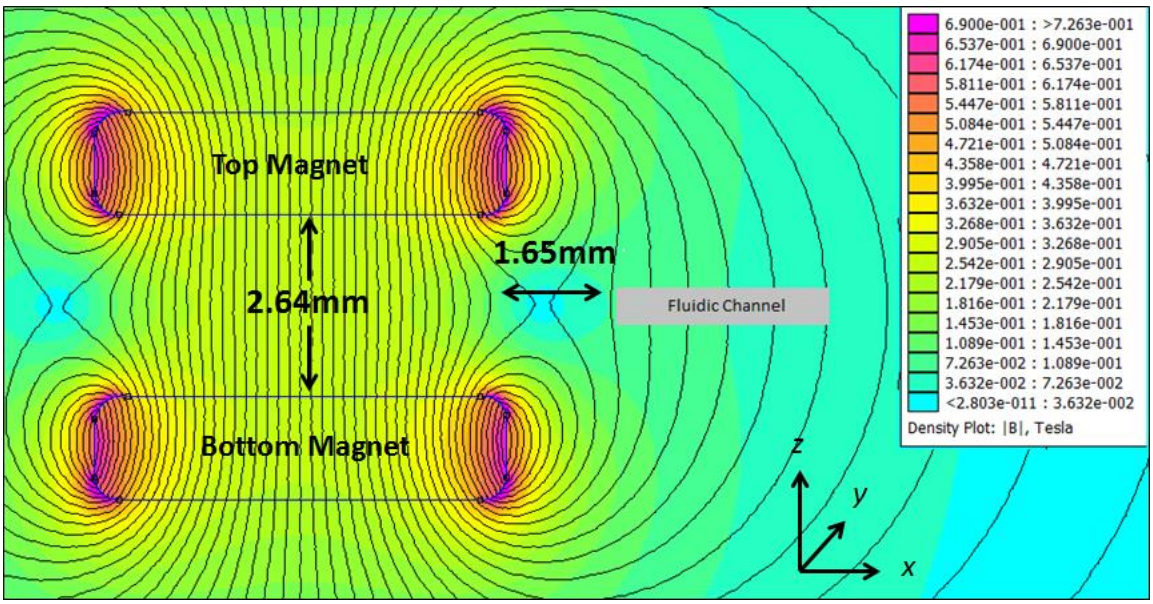

Figure 4.6. The magnetic flux lines of the double magnet configuration as modelled in FEMM

Careful positioning of the magnets 1.65 mm from the fluid-channel's edge, with the optimum 2.64 mm separation (data not shown) between the magnets, the ROM in the horizontal plane could be accurately positioned in channel 1, at 0.5 mm away from the channel's side wall (Figure 4.6). MPs entering the device in channel 2 were separated through magnetophoresis from the sample flow into the ROM, where no magnetic force is experienced. The MPs were removed from the MFD by the hydrodynamically focussed flow in channel 1.

The advantage of using a magnetic field of this design is the minimising of the number of MPs at the edges of the MFD, where the velocity profile is zero. Due to the zero magnetic force acting on the MPs in the ROM, theoretically, MPs of any susceptibility, size and concentration can be separated from a sample flow.

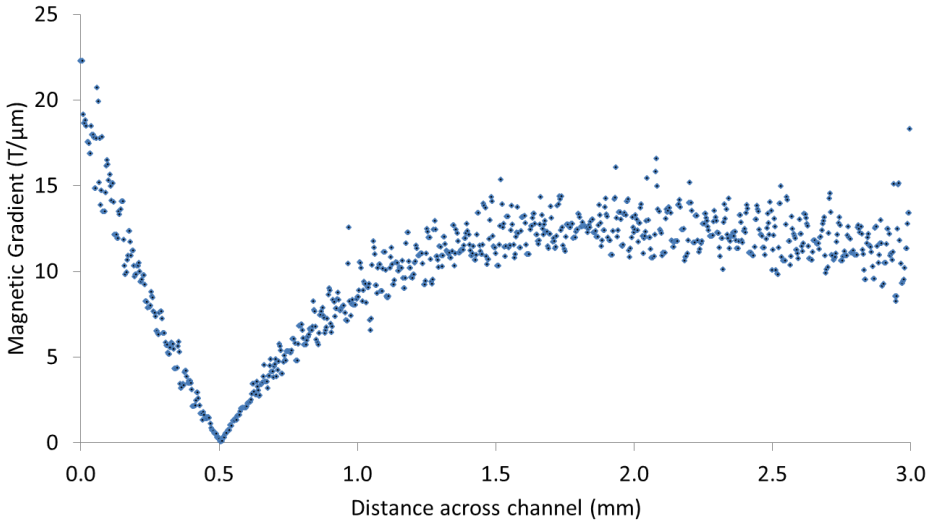

Figure 4.6. The magnetic force acting upon a magnetic particle across the width of the microfluidic device as modelled in FEMM

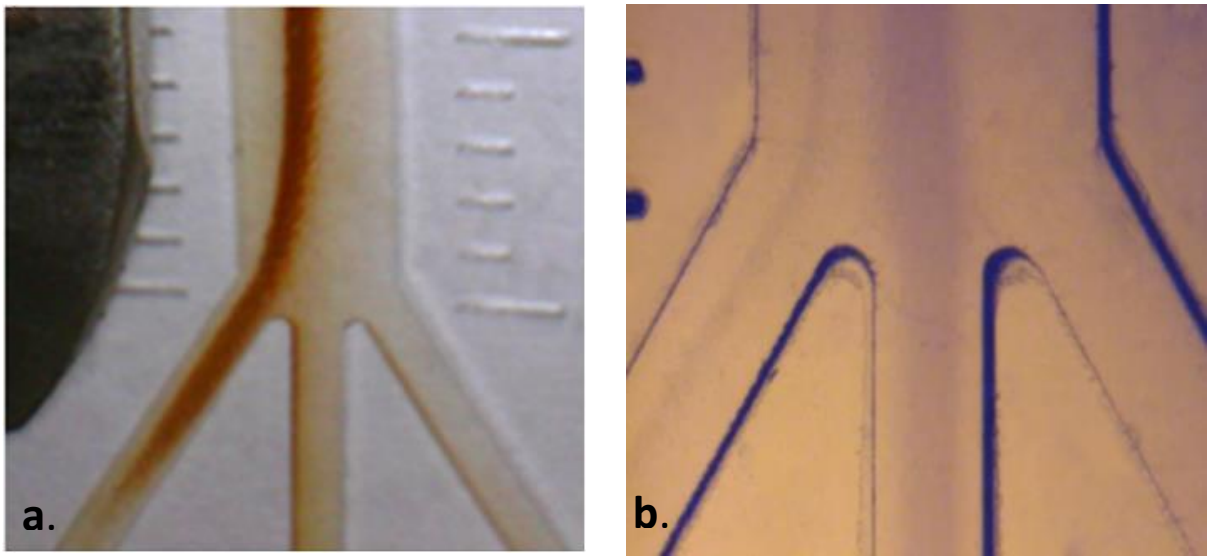

Figure 4.7. The exit end of the microfluidic device, highly concentrated magnetic particles aligned in the region of equilibrium starting from the sample inlet, channel 2, and exiting through exit channel 1 under a) zero flow conditions and b) continuous flow at higher magnification.

Figure 4.7a) displays the concentrated MPs under static conditions (i.e. zero flow) aligned in the ROM, exiting the device through channel 1. Figure 4.7a) shows that a clear separation of magnetic material was achieved. Figure 4.7b) shows a higher resolution image of the transport of MPs out of the exit channel away from the sample flow. This separation is again demonstrated in Figure 4.8; the orange coloured MPs are

separated from a mixture of magnetic and non-magnetic particles (blue) in the central flow, channel 2.

4.4.4. Separation of MPs using the double magnet configuration

The separation of MPs using the MFD-magnetophoretic separation device was determined using flow cytometry. The MPs, which were introduced through the channel 2, migrate to the ROM, where no horizontal magnetic force is acting upon them (Figure 4.8). A clear separation was visible; however, the percentage of MPs exiting through channel 1, when measured by flow cytometry, was low (Figure 4.10).

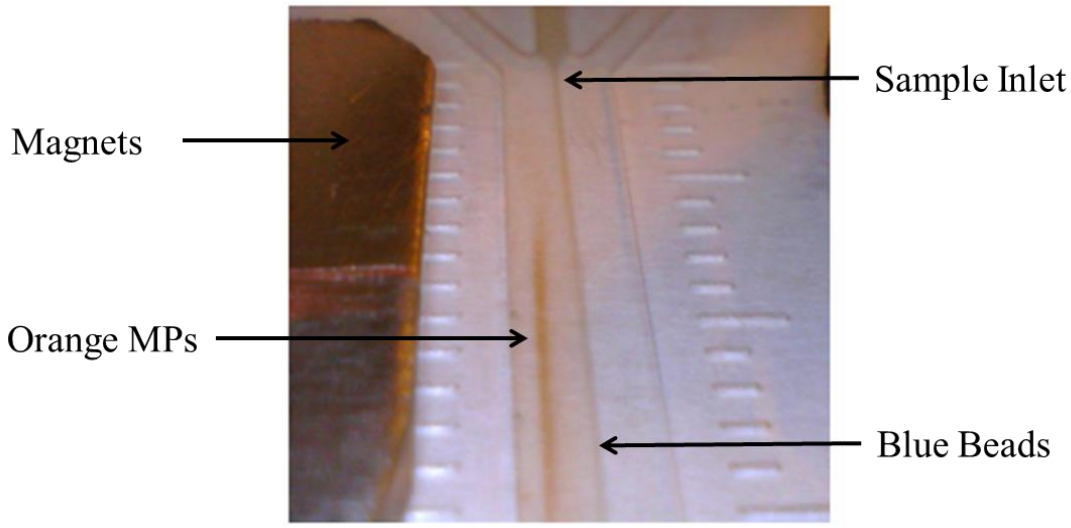

Figure 4.8. The separation of magnetic particles (orange) from a mixture of magnetic particles and blue non-magnetic beads achieved in continuous flow using the double magnet configuration

The results indicated that the majority of MPs were not deflected by the magnets and travelled straight through the device in the sample flow. The separation efficiency of the double magnet configuration was found to be negatively correlated to the total flow rate in the MFD (Figure 4.9). Flow rates lower than 50µl in each inlet could not be used due to instrumental limitations that interrupted the flow, making it appear turbulent with the introduction of mixing between flows within the MFD.

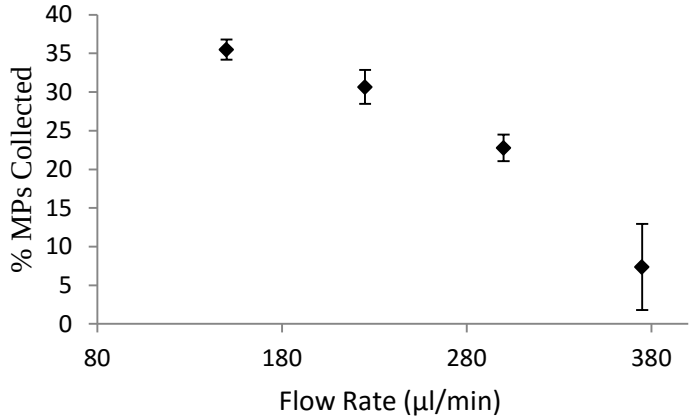

Figure 4.9. The correlation between flow rate and the percentage of the collected magnetic particles that were separated into exit channel 1 compared to the total magnetic particles collected from all three outputs (Error = 1 SD; n=3).

The field strength of the magnet and the magnetic susceptibility of the MPs will limit the maximum flow rates [355]. The aspect ratio of the flow rates in the channel inlets is kept as close to 1, whilst maintaining complete HDF. The device was designed so that MPs are drawn into and exit through channel 1. However, it can be seen from Figure 4.10 that the majority of MPs (> 65%) exited through channel 2.

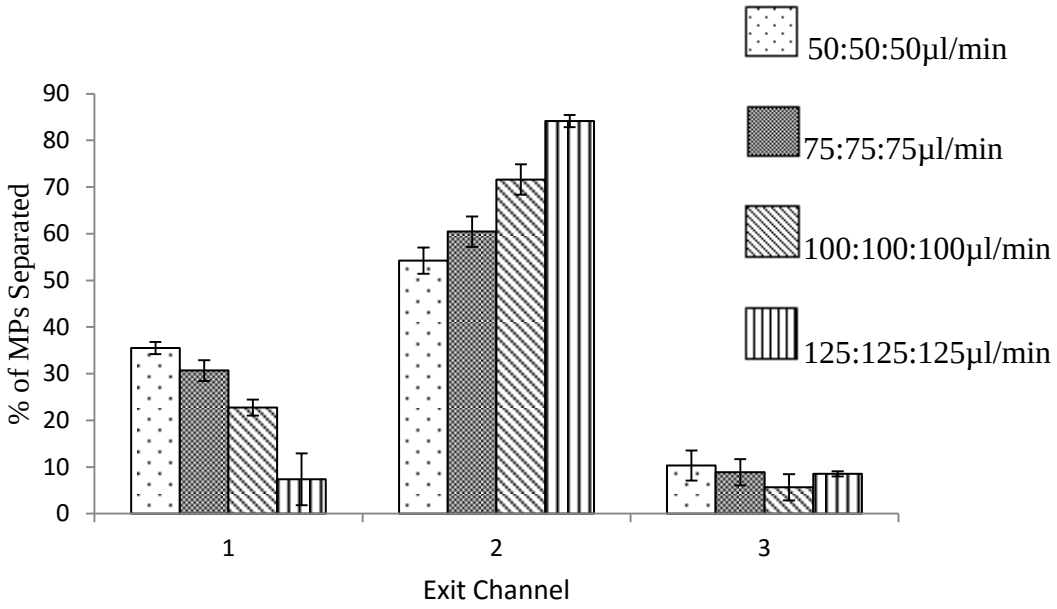

Figure 4.10. The percentage of magnetic particles recovered from each exit channel at different flow rates (Error = 1 SD; n=3)

Visual observations suggested that separation of MPs from the sample flow was achieved. MPs were deflected by the magnet from the central sample flow into the buffer flow. By eye, and using the low magnification of a stereomicroscope, this observation was confirmed. Further examination using higher resolution microscopy, revealed that the MPs were being deflected from the sample flow in both the *x* and *z* direction and were becoming trapped at the surface of the MFD, where they agglomerated and exited slowly out of channel 1 by rolling along the top surface. It was very difficult to centre the ROM in the middle of the MFD in the *y* plane. It is anticipated that slight misalignment of the magnets increased the number or collisions with the top of the MFD, increasing agglomeration. MPs became trapped at the surface and were separated by rolling along the top surface and out of exit channel 1.

Analysis using flow cytometry supported this observation, it was found that the majority of MPs (>65%) were not deflected from the main sample flow; the MPs did not have large enough residence time within the magnetic field to be separated. It is assumed that agglomerates were separated due to their increased magnetophoretic mobility, but single MPs passed straight through the device.

4.4.5. Optimisation of the quadrupole magnet configuration

Due to the low separation efficiency found for the double magnet configuration, a quadrupole magnet configuration (4.11) was used in further experiments.

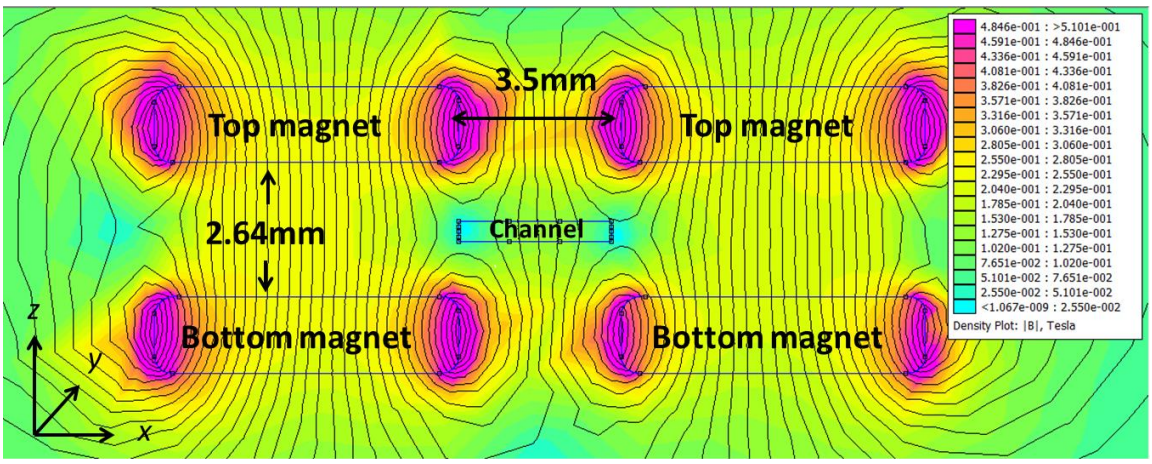

4.11. The FEMM model of the magnetic flux lines of the quadrupole configuration

The force acting upon the MPs was increased through use of the four magnets in the quadrupole configuration (Figure 4.12). The gap between the magnets was 3.5 mm, with a separation of 2.64 mm; the ROM in the horizontal plane was located at 1.5 mm away from the channel edge of the iBidi MFD.

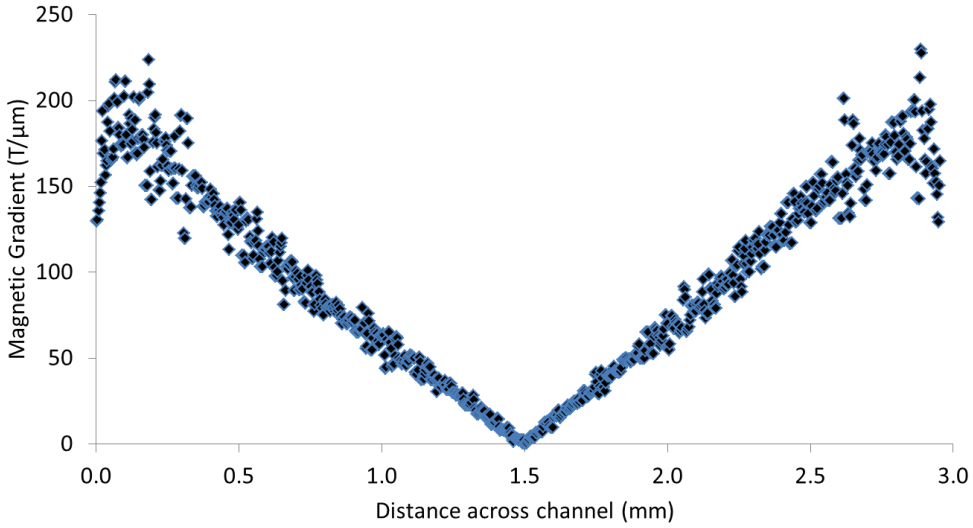

Figure 4.12. The magnetic force acting upon a magnetic particle across the width of the microfluidic device as modelled in FEMM

When using the quadrupole magnet configuration MPs were introduced in inlet 1, and separated from the sample flow into channel 2 (Figure 4.4). The ROM was positioned along channel 2 so that MPs migrated along the magnetic gradient to this point; the MPs

were then separated using the buffer flow, exiting through channel 2. As displayed in Figure 4.13, MPs located at the channel's edge will be situated within an area of high gradient and will be manoeuvred towards the centre of the device.

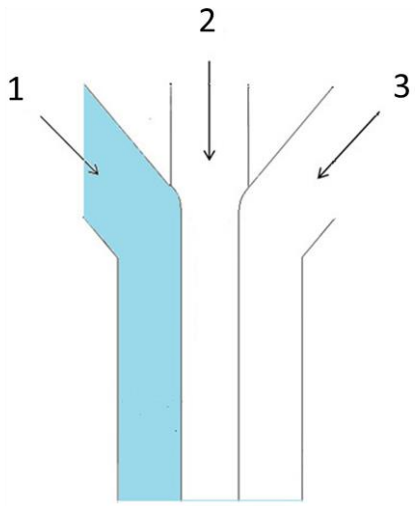

Figure 4.13. A schematic of the hydrodynamic focussing used with the quadrupole configuration, magnetic particles are introduced in channel 1 and separated into channel 2.

4.4.6. Separation using the quadrupole magnet configuration

The quadrupole configuration was more successful at focussing the MPs away from the sample stream and into a channel for separation. Although there was a definite migration of the MPs sideways into the central stream, there was also an upwards force acting upon the MPs, causing them to agglomerate at the surfaces of the device.

The separation efficiency using the quadrupole configuration in continuous flow was 55% (Figure 4.14). It was again observed that separation using the magnetophoresis-MFD under continuous flow did not allow enough time for all MPs to migrate into the central exit channel. Many were still found in the introductory exit channel. To improve this separation, a strategy of introducing MPs for 30 seconds, then pausing all flow for 60 seconds and repeating this for ten cycles, before using a fast flush of 1000 μl/ min for 10 seconds; termed a "pulsed" mode. This strategy aimed to increase the residence time of the MPs in order for them to migrate into the ROM and to be separated. Nearly 80%

of the MPs were separated from the sample flow using the pulsed mode and the quadrupole magnet configuration.

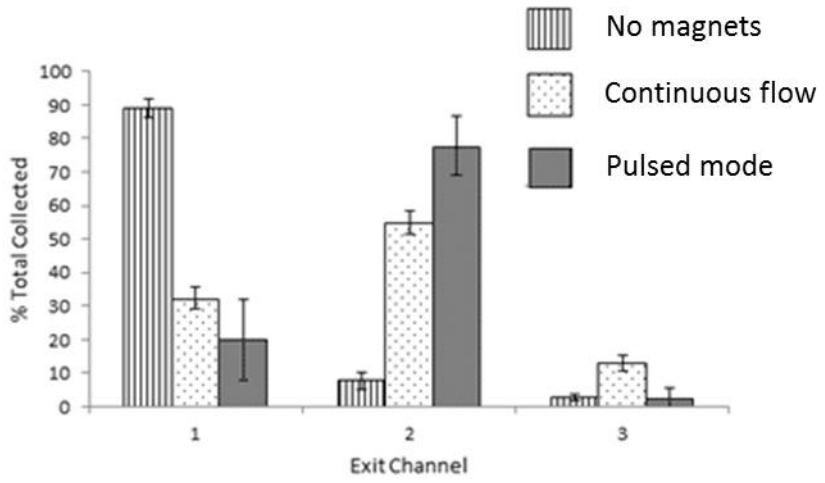

Figure 4.14. The separation efficiency of the quadrupole configuration in continuous and pulsed mode compared to the control of no-magnets (Error = 1 SD; n=3).

4.4.7. Separation and concentration of MPs from a sample

Although numerous microfluidic devices have been described [210, 236, 237, 310, 311], further development is required to establish higher separation efficiency whilst maintaining target cell purity [240]. The MFD incorporating magnetophoresis as described in this Chapter goes someway to improving upon previously described devices. It enables the continuous separation of MPs from a complex sample without pre-enrichment and is comparable to separation described by Xia *et al*, [369] where separation efficiencies are detailed as being between 50 and 90%.

The MPs that were initially freely dispersed throughout the larger water sample were concentrated and separated from the original sample matrix. The separated and concentrated MPs will contain bound and unbound MPs. A further analytical step is necessary in order to determine the number of bacteria that have been captured by the MP. This is described in the Chapter 5.

The separation efficiency may be improved by reducing the dimensions of the channel. The described MFD is 3 mm in width. The MPs need to migrate at least 0.5 mm in the *x*

direction before they are “separated” and can be transported in the buffer flow. When operating in the pulsed mode, an increase in the “pause” time will allow an increased residence time for the MPs to migrate to the ROM. This is expected to increase the separation of MPs from the sample flow.

The magnetic susceptibility of the MPs determines the magnetic moment and hence the force exerted upon the MPs within a magnetic field [370]. In order to increase the flexibility of the MFD, MPs with a higher magnetic susceptibility will enable the use of increased flow rates due to the increased magnetic force; the residence time required within the MFD will be reduced. A study into suitable commercially available MPs is conducted in Chapter 5.

The separation efficiency using the “pulsed” mode may be further improved through physical alterations to the magnet. Shaping and tapering of the magnets at the exit ends will reduce the magnetic flux, and therefore the pull on the MPs, allowing them to be flushed from the device more easily.

An exploration of the vertical forces experienced by the MPs should be conducted using 3D finite element methods to explore the trajectories of the MPs within the magnetic field. Studies on continuous separation using magnetophoresis have neglected the migration of MPs in the *z* direction [197]. A method for counteracting the loss of MPs within the MFD could be to introduce a viscosity gradient. Increasing the viscosity of the buffer flows would reduce the velocity of the MPs as they migrate towards the magnet. This would also slow the movement of MPs in the *z* direction.

Despite the HDF, MPs are introduced at different positions into the MFD and were therefore subjected to different forces. These different forces are responsible for the trapping and “loss” of MPs in the MFD. 2D HDF was described in the MFD, however, the particles will still experience vertical forces [139]. To overcome the limitations of 2D HDF, a 3D HDF MFD should be considered. Flow cytometers achieve HDF by

introducing flows via a smaller capillary within a larger capillary, thus obtaining a simple, yet effective method of circular and 3D HDF. The use of 3D HDF and a magnetic separator was described by Zborowski & Chalmers [371]. In order to increase the predictability of the trajectories of the MPs, a more localised introduction of the MPs into the device should be found. Reducing the dimensions of the device and making use of HDF, but in 3D, might help mitigate this problem.

Magnetic separation permits the isolation of target cells from heterogeneous, crude samples [282]. Microfluidics has increased in popularity within scientific research over the past decade. The versatility they offer in design allows for an array of applications. Laminar flow that is achievable at the micro-scale enables highly predictive characteristics and for continuous separation to be achieved. The ability to incorporate automation and analysis on-chip is an attractive characteristic. Microfluidic separations are still troubled by trapped air-bubbles and blockages. Such phenomena are mitigatable, but are still an occurrence that can disrupt separation. The low flow limits observed in this experiment will restrict the amount of sample that can be processed. Running multiple MFDs in parallel will increase the concentration and separation of larger volumes, and could also facilitate multi-analyte detection, which is desirable when monitoring water for contaminants.

4.5. Conclusions

An MFD incorporating magnetophoresis was designed to separate MPs from a sample flow. A dilute sample of MPs was concentrated and presented for further analysis. Two novel magnet configurations were designed to remove MPs from a sample in continuous flow.

Low magnification viewing of the separation indicated a good separation of the MPs. However, analysis by flow cytometry highlighted that many MPs passed through the device without being deflected from the sample flow. Increasing the residence time of

the MPs by introducing a “pulsed” flow regime increased the separation of MPs from the sample flow. The quadrupole configuration, when operated in a pulsed mode, was able to separate nearly 80% of the MPs from the sample flow

.

5. Magnetophoretic velocities of superparamagnetic particles, agglomerates and complexes

The objective of this Chapter is to explore the understanding of how MP-capture assays perform by measuring mobilities of MPs, when aggregated together or attached to non-magnetic beads (NB). The magnetically induced velocities of self-assembled MP chains were measured and found to meet the proposed models. A study into the zeta potential of the MPs was completed to determine a scenario for maximal electrostatic interactions and efficient capture of the MPs to a target. MPs were bound to biotinylated NBs, representing attachment to a disease biomarker. The drift velocity of MP chains and MP-NB complexes in a gradient magnetic field was compared. This study will enable the accurate prediction of particle velocities and trajectories and can mimic the case of a bacterium or other cell bound to an MP.

5.1. Introduction to magnetophoretic separations

Due to the commercial availability, low cost and easy functionalization of MPs, their use in the separation and detection at the micro-scale is ever increasing. MPs have been described in many batch applications, which include but are not limited to the detection of pathogenic bacteria in the environment [141, 354] and in food [372, 373].

In clinical settings, the use of MPs for the recognition of biomarkers from blood [374–376], including nucleic acids, microvesicles [345] and proteins [377], have been documented along with applications in biomedical imaging [378]. Environmental contaminants have been removed through adsorption to MPs [379], and algae have been harvested using the same technique [380].

A simple and reliable method is required to determine the magnetic characteristics of MPs in order to enhance the predictability for *in vivo* applications. A better

understanding of the properties of MPs will allow for their use in more advanced, continuous-flow systems [381].

A study was conducted into the magnetic properties of four commercially available MPs, using light microscopy. The aim was to develop a better understanding of the movement of the particles within a magnetic field, as single particles, self-assembled chains and as complexes bound to a NB. A diameter of 1 μm was chosen for the NB as this is representative of the approximate size of bacteria and specifically *E. coli*.

5.1.1. Superparamagnetic particles

Superparamagnetism refers to the random magnetisation of magnetic crystallites in the absence of an external magnetic field [370]. The unique properties of superparamagnetism enable the free dispersion of MPs throughout a sample matrix. The later application of an external magnetic field allows MPs to be focused, separated or concentrated from a sample, at a specific location. When required, removal of the magnetic field results in magnetic relaxation of the MPs, i.e. they "switch off" [276], allowing the MPs to be re-dispersed and removed from the location.

There are a variety of commercially available MPs with different manufacturing procedures and therefore differing characteristics. The loading of iron oxide nanoparticles into a silica shell, for example, occurs either as dispersed particles within the silica shell or as a group forming the core [382]. It can then be expected that each brand of MPs will behave differently when subjected to a magnetic field.

The response of a magnetic material to an applied magnetic field is termed magnetic susceptibility [362]. Magnetic susceptibility is an important parameter, but may vary greatly [370]. Given this variation, it is not sufficient to determine only the magnetic susceptibility. The susceptibility provides an approximation of magnetic responsiveness in *in vivo* applications [383]. However, the MPs' trajectory and induced magnetic velocity can be better calculated from experimentally determined magnetic mobility.

5.1.2. Functionalised magnetic particles

The ability to coat several superparamagnetic nanoparticles with a silica or polystyrene shell allows the magnetic content to be maximised, increasing the magnetic mobility of the particle, while maintaining the superparamagnetism (which is dependent upon the nanoparticle size) [384]. The coating encases the toxic iron oxide content; as such the conjugate becomes biocompatible [378].

Functional MPs are used in a variety of applications for the capture, transport and detection of magnetically labelled cells [185]. The functionalization of a microparticle is achieved through the attachment of a biologically active component to its surface, for example, a ligand, an amino acid or a protein [385]. A specific capture molecule may be immobilised upon the surface of an MP [220]. When a particle comes into contact with a target cell, a binding event occurs. The target cell inherits the magnetic properties of the MPs [350] and will thus be influenced by a magnetic field. The most widely used capture method is the immunological antibody-antigen interaction [354], or a protein-ligand interaction (as was used in this study). Immuno-magnetic separation is generally an efficient and rapid method to perform and can be achieved in almost any sample matrix [370].

5.1.3. Streptavidin-biotin binding

Streptavidin-biotin binding has one of the highest association constants in biochemistry [386]. This ligand-protein interaction acts as a good model for binding due to its low cost and the considerable enthalpy generated (approximately 10^7 kJ/ mol) [387]. Biotinylation is a popular method for attaching proteins, carbohydrates and nucleic acids to particles. Due to the small size of biotin, it is unlikely to change the natural functions of the molecule to which it is attached [388].

Given the strong binding properties to biotin and the ease with which proteins may be biotinylated, many manufacturers offer MPs coated with streptavidin. This binding

interface was used in this study to demonstrate the potential for using immuno-labelling of MPs for target detection through attachment of a biotinylated antibody to streptavidin coated MPs.

There are many conjugation methods for coating particles with binding molecules. The linkers that are used to attach the molecule to the particle surface vary in length. Two types of biotinylated beads were used as mock biomarkers in this study. The first bead had biotin attached via a “short” linking arm (SLB); the second with biotin attached by a bespoke “long” linking arm (LLB) as supplied by Chemicell (Germany), with four additional methylene bridges in the linking arm attaching biotin to the bead. The particles used in this study are listed in Table 5.1.

5.1.4. Zeta potential of magnetic particles

All suspended particles carry a charge; the components of the MPs and interaction with surrounding media give the particle an electrical charge. A double layer is formed between a particle and the suspending medium, the first layer, named the Stern-layer, contains immobilised ions surrounded by the diffuse layer [81]. The potential between the diffuse layer and the suspending medium is measurable and is termed the zeta potential [389]. The zeta potential is measurable by commercially available instruments such as Malvern Instruments’ Zetasizer Pro. Electrophoretic light scattering is used to measure the electrophoretic mobility of a particle towards either the cathode or anode, and the Helmholtz-Smoluchowski equation [324] used to extrapolate a value for the zeta potential.

To establish efficient binding of MPs to a target, it is important to know the charge of the binding particle and the charge of the target particle. If both particle types carry the same charge when suspended in the solution, then rather than binding of the MP to the target, the particles will be repelled from each other and will remain isolated.

Table 5.1. The six types of micro-particles used in the study and their individual physical and surface characteristics

Manufacture	Brand	Size (um)	Magnetism
Chemicell	ScreenMAG/G - Streptavidin	1.00	Superparamagnetic
Dynabeads	MyOneT	1.05	Superparamagnetic
Dynabeads	MyOneC	1.05	Superparamagnetic
Dynabeads	M270	2.8	Superparamagnetic
Chemicell	screenCORE/RR-Biotin Short	1.00	None
Chemicell	screenCORE/RR-Biotin Long	1.00	None

Information regarding the charge of Dynabeads, as used in this study, is available from the manufacturer [390]. However, charge information for the Chemicell particles was not available. A study into the zeta potential of the Chemicell particles was conducted in order to gain an approximation of the isoelectric point and charge of the particles across a pH range. Ideally, the solution should have a pH such that the MP and NB have opposite charges to promote binding.

5.1.5. Continuous separation

In order to maximise the potential for MPs in ultrasensitive detection of *E. coli*, there is a need to improve their extraction from a continuous flow of assay solution. The continuous separation from a sample flow will allow the use of MPs in even more diverse and complex systems. This will have advantages; for example within environmental applications for the removal of contaminants from wastewater, or in a medical context, for the extraction of bacteria from a patient with septicaemia [391].

Continuous methods have been described [355]. However, these methods meet certain difficulties. The agglomeration of MPs is a particular problem. The greater the number of MPs within close proximity to each other, the greater the magnetic force acting upon them. When in high concentration, particle agglomeration is unavoidable [392]. An understanding of the magnetic properties of particle agglomerates is required to allow for predictability when designing a continuous flow system.

5.2. Transport model

There are two dominant forces which act upon MPs when in a magnetic field. Primarily, the magnetic force imposed by a gradient field and secondly the Stokes's Drag which is generated in the opposite direction to movement, these formulae are detailed in Chapter 4 (equations 4.8 and 4.9).

5.2.1. Magnetophoretic velocity

The magnetically induced velocity, **u**, upon an MP is then determined when these forces balance:

$$\mathbf{u} = \frac{\Delta\chi V}{6\pi r\eta}\frac{\nabla|\mathbf{B}|^2}{2\mu_0} = \mu\frac{\nabla|\mathbf{B}|^2}{2\mu_0} \tag{5.1}$$

where $\Delta\chi$ the difference in magnetic susceptibility of the MP and the surrounding solution, and V the volume of the magnetic body, r the radius, η the viscosity of the suspending medium μ_0 is the magnetic permeability in a vacuum and **B** is the magnetic flux density and μ is the magnetophoretic mobility of an MP [362]. The magnetic flux density was determined by modelling the magnetic configuration in the finite element software FEMM.

The velocity of the MPs as they traversed the FOV was determined using the tracking mechanism of ImageJ and the plug-in MJtrack. Rearranging Equation 5.3 enables the magnetic mobility to be derived from the measured velocity:

$$\mu = \frac{u}{\nabla|\mathbf{B}|^2/2\mu_0} \tag{5.2}$$

5.3. Materials and methods

The magnetophoretic mobility of four types of MPs was determined using light microscopy, and tracking of individual MPs using the ImageJ software package

(http://rsb.info.nih.gov/). The magnetically induced velocity was determined for a single MP, chains and MP-NB complexes. The zeta potential of particles was determined using a Malvern Zetasizer Pro and the isoelectric point of the Chemicell particles was derived from this data. In total, this study extends to six types of particles.

5.3.1. Superparamagnetic particles

Commercially available ScreenMAG-streptavidin coated MPs and ScreenCORE biotinylated silica beads were obtained from Chemicell (Germany) of 1 µm in size. Dynabeads MyOneC, MyOneT both of 1.05 µm in size and 2.8 µm particles M270 were purchased from Invitrogen, UK [390].

5.3.2. Mobility study

To compare the mobility of the four types of MPs, the drift velocity of the particles, in stationary liquid, within a known region of the magnetic B-field was determined. Using an inverted microscope and magnification that allowed the clear viewing of 1 µm particles, the particles were observed in a Fast-read microscope slide (Immune Systems, UK) which contains a set of easy-fill fluid "observation chambers" (Figure 5.1) of dimensions 190 × 100 × 0.1 mm. Each observation chamber has a counting grid pre-etched to its surface for easy determination of viewing location. MPs were observed moving towards the magnet and their velocity measured, but data from MPs that travelled with atypical velocity were ignored from the analysis. Selecting velocity data in this way is necessary to avoid including data from beads that are clearly interacting with the chamber's internal surfaces or close neighbours, noting that the channel depth size is just 100 µm.

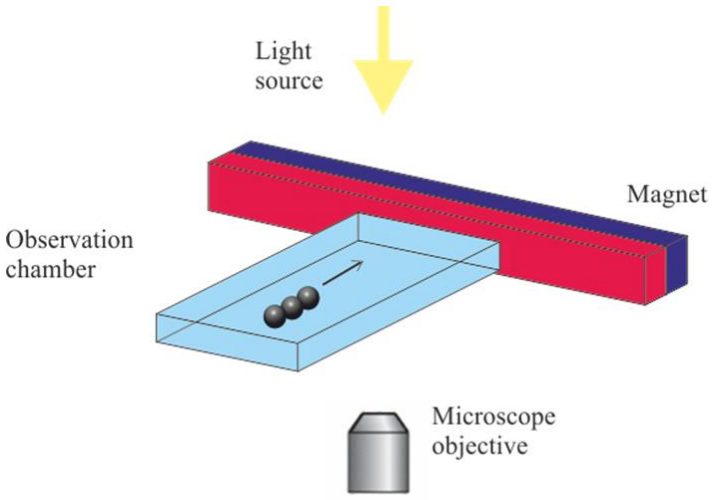

Figure 5.1. A schematic of the experimental setup used to determine the magnetically induced velocity of magnetic particles, as single particles and self-assembled chains

5.3.3. Binding observations

All particles were washed in TE buffer three times before being diluted to a concentration between 6 -7 × 10^7 particles/ ml. MPs were re-suspended in DI. In order to enable the binding of MPs to the biotinylated silica beads, 250 µl of the silica beads were added to the 250 µl MPs and incubated with steady rotation for two hours.

5.3.4. Observations

All particle types were diluted to within a range of 6-7 × 10^7 particles/ ml in DI. A volume of 20 µl of each MP solution was pipetted into the Fast-read observation chamber. After the particle solution had filled the chamber and particles were stable, an external magnetic field was applied by accurately positioning a permanent N42 neodymium magnet (Magnets4U, UK) adjacent to the observation chamber (8 mm from the viewing area) as illustrated in Figure 5.1. Video frames were recorded of the particles moving towards the magnet using µEye software and a CCD camera (Imaging Development Software, Germany) (33 frames/ second) and were analysed offline using the ImageJ software. MPs were tracked over a distance of 55 µm; the equivalent of one traverse of the field of view (FOV) of the camera. The velocity of the MPs was calculated using the ImageJ software.

5.3.5. Zeta potential

Zeta potential measurements were taken using a Zetasizer (Malvern Instruments, UK) and the method followed as described in Section 3.2.2. The zeta potential measurements were taken across a range of water with pH between 3 and 10.

5.3.6. Software packages

The B-field of the magnet through the observation channel was modelled using FEMM (http://www.femm.info/wiki/HomePage) a finite element method software package for magnetics; $\nabla|\mathbf{B}|^2$ was estimated to be of the order of 10^{-6} T^2/ m. Particle trajectories were tracked using ImageJ video tracking software.

5.4. Results for the magnetophoretic mobilities of magnetic particles

A study into the magnetophoretically induced velocity upon MPs was conducted. Single particles, chains and MP-NB complexes were analysed. Velocity data was compared to predictions derived from a simple drag force model to determine if relative drift velocity of MP-NB complexes could be a useful parameter in a biosensor. MPs bound to a non-magnetic biomarker, for example, are predicted to have a lower drift velocity (i.e. mobility) compared to a single MP; detection of bacteria is given by interpretation of the relative mobility of a population of such particles.

5.4.1. Magnetophoretic mobility of magnetic particles

The Dynabeads M270 of size 2.8 μm had the largest drift mobility, attributed to the larger quantity of iron present in this type of MP. The Chemicell MPs had the lowest mobility. The magnetically induced drift velocity of the MPs is given in Table 5.2.

*Table 5.2. The magnetophoretic induced velocity obtained for the four different types of magnetic particles in water (n = 20). (*Not specified by manufacturer)*

Particle	Diameter μm	Iron %	Velocity μm/ s	Velocity SD
Chemicell	1	*	12.19	0.36
MyOneC	1.05	26	15.58	0.28
MyOneT	1.05	26	17.32	0.13
M270	2.8	14	59.01	0.18

Given the heterogeneity of the MPs used within this study, inevitably there is a range of mobilities which may be attributed to the different size, shape and iron content. As described in Section 5.3.4, care was taken, when recording observations, to discount MPs interacting with internal surfaces of the observation chamber.

5.4.2. Magnetically induced velocity on magnetic particle chains

Chains of MPs were evaluated for their velocity as they passed through the FOV. As the chains self-assemble along the direction of the magnetic field lines, it is possible to establish drift with either orientation of the chain, by using a different configuration of the permanent magnet. The orientation of the chain is in the same direction as the pole axis of the magnet as illustrated in Figure 5.2. In order to explore further the effect of Stokes's drag force upon chains of MPs and to demonstrate the models proposed, two experimental configurations were investigated.

In the configuration shown in Figure 5.2i, the long axis of the magnet was placed parallel to the observation chamber (Figure 5.2iii). MP chains are formed along the direction of the magnetic field lines and the chain drifts in the direction of increasing magnetic energy density, i.e. towards the magnet. In configuration Figure 5.2ii, the long axis of the magnet was rotated 90 degrees, perpendicular to the observation chamber, and the magnetic pole axis rotated. The MP chains will again form along the magnetic field lines but the direction of the drift orthogonal to the long axis of the chain. The chain travels towards the magnet but in an orientation with higher Stokes's drag (Figure 5.2iv).

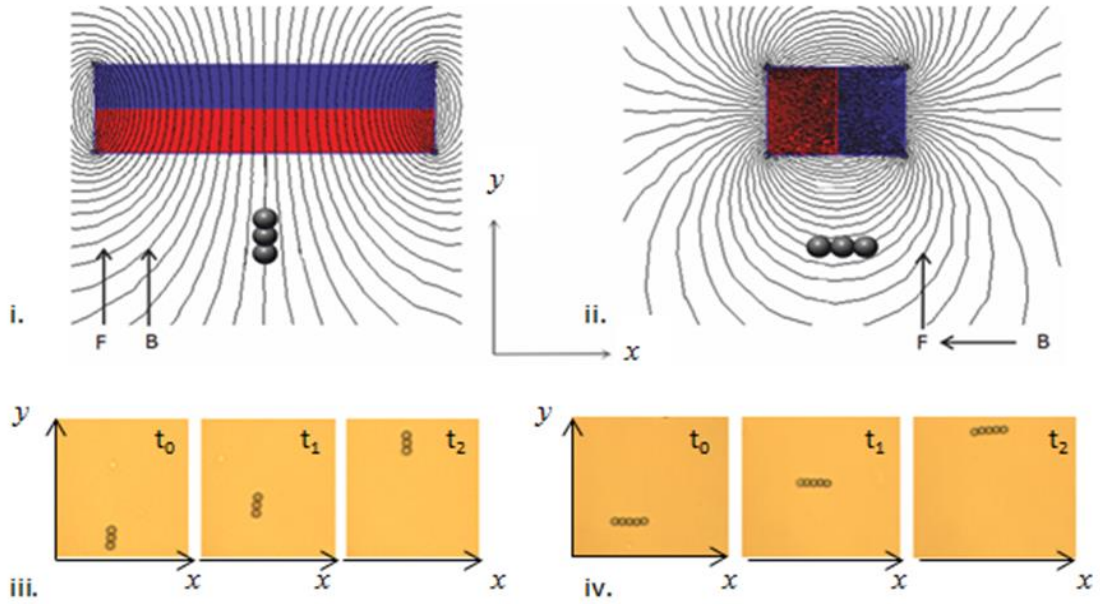

Figure 5.2. A schematic of magnetic particles travelling towards a permanent magnet in configuration (i) showing the B-field lines, the direction of B-field (B) is parallel to the direction of maximum magnetic force (F). In configuration (ii) the B-field and force are perpendicular

(iii) Sequential images of a chain of three MPs travelling towards the magnet at three time intervals (t_0, t_1 and t_2), and (iv) a chain of five MPs aligned perpendicular to the magnet at three time intervals (t_0, t_1 and t_2). Chains assemble in the B-field direction. [Not to scale.]

The magnetic drift velocity observed for the case of a chain of n identical spherical particles, moving either with the long axis of the chain in the direction of the drift or perpendicular to the drift, can be estimated by equating the magnetic forces to an approximation of the corresponding drag force. Following [393] the drag on a longitudinal elliptic body in low Reynolds number flow can be adapted for this study by assuming a circular cross-section equal to the diameter of the spherical particles, a, and the length of the long axis determined by the number of particles in the chain, $n \times a$.

$$F_{\parallel} = 4\pi\eta a v \frac{n^2 - 1}{\frac{2n^2 - 1}{(n^2 - 1)^{1/2}} \ln[n + (n^2 - 1)^{1/2}] - n} \tag{5.3}$$

The above equation applies for the case when $n \geq 2$ and is the drag force when the long axis of the n-particle chain is aligned in the direction of a scalar drift velocity, v, i.e. configuration (i). When the drift velocity is perpendicular to the long axis of the chain, i.e. configuration (ii), the drag force approximates as

$$F_{\perp} = 8\pi\eta a v \frac{n^2 - 1}{\frac{2n^2 - 3}{(n^2 - 1)^{1/2}} \ln[n + (n^2 - 1)^{1/2}] + n} \qquad (5.4)$$

The magnetic force acting on a body of n MPs in a linear chain will be taken as simply n times the force on a single MP. In other words, dipole interaction between neighbouring MPs has been determined to be negligible compared to changes in the drag force. Using equation (5.1) equated to either (5.3) and (5.4) leads to the magnetic drift velocities for the two orientations of the chains. In order to compare the mobility of an n-MP chain with the model described above it is sufficient to consider a normalised velocity obtained by dividing by the magnetic drift velocity for a single bead, u. Figure 5.3 shows the experimental data compared to the model (dotted curve), and within the expected statistical error confirms that the longitudinal elliptical body approximation is a sufficient predictor of the drift velocity of n-MP chains.

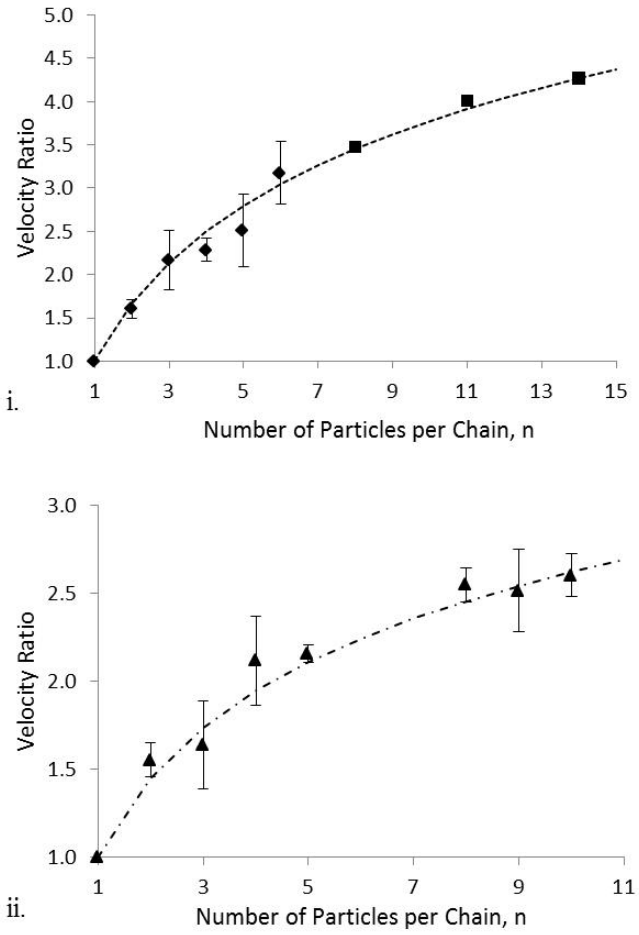

Figure 5.3. The normalised ratio of the magnetophoretically induced velocity per chain of magnetic particles to the magnetophoretically induced velocity of a single magnetic particle travelling towards a magnet i) parallel and ii) perpendicular to the field lines. The dotted curves represent the data calculated from the proposed model. Error = 1 SD. The data points represented by a square are single data results with replicates.

The magnetically induced velocity on a single MP of each type was normalised to 1. This enabled the data collected from all four MP types and, the chains they formed, to be directly comparable. Figure 5.3 displays the normalised velocity data of the chains formed by all MP types.

5.4.3. Zeta potential measurements

The zeta potential of all Chemicell particle types was measured at different pH values. An estimation of the isoelectric point was found to be at pH: 5.5 for the ScreenMAG-G MPs, 6.2 for the SLBs and 6.9 for the LLBs (Figure 5.4). The zeta potential measured for the Dynabeads varied from that listed by the manufacturer (Table 5.3). The conditions

under which the manufacturer measured the charge are not specified. The zeta potential is influenced by many characteristics, such as concentration and the suspending solution [394]. Consequently the charge measurements tabulated here are only comparable within this study.

In order to maximise binding of an MP to a target, the zeta potential of the particles was investigated to determine the charge of particles and to predict electrostatic interactions. The charge of the particles at pH 7 was determined to be negative and results in an electrostatic repulsion rather than an attractive force to the NB. Secondly, the zeta potentials of the formed MP-NB complex should be the same as the internal surfaces of the device they are within. The same electrostatic charge will create a repulsive force between the internal surfaces of the observation chamber and the MP-NB complex; reducing MP-surface interactions.

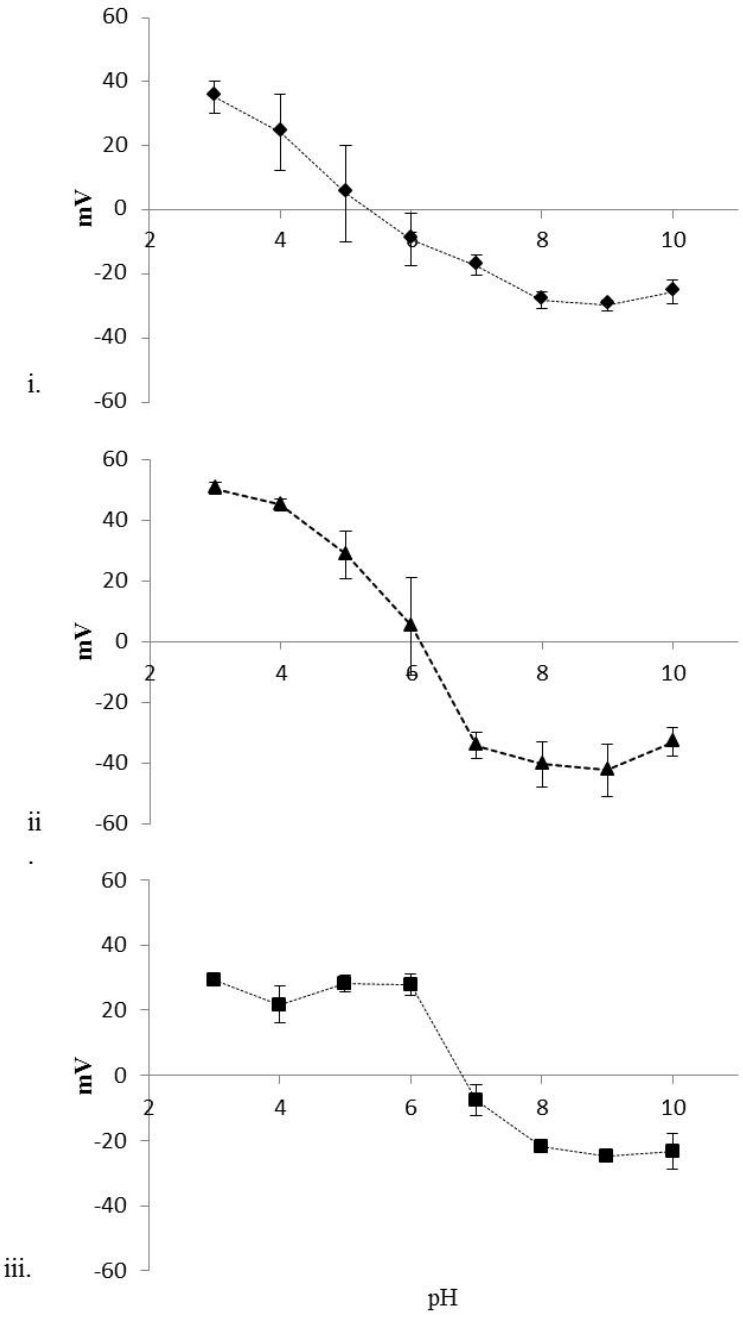

Figure 5.4. The zeta potential of Chemicell i) streptavidin-ScreenMAG-G ii) short-linker biotinylated silica and iii) long-linker biotinylated silica beads, suspended in water adjusted to different pH values. The crossing of the horizontal axis determines the isoelectric point. Error bars denote the standard deviation of the individual measurements (Error =1 SD; n =15).

Table 5.3. The surface properties of the magnetic particles and silica beads used within this study (data not provided by manufacturer).*

Particle	Isoelectric Point pH	Charge pH 7 mV	Zeta pH7 mV	Protein/Ligand Attachment
ScreenMAG/G	5.4	*	-17.39	Aminated
MyOneT	5.0	-10	-16.04	Tosylactivated
MyOneC	5.2	-35	-20.57	Carboxylic
M270	4.5	-50	-28.28	Carboxylic
ScreenCORE/SL	6.1	*	-34.22	Aminated
ScreenCORE/LL	6.9	*	-7.68	Aminated

5.4.4. Bound particles

When incubating MPs with the SLBs, paired bindings were observed to be extremely rare. The same difficulty was not found when binding MPs to the LLBs. The binding of the SLBs was difficult for all MPs types in DI. However, little or no binding was seen with the SLBs with the larger M270 MPs. As discussed in Section 5.4.3, the electrostatic forces may inhibit binding. The short linking arm may not be brought into a region that would enable linkage with the streptavidin site. The same phenomenon was not experienced when binding the LLBs, i.e. in this case binding appeared to be immediate, suggesting that the electrostatic forces were circumvented by the extra length of the binding linker (data not shown). The results presented are for only the LLBs bound to the various types of MPs.

The bound MP-NB complexes were tracked and the velocities calculated. The complexes travelled at 75 – 85% of the velocity of one MP. The predicted velocity is a factor of 0.8 times the velocity of a single MP due to the additional Stokes's drag introduced by the bound NB (as per equation 5.4). In all cases the NB aligns behind the MP, in the direction of travel, regardless of the magnet configuration.

The data in Figure 5.5 displays single MPs bound to single NBs with a 1 µm diameter. *In vitro* experiments may find single MPs bound to smaller or larger, bacteria or even multiple bacteria. In such cases the velocity of a particle-bead complex will be further reduced with increasing diameter or number of attachments. The model fits with the observations made, although there are some variations between the different MPs types. MyOneC and MyOneT both have the same iron oxide content and should therefore have the same magnetically induced velocities; it may be seen from Figure 5.5, that the induced velocities are similar but not identical. The variations may be attributed to the heterogeneity of the MPs and the variance in the magnetically induced drift velocity this creates.

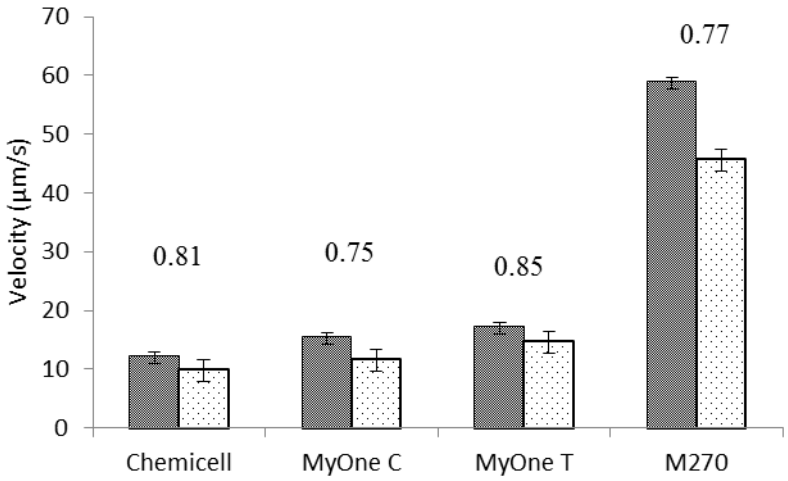

Figure 5.5. The velocities of single magnetic particles (hatched) and single magnetic particles bound to a single biotinylated silica bead (dotted). The number above each column represents the velocity ratio of the magnetic particle-silica complex, to the velocity of a single MP of the same type. Error = 1 SD; n = 5.

5.5. Conclusions

A method has been developed that allows the analysis of the magnetically induced drift velocity of MPs in a known magnetic gradient. The trajectories of the MPs within a magnetic field, as single particles, chains and complexes, were observed. The Dynabead

M270 had the greatest magnetophoretic mobility. Chains of MPs aligned with the field lines of the magnet.

This study shows that the magnetic drift velocity of MPs formed into chains or attached to NBs can be predicted using simple approximations to the increase in drag forces. Tracking the movement of MPs attached to a biomarker will enable the quantification, and a method to separate, successfully captured biomarkers. The measurement of magnetophoretic mobility may be an effective tool for the detection of captured bacteria by the MP if the attachment is of comparable size.

6. The separation and detection of single, viable *Escherichia coli* from drinking water

The separation method, as described in Chapter 5, to discriminate between bound and unbound MPs was used to evaluate captured *E. coli* from DW. The research in this Chapter describes the labelling of MPs with an anti-*E. coli* antibody and the optimisation of the method. The magnetophoretic drift velocities of MP-bacterial complexes were explored and the drift-velocities of viable and non-viable bacteria compared.

6.1. Introduction

Whilst many of the novel biosensors, that have been described, offer great promise and low-detection limits (as low as 1 CFU/ ml) [18, 169], many require highly trained scientific users and are costly in their use of reagents and equipment. MPs, in conjunction with immuno-labelling are a cost-effective, sensitive method for capturing target bacteria from environmental samples and are used within this study to analyse captured *E. coli* at the single-cell level.

6.1.1. Superparamagnetic microparticles

Functional magnetic micro-particles are used in bioanalytical applications as solid carriers for capture, transport and detection of magnetically labelled cells [185]. The MPs are able to be freely dispersed within a sample. Colloidal suspensions of MPs provide a large surface for chemical binding. MPs are easily dispersed throughout a sample which enables the highly efficient interactions with the target cells [215]. Functionalising the surface of the MPs with an antibody allows the binding of species-specific bacteria.

6.1.2. *Escherichia coli* as a biosensor target

The physiology and virulence of *E. coli* is well reported. Most strains of *E. coli* are not harmful and are ubiquitous in the mammalian digestive system. However, some strains are enterohemorrhagic and cause diarrhoea, severe illness and even death. An indirect, but common secondary consequence of *E. coli* gastroenteritis is that of haemolytic uraemic syndrome which is characterised by the onset of fragmentation of red blood cells and renal failure, for which there is no direct treatment [395]. *E. coli* was first recognised as a cause of illness in 1982 during an outbreak causing severe bloody diarrhoea due to contaminated hamburgers [396].

"*Indicators are used to provide an early warning of potential microbial contamination*" [74]. The bacteriological quality of DW is determined using indicators of microbial contamination; *E. coli* is a universally used indicator [30]. Although the use of an indicator organism such as *E. coli* has received discussion over its suitability for indicating water contamination, there are no reliable alternatives [33]. Due to the widely reported cases of *E. coli* as a water- and food-borne pathogen [397], many sensors have been described which target this bacterium [397–400]. It was therefore used as an indicator in this Chapter.

6.1.3. *Escherichia coli* carriers and vectors

E. coli resides in the intestine of many animals. Most pathogenic strains of *E. coli* are carried by healthy cattle in their faeces [401] and cattle farming has been attributed for the distribution into groundwater. Rain is an important vector in the distribution of *E. coli* however, and temperature is equally as important to the presence of pathogenic strains [26].

The physico-chemical intestinal environment is vastly different from that of the extra-intestinal habitat. *E. coli* is a facultative anaerobe which can adapt in order to survive and maintain its virulence in both environments [20]. Additional reported sources of *E. coli*

contamination are from minced beefburger, unpasteurised milk, cider and vegetables (e.g. lettuce and radish sprouts) [395].

6.1.4. Immuno-labelling of magnetic particles and magnetophoresis

Antibody or nucleic acid probes are utilised in a vast number of detection sensors [402]. A capture molecule may be immobilised on the surface of an MP, once bound to the target, the target also inherits the magnetic properties [350]. Antibodies can be either polyclonal (multi-strain specific) or monoclonal (single-strain specific) and can target specified antigenic sites on a cell, in this case a bacterium. The number of strains of *E. coli* has been reported to be 173 'O' antigens, 103 'K' antigens and 56 'H' antigens, with more ever being discovered [401].

Given the strong binding properties to biotin and the ease with which proteins may be biotinylated, many manufacturers offer MPs coated with streptavidin. This binding interface was used in this study to demonstrate the potential for using immuno-labelling of MPs for target detection through attachment of a biotinylated antibody to streptavidin coated MPs. The biotinylation of the "heavy chain" of antibodies allows specific orientation of the antibodies upon the MP, ensuring the antigenic binding sites are available for binding and not blocked by the surface of the MP. This increases the affinity of the biosensor.

Once a cell has been captured by an immuno-labelled MP, the cell can be manoeuvred by a magnetic field. *"Magnetophoresis is the physical migration phenomenon of a particle in a liquid due to the magnetic susceptibility of the particle under a magnetic field gradient*" [403]. A static magnetic field is applied to the sample; only magnetic material will migrate. An advantage of using a static field is that it will not impact the transport of charged solutes and ions in aqueous solutions, unlike an electric field [282].

Target bacteria are present in environmental samples in low concentrations. A high concentration of MPs is required in order to move through a sample and ensure the

binding and isolation of the target bacteria. Chapter 4 details the microfluidic concentration method used to achieve this separation. In order to successfully identify the percentage of bound MP to bacteria, the unbound MPs must be removed. To achieve this, a non-uniform magnetic gradient is applied. Bound MP-bacterial complexes migrate along the gradient at a reduced velocity and are therefore separable from the unbound particles. The bound MP-bacterial complexes, once isolated, can be viewed at the single MP-bacterial level using the magnetophoretic observation chamber as described in Chapter 5.3.4.

A prerequisite of designing a novel biosensor technology is the ability to determine the physiological state of the captured bacteria. An investigation into the magnetophoretic drift velocities of viable and non-viable cells was conducted to ascertain whether a relationship could be found between the magnetically induced drift velocities and viability.

6.2. Transport model

There are two known dominant forces which act upon MPs when in a magnetic field. Primarily, the magnetic force imposed by a gradient field and secondly the Stokes's Drag which is generated in the opposite direction to motion through a fluid, a detailed description of these forces may be found in Chapters 4.2 and 5.2.

6.3. Materials & method

The method for preparing the immuno-labelled MPs is described here, along with a description of the magnetophoretic chamber used for separating bound and unbound MPs, and viable and non-viable *E. coli* cells.

6.3.1. Immuno-labelling of magnetic particles

The five types of MPs used within the optimisation study were ScreenMagG (Chemicell, Germany) of approximately 1 µm diameter, Dynabeads MyoneC and MyOneT of 1.05 µm diameter and Dynabeads M270 and M280 of 2.8 µm diameter obtained from Invitrogen, UK.

Superparamagnetic microparticles Dynabeads MyOneC coated in streptavidin, 1.05 µm in size, were purchased from Invitrogen, UK. A concentration of 7-12 × 10^7 beads/ ml were washed in PBS three times and re-suspended in 100 µl of PBS. Anti-*Escherichia coli* polyclonal antibody (Biotin) (ab20640) was purchased from Abcam, UK. Aliquots of 20, 40 and 120 µg/ ml were added to the MPs. The antibody-MP samples were incubated for 40 minutes at 100 rpm in an orbital shaker. The MP-antibody conjugates were washed by collecting the MPs at the bottom of the Eppendorfs, by using a permanent magnet and removing the supernatant. The antibody-MPs were then washed four times in PBS with 0.1% bovine serum albumin, to block excess binding sites. The MPs were re-suspended in 100 µl of the same buffer and stored at 4 °C, the surfactant Pluronic F-127 (Sigma Aldrich, UK) was added a 0.1% w/v.

6.3.2. Binding calibration

To measure the amount of biotinylated antibody that had attached to the streptavidin-coated MPs, the absorbance of the antibody suspended in a quartz curvette, at a wavelength of 280 nm, was established over a range of concentrations using a Schimadzu spectrophotometer to determine a calibration curve.

Absorbance is given as a logarithmic ratio of a quantitative measurement of the radiation falling upon a material and the radiation transmitted through the material:

$$A_\lambda = -log_{10}\frac{I_1}{I_0} \tag{6.1}$$

where A_λ is the absorbance at a certain wavelength of light (λ), I_1 is the intensity of the light that has passed through the material and I_0 is the intensity of the light before the material [404].

After binding the antibody to the MPs, the supernatant was removed and the absorbance measured. The extinction coefficients at 280 nm [141] were derived from the calibration and were used for estimating the amount of conjugated antibody with the MPs.

6.3.3. *Escherichia coli* preparation

E. coli (HB101) was obtained by, kind permission, from the stores of Professor Thompson's laboratory at the Engineering Science Department, University of Oxford. A single colony was inoculated in pre-autoclaved Luria broth and incubated in an orbital shaker at 30 °C overnight. The bacteria were centrifuged into a pellet, at 10,000 rpm and cooled to 10 °C, the supernatant was removed and the pellet re-suspended and washed three times in PBS. The bacteria were finally re-suspended in ambient DW for further experimentation.

6.3.3.1. *Viable and non-viable cells*

To prepare the cells for the viable and non-viable analysis, a sample of *E. coli* was treated using chlorine at a concentration of 5 mg l^{-1}. Cells were suspended in the chlorinated solution for one hour. The cells were centrifuged as above and washed five times in DW to remove the chlorine from the sample. To ensure the cells were non-viable, samples were analysed using the traditional plating method as described by Miles and Misra [323]. The concentration of the sample of viable *E. coli* was 1.4×10^7 CFU/ml.

6.3.4. Antibody-MP-bacterial binding

The 100 µl antibody-MP stock solutions were added to 900 µl of *E. coli* suspended in DW and incubated at room 25 °C in an orbital shaker at 100 rpm for 2 hours. The Antibody-MP-bacterial complexes were collected at the bottom of the Eppendorfs and unbound *E. coli* cells were removed in the supernatant. The complexes were washed in DW twice before further analysis.

6.3.5. Mobility study

To determine the magnetophoretic mobility, the velocities of single MPs, and MP-bacterial complexes were measured within a known region of a magnetic B-field. Using an inverted microscope and magnification that allowed the clear viewing of 1 µm MPs, the MPs and MP-bacterial complexes were observed in a Fast-read microscope slide (Immune Systems, UK) which contains a set of easy-fill fluid "observation chambers" (see chapter 5.3.4).

6.3.6. Observations and software packages

Observations were made as described in section 5.3.4 and 5.3.6.

6.3.7. Statistics

The significance of the results described were tested using the Student's T-Test. The use of '*' denotes a statistically significant difference between means with $P<0.05$.

6.4. Results

The capture of *E. coli* cells was demonstrated using five types of MPs. An example of light microscopy images of *E. coli* attached to M270 and Chemicell MPs is pictured in Figure 6.1.

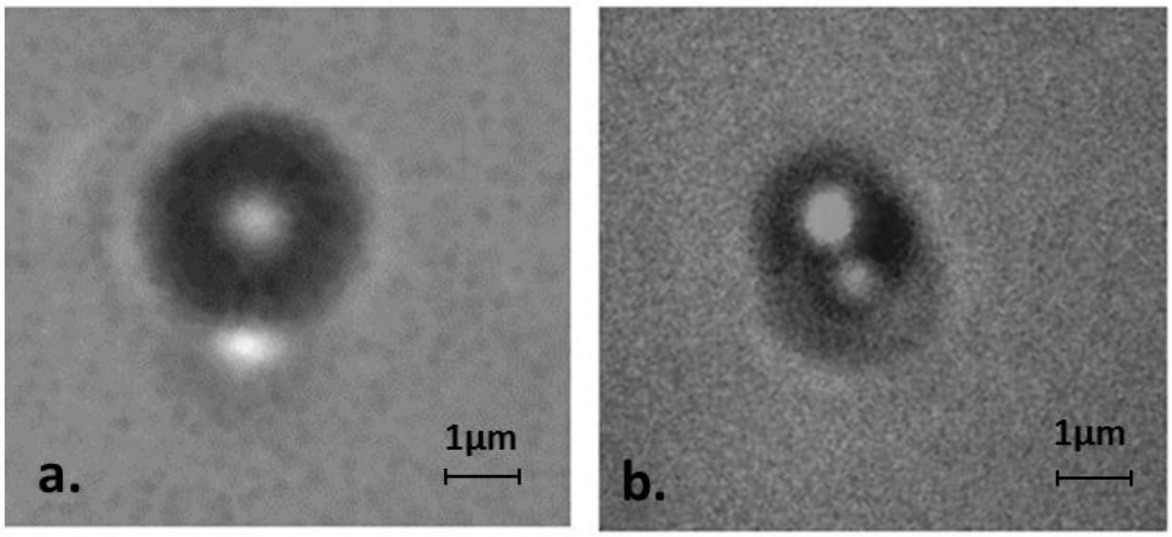

Figure 6.1. a) An M270-Escherichia coli complex and b) a Chemicell-Escherichia coli complex

6.4.1. Antibody Specificity

To determine the specificity of the antibody-MPs, a control sample of unfunctionalised MPs and two samples of anti-*E.coli*-MPs were incubated for eight hours with a sample of *E. coli* HB101 and a sample *Staphylococcus warneri* (ATCC 27836). The capture efficiency was determined using light microscopy, and was found to be 82% for *E. coli* and 1% for *S. warneri.* This demonstrated the specificity of the functionalised MPs to capture *E. coli* (Figure 6.2).

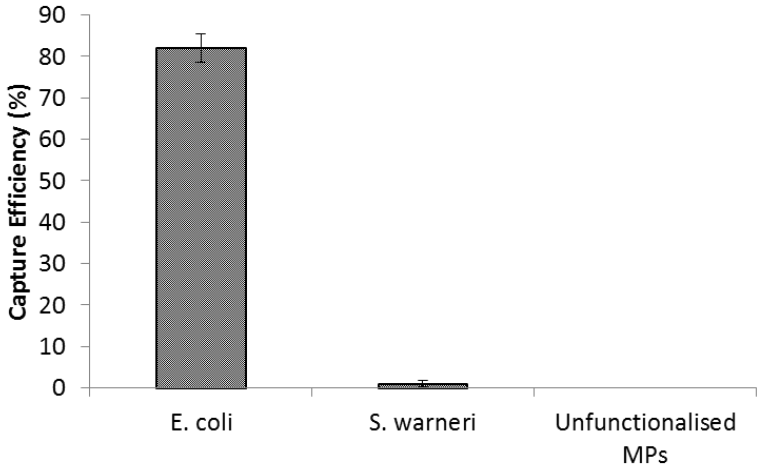

Figure 6.2 The capture efficiency of anti-Escherichia coli-MPs of <u>*Escherichia coli,*</u> <u>*Staphylococcus warneri*</u> *and unfunctionalised MPs* (Error = 1 SD; n=4)

The optimised binding conditions used to capture viable and non-viable *E.coli* cells were determined. The magnetically induced drift velocity of viable and non-viable cells was calculated using the magnetophoretic chamber as described in Chapter 5.

A calibration between concentrations of anti-*E. coli* antibody suspended in DI, and absorbance measurements at wavelength 280 nm was made (Figure 6.3). A good correlation was established between the two parameters (R^2 = 0.99) and the equation of the straight line was found to be y = 0.0018x.

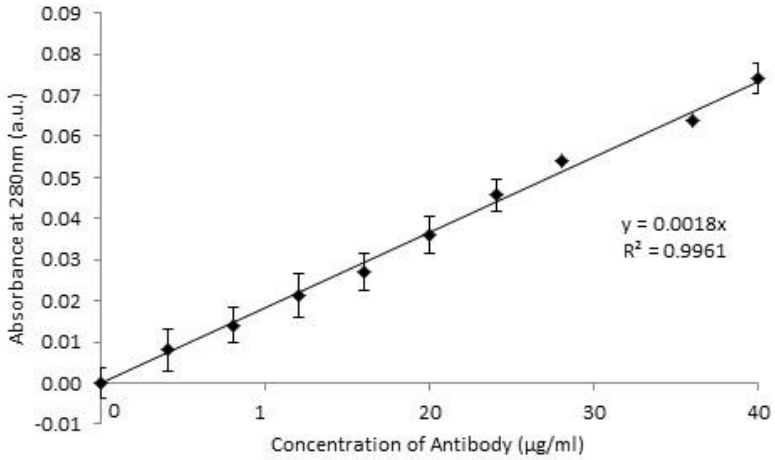

Figure 6.3. The antibody absorbance calibration conducted at a wavelength of 280 nm (Error = 1 SD; n=3)

The amount of antibody used to functionalise each type of MP was determined using this equation and the amount of antibody conjugated to the respective MPs was calculated and is detailed in Table 6.1. The density of the MP types and the surface area was obtained from the manufacturers' data sheets [351, 390].

The absorbance measurement of the supernatant showed that the greatest amount (65%) of the total antibody was attached to the MyOneC MPs. The MP type M280 had the lowest amount of antibody bound to its surface, retaining only 25% of the original antibody concentration.

The use of biotinylated antibody-streptavidin labelling was overall successful, and found to be a simple method for fuctionalising MPs.

Table 6.1. The magnetic particles used in the immunoassay to capture Escherichia coli, physical attributes and the amount of antibody applied and attached to the MPs with the calculated antibody surface area

Bead	Size (µm)	Applied (µg/ ml)	Bound (µg/ ml)	Bound %	Beads (per µg)	Surface Area (μm^2/ g)	Surface Antibody (ng/ m^2)
Chemicell	1.00	40	23.15	57.87	9.0×10^7	5.0×10^{13}	46.30
MyOneT	1.05	40	22.22	55.56	9.5×10^6	3.3×10^{13}	67.54
MyOneC	1.05	40	25.93	64.81	9.5×10^6	3.3×10^{13}	78.79
M270	2.80	40	20.56	51.39	6.5×10^5	1.6×10^{13}	128.4
M280	2.80	40	9.81	24.54	6.5×10^5	1.6×10^{13}	61.31

6.4.2. Antibody-magnetic particle functionalisation capture efficiencies

The optimal binding conditions were explored by coating the five types of MPs with different concentrations of the antibody. The larger beads (M270 and M280) were trialled with three concentrations of antibody: 20, 40 and 120 µg/ ml. A maximum binding percentage was found for both particle types between 8 and 10 hours of incubation. A decline in the percentage of binding was observed after 10 hours. The

incubation step was conducted in an orbital incubator maintained at room temperature. The decline in binding efficiency may be attributed to the denaturing of the antibody [405].

The concentration of antibody 120 µg/ ml achieved the highest binding capacity for particle types M270 and M280 (Figure 6.4). Even at this high concentration of antibody, only 55% of the MPs were bound to bacteria. This poor binding efficiency does not make the MPs suitable for capturing *E. coli* from environmental samples.

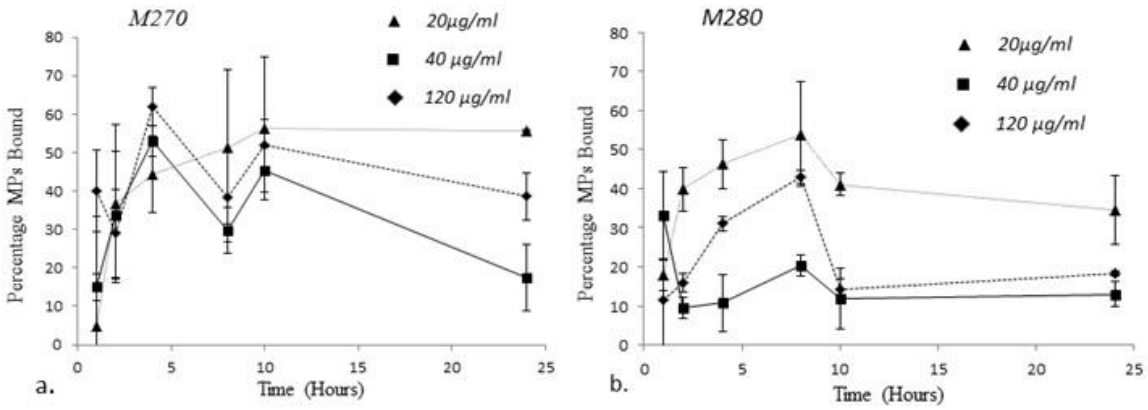

Figure 6.4. The binding efficiencies of the 2.8µm magnetic particles M270 (a) and M280 (b) functionalised with different concentrations of antibody (Error = 1 SD; n=3)

Of the 1 µm MPs the maximum binding percentage was 80%, obtained using the Dynabead MyOneC at both 20 and 40 µg/ ml. Chemicell MPs had the second highest binding efficiency, reaching greater than 60%. The optimal conditions for attaching the antibody to MyOneC and were a concentration of 40 µg/ ml and an incubation of eight hours (Figure 6.5) and similarly for the Chemicell MPs the conditions are 4 hours and 20 µg/ ml of antibody.

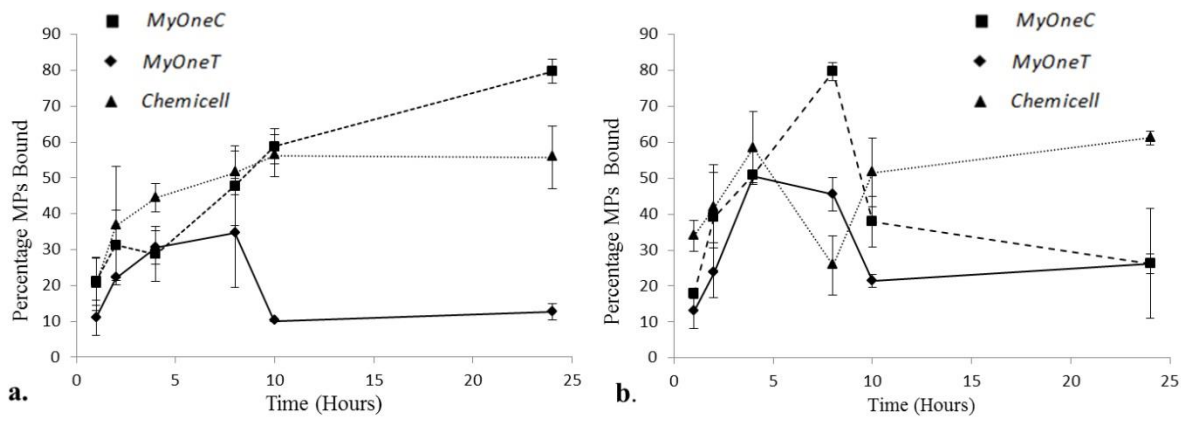

Figure 6.5. A comparison of the three types of magnetic particles functionalised with a) 20 µg/ ml and b) 40 µg/ ml of anti-Escherichia coli antibody (Error = 1SD; n=3)

A higher percentage of antibody was attached to the smaller MPs, providing more sites for the antibody to bind to the target. This has been previously reported [141] and may be explained by the larger surface area to volume ratio for the smaller MPs.

6.4.3. Magnetophoretic velocity of *Escherichia coli*

Given the higher capture efficiencies of MyOneC and Chemicell particles, they were used to explore the magnetophoretic-drift velocities of captured *E. coli.*

MP-bacterial complexes and unbound MPs were observed as they traversed the FOV. The velocity was determined by tracking the individual trajectories using ImageJ software. Single MyOneC MPs travelled at an average velocity of 20 µm/ s and Chemicell MPs at 18 µm/ s. The drift velocity is expected to reduce as the number of bacteria attached to the MPs increased.

A comparison of the drift velocities induced on the MyOneC and Chemicell MPs was conducted (Figure 6.6). Surprisingly, the drift velocities for the Chemicell MPs did not differ significantly between the single MPs, and complexes (T-Test $P>0.05$). Unbound and bound complexes of the MyOneC MPs, however, could be determined by the magnetically induced drift velocity of the MyOneC MPs and were therefore used in the later separation experiments.

A comparison was made between the MP types: Chemicell and MyOneC. The aim of the experiment was to select the most suitable MP type for use in bacterial-magnetophoretic separations. As mentioned previously, no clear distinction could be made between the unbound and bound spread of velocities of the Chemicell MPs. This may be explained by the size distribution of the Chemicell MPs as found in Chapter 5. It was noted that the range of the magnetic mobility of a single MyOneC particle type was narrower than that of single Chemicell particles (see Chapter 5).

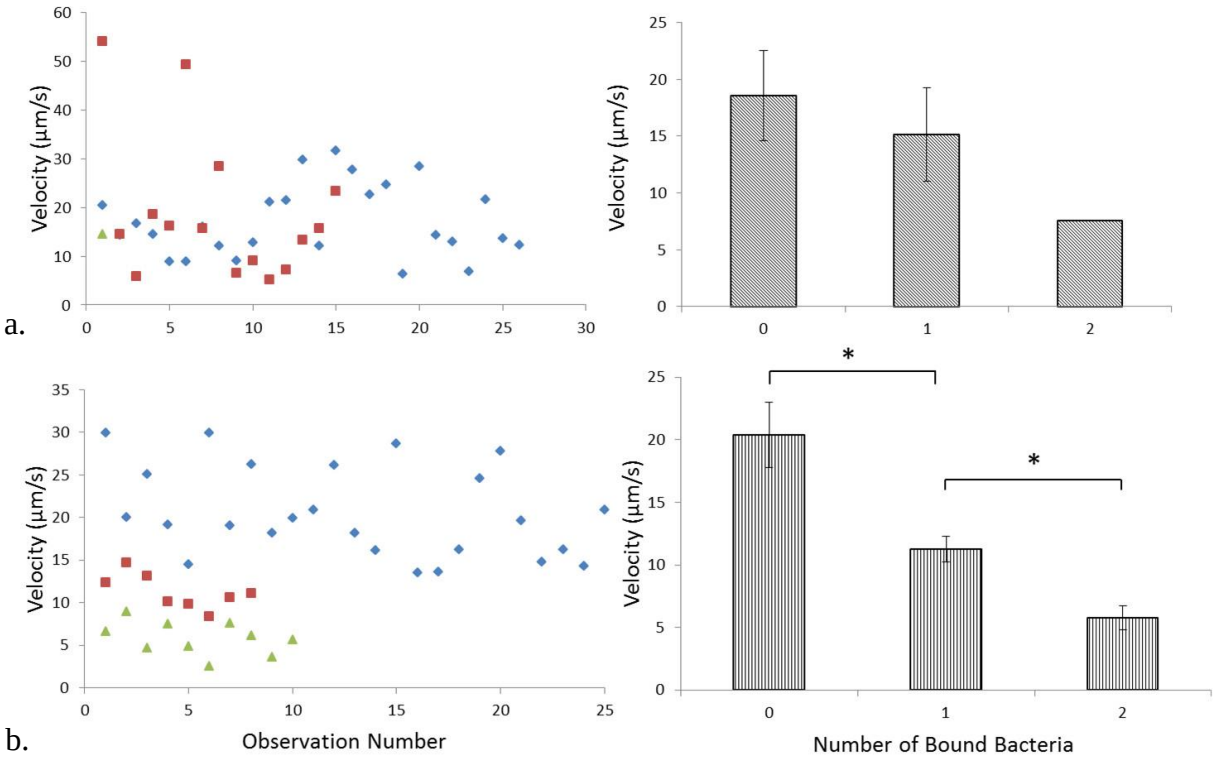

Figure 6.6. The scatter graphs (◆ represent single MPs, ■ MP+1 bacterium and ▲ MP+2 bacteria) and respective bar graphs obtained for the velocity of magnetic particles attached to one and two viable Escherichia coli cells a) Chemicell and b) MyOneC

*(Error = 1SD; * denotes T-test P<0.05)*

Figure 6.7 displays the magnetically induced drift velocities of the MyOneC MPs attached to viable *E. coli* cells. It was observed that in rare cases, as many as seven bacterial cells could attach to a single MP at any one time. Pathogenic bacteria express

and utilise an array of adhesions, which can occur as protein-protein or protein-carbohydrate interactions [83]. Adherence molecules on the cell membrane of *E. coli*, such as fimbriae, lock the cells together, and though not directly attached to the MP, the complex moves as one. Even with vigorous vortexing and ultrasonication of samples before analysis, these clusters of bacteria were still visible.

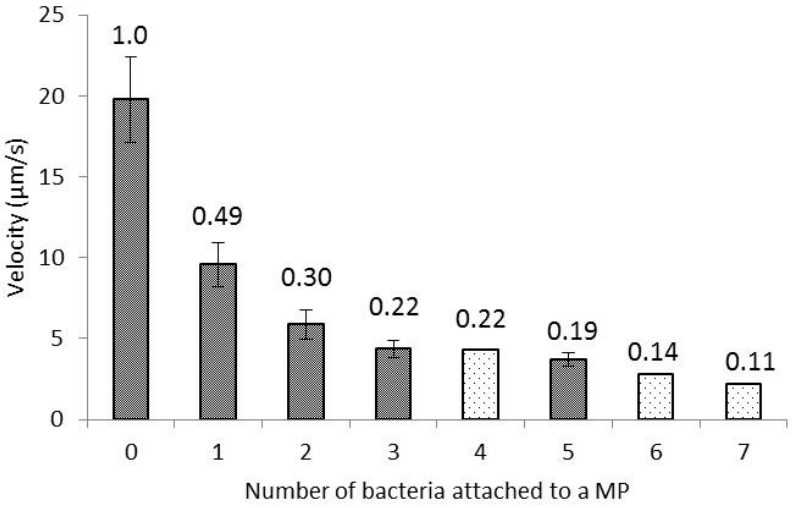

Figure 6.7. The magnetically induced velocity of Dynabeads MyOneC as the beads traversed the observation chamber. The number above each column is the ratio of the velocity of the complex to a single MP. The dotted data points denote single observation results (Error = 1 SD)

6.4.4. Magnetophoretic velocity of viable and non-viable *Escherichia coli* cells

Viable and non-viable cells were prepared by using chlorine to render one population of cells non-viable. Plate counts determined that no viable cells were present in the chlorinated sample 0 CFU/ ml and 1.59 x 10^7 CFU/ ml in the untreated sample.

There was a significant difference between the magnetically induced drift velocities of MPs when attached to viable *E. coli* cells and non-viable cells (Figure 6.8). The viable cells had a velocity of approximately 0.49 that of a single MP, whereas the non-viable cells travelled at a velocity of 0.75 that of a single MP.

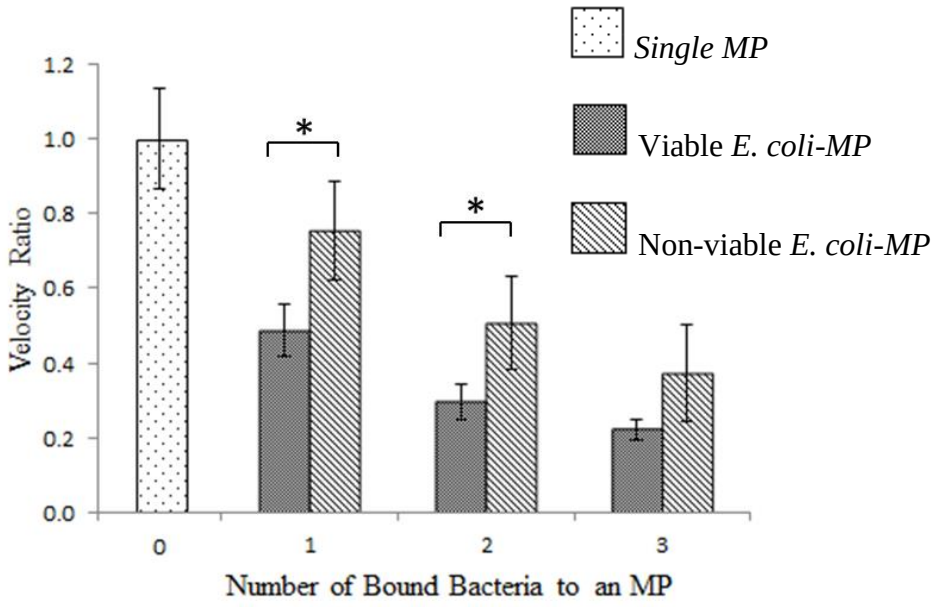

*Figure 6.8. The magnetically induced drift velocities of magnetic particles attached to Escherichia coli in non-viable and viable physiological states relative to the drift velocity of an unbound single magnetic particle (Error = 1 SD; n=10 * denotes T-test P<0.05)*

The magnetic drift velocities of single MyOneC MPs bound to different number of *E. coli* cells from viable and non-viable sample sets was found to fit an exponential expression.

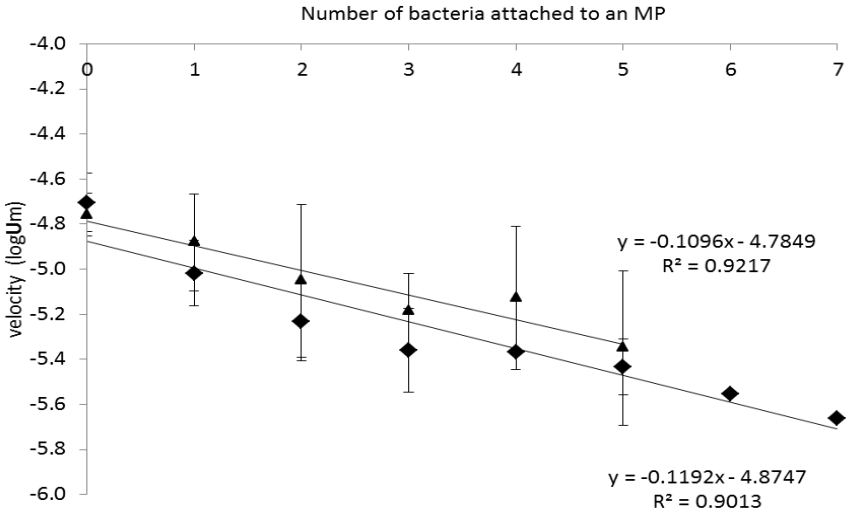

Figure 6.9. The logarithmic values of the magnetically induced drift velocity upon a single magnetic particle bound to increasing numbers of bacteria (N) for ▲ dead Escherichia coli; and ◆ for viable Escherichia coli, (Error =1 SD n is dependent upon the number of observations made which were random)

The logarithmic plot in Figure 6.9 displays a linear relationship with high regression values for both the chlorinated (R^2=0.9217 and equation of the line *y = -0.1096x – 4.7849*) and viable (R^2=0.9013 equation of the line y = *-1192x -4.8747*). Using these equations, it will be possible to determine the number of bacteria attached to an MP and an estimation of the viability of the captured bacteria. Using these equations, it will be possible to determine the number of bacteria attached to an MP and an estimation of the viability of the captured bacteria.

Previous results (Chapter 5) displayed a decrease in the drift velocity of an MP-NB complex to 0.8 of the velocity of a single unbound MP. A single viable *E. coli* bound to an MP travelled at 0.49 times the velocity of a single MP, and a single non-viable *E. coli* travelled at 0.75 that of a single MP. It is hypothesised that viable *E. coli* induced some resistance to the magnetic transport of the MP. *E. coli* are widely documented as being motile organisms. When the bacteria have sufficient ATP within the cells, the bacteria search for food sources by chemotaxis, rotating their flagellar to search for food. This movement would increase the resistance to the magnetically induced drift velocity, and would reduce the velocity of the complex. The viability of bacteria is therefore demonstrated by motility.

6.5. Discussion

E. coli cells were captured by functionalised MPs using a biotinylated polyclonal anti-*E. coli* antibody that was attached to the surface of the streptavidin-coated MP. Of the five MPs trialled, the Dynabead MyOneC was selected to use in further experiments due to its high *E. coli*-capture efficiency, in the shortest duration (8 hours) and the uniformity of the MPs.

6.5.1. Antibody conjugation of magnetic particles

It was observed during this investigation that, after 10 hours of incubation at room temperature, the immuno-labelled MPs lost the ability to bind bacteria. This may be attributed to the loss of biological function and overall stability of proteins above 4 °C due to the degradation by proteases [405]. Long-term use of an antibody under environmental conditions is therefore not appropriate, as the sensing technology will be compromised by a denatured antibody. The addition of a protease inhibitor may be a solution to prevent the rapid degradation of the protein and is suggested for further research.

An explanation for the lower than expected capture efficiency exhibited by the MPs when labelled with the polyclonal antibody is that the antibody is designed to target the O-saccharide of *E. coli.* The strain of *E. coli* used in this experiment was HB101. The naming of the strains of *E. coli* i.e. O, K and H, is due to the presence of an antigenic site at different locations on the cell surface. The antibody region of HB101 is located on the flagellum and the specificity of the polyclonal anti-*E. coli* from ABCAM had not been previously tested upon strains with the H antigenic site. Different strains of *E. coli* interact differently to the same MPs, due to the different antigenic differences between strains [141]. *E. coli* HB101 was used in this study to demonstrate the capture of bacteria using immuno-labelling of MPs. To optimise this assay, an environmental strain of *E. coli* indigenous to the sensor-sampling area could be used as an indicator of contamination. There has been advancement in the development of synthetic oligonucleotides (aptamers) during recent years [96]. It is proposed, to increase the capture efficiency and the shelf-life of the MP-capture biosensor technology, aptamers [103] are investigated as an alternative labelling method.

Only 55% of the MPs for M270 and M280 were bound to bacteria. As the M270 and M280 are negatively charged (see Chapter 5.4.3), and when suspended in water, *E. coli*

is also negatively charged (see Chapter 3.3.1.1). These particles repel each other and are likely to have a minimum separation distance that depends on the repulsive charge magnitude. A reason for the poor percentage of MPs bound to bacteria is that the linking arm attaching the antibody to the MP is not long enough to circumnavigate the electrostatic repulsion region. Tu *et al.* [141] observed that larger MPs were more effective at capturing bacteria than smaller MPs at the same density. They attributed this to the ability of the larger MPs presenting a larger volume, and therefore increase the possibility for target-collisions. An investigation into the optimal pH should be conducted to improve the capture efficiency of the antibody-coated MP; it has been reported that the interaction between antibodies and antigens was dependent upon the pH of the reaction system [220]. The proposed sensor is designed to reduce the detection time for identifying contaminated environmental samples; an incubation time of 8 hours is too long. In order to improve the proposed sensor and move towards a commercial product, this incubation period must be reduced significantly. It is proposed that mixing should be conducted on-chip using a spiral microfluidics channel [232], thus encouraging immediate MP-bacterial interaction. This will shorten the incubation step and improve capture efficiency.

The detection of *E. coli* has been demonstrated here. However, there is no reason to suggest that this technique is limited to *E. coli*, as a plethora of antibodies exist for the detection of not only bacteria but of biomarkers of disease also. Using a magnetophoretic gradient along a microfluidic chip, it is possible to separate viable and non-viable bacteria. It is hypothesised that this technique may also be used to separate damaged cells from intact cells, given the induced drift velocities.

6.5.2. Magnetophoretic velocity of viable and non-viable *Escherichia coli* cells

There was a significant difference observed between the viable and non-viable drift velocities of *E. coli* cells. It is well documented that when bacterial cells are treated with chemicals, the cell membrane is permeabilised and stressed cells can change in shape. The loss of membrane integrity results in the free transport of ions in and out of the cell, the cell is expected to lose its rigid structure, becoming much like a deflated balloon. Viable cells of *E. coli* are motile through the use of a single flagellum. The viable cells may be altering the trajectory of the MP by "swimming", thus increasing the drag force exerted on the MP-bacterial complex, motility therefore defining viability in this study.

Viable and non-viable bacteria have morphological differences that are not visible using conventional light microscopy. The loss of cell integrity may also play a role in the increased velocity of non-viable cells. It is recommended that environmental scanning electron microscopy (SEM) is conducted upon viable and non-viable bacteria, to observe any morphological differences.

6.6. Conclusions

The magnetophoretic chamber described here is a useful tool to distinguish between unbound and MP-bacterial complexes. Bound MPs traverse the chamber at a slower velocity than single MPs. It is possible to distinguish between viable and non-viable *E. coli* cells, by viable cells motility, using the magnetophoretic chamber described due to the difference in the magnetically induced drift velocities.

The use of video-tracking will enable the automation of the analysis and a digital readout of the magnetically-induced velocities of single MPs, MP-bacterial complexes, and differentiate between viable and non-viable bacteria within a sample.

7. Summary, conclusive remarks and future work

The objective of the work described in this thesis was to develop a biosensor to detect pathogenic bacteria in water. The key features of the biosensor were: to enumerate and assess the viability of captured bacteria from continuous flow, and to reduce the detection time of current microbiological methods.

7.1. Summary of research and discussion

Available microbiological techniques were investigated to ascertain whether they could provide a basis for viable, rapid detection of bacteria. An MFD was designed, incorporating magnetophoresis to separate and concentrate bacteria from water. MPs were used as solid-capture bodies to isolate *E. coli* from water. The research conducted for this thesis is summarised and discussed in this Section.

7.1.1. Microbiological viability analytical techniques

The biosensor developed in this thesis, should produce a rapid reading on the physiological state of the detected bacteria. The industry standard for pathogen detection is by use of plate counts, where a response time takes greater than 24 hours. An exploration of suitable microbiological techniques was conducted with the aim of identifying a replacement method for the rapid analysis of the viability of bacteria in DW.

Flow cytometry offers a fast and efficient method for analysing bacterial populations with the addition of organic fluorochromes [298]. Flow cytometry was used to assess the bacterial populations and the physiological response of the cells when subjected to different environmental stressors and conditions. The fluorochromes utilised in this study were selected as a function of the different physiological pathways they targeted, and they were indicators of different physiological states such as loss of membrane potential ($DiBAC_4$) and permeability (SG and PI).

Berney *et al.,* [406] suggested that the use of membrane-permeable nucleic acid fluorochromes, such as Syto 9, with Gram-negative bacteria may be limited, due to the outer membrane acting as a barrier preventing the uptake of these dyes. A correlation with plate counts was found with one fluorochrome, 2-NBDG. Further development of the 2-NBDG protocol highlighted areas of concern and variable results when used to assess different disinfection techniques. Viable bacteria may be active or inactive with respect to metabolic activity [407]; therefore 2-NBDG is not a reliable indicator of viability. It has been reported that flow cytometric analysis can overestimate viability in bacteria by as much as 20% [408]. No satisfactory results were obtained that enabled the confident use of flow cytometry to identify viable and non-viable bacteria as an alternative to plate counts.

When cells are exposed to electric fields within the range of radiofrequencies, interfacial polarisation across the cell membrane causes cells to become polarised [158]. The bacterial cell membrane is highly insulating, presenting a conductivity of 10^{-7} S/m, whereas the inside of the cell, with: DNA , nutrient storage granules, ribosomes and many more dissolved charged molecules, is more conductive (1 S/m) [157]. Permeabilisation of the cell membrane will result in the breakdown of the membrane and it can no-longer act as an insulator. The conductivity of the cell membrane will therefore increase.

Measurement of the zeta potential of bacteria provided an array of information of bacterial populations. The zeta potential of different species of bacteria was found to be significantly different. Importantly, zeta potential, as measured using a commercially available instrument, is dependent upon concentration and the suspending solution [266, 328]. The zeta potential is measured at the slipping plane, a distance away from the surface charge of a bacterium, in microbiological terms. To improve upon these results and to better interpret the change in the charge of bacteria when subjected to different

stressors, a measurement of the surface charge would be beneficial and could improve upon the results that are reported.

In order to obtain confidence of a rapid bacterial viability technique, a direct comparison with plate counts is required, or a consistency of results reported. Although there has been advancement in real-time microbiological techniques, the tested techniques did not meet all of the requirements for the proposed sensor. No reliable correlation was found between flow cytometry and zeta potential analysis of bacterial populations and traditional plate counts. This background investigation highlighted the need for a novel method to assess bacterial viability.

7.1.2. Microfluidics and magnetophoresis for the continuous separation and concentration of pathogenic bacteria

Microfluidics enable measurements from small volumes of complex fluids with speed and sensitivity. MFDs are a powerful and versatile tool for biosensors [366]. In this study an MFD was designed to incorporate magnetophoresis to separate and concentrate bound bacteria from a sample flow. A novel quadrupole magnet configuration was designed that enabled the focussing of the MPs away from the sample flow. A separation of 80% of the MPs from the sample flow was established which is a marginal improvement on the 75% trapping efficiency of the MFD reported by Ramadan *et al*., [377].

The described MFD had limitations; the magnet design encouraged surface collisions and loss of MPs. Further developments are required to optimise the configuration; these are described later in this Chapter. MFDs reported in the literature, incorporating magnetophoresis to separate micro-particles from continuous flow, have not addressed the vertical forces experienced by the MPs [197], and the problematic removal of these MPs. This study highlights that there are additional areas within the topic of magnetophoresis that need to be addressed to better design a continuous magnetophoretic separation devices.

The device enables the separation of MPs with different mobilities, providing a separation platform that is not affected by agglomerates that occur inevitably when magnetic material is used in biological separations. The microfluidic design has a higher throughput (3000µl/hr) than described magnetophoretic devices (40 µl/hr) [354]. The described magnetophoretic device utilises low-in-cost, commercially available materials and therefore provides a simple platform to separate biological material. Multiple devices can be run in parallel to increase throughput further and to enable multi-target detection. In addition, the separation efficiency of the here described magnetophoretic-microfluidic device was determined after the MPs had exited the device, and not within the chip, as reported by [197]. Determining the separation of MPs on-chip does not take into account the starting and final concentrations and is therefore not an accurate method for determining the overall separation efficiency of magnetic material from a sample.

7.1.3. Magnetophoretic mobilities of magnetic particles

MPs have been used in numerous biotechnology applications over the past decades which include areas of drug delivery [409], culture assays [410] and biomarker concentration [411]. To understand better the characteristics of MPs and their behaviour within a magnetic field, a simple method was developed to determine the magnetic mobility of MPs and a predictive model was established to calculate the magnetic drift velocities of the MPs. It was found that some brands of MPs have better uniformity in size and magnetic content than others. When used in continuous separations, to allow for predictability, MPs should be chosen on their uniformity. Predictability of the trajectories of MPs is not as important a characteristic when using MPs in batch applications. The self-assembly of MPs into chains is a phenomenon that must be carefully considered when using MPs in a continuous flow separation device. The magnetically induced drift velocity of chains of different numbers of MPs was determined by a simple model.

The charge of MPs is an important consideration. The MPs used within this study were all found to have a negative charge when suspended in DW at pH 7; bacterial cell surfaces are usually negatively charged at pH 7 [335]. The length of the linking arm attaching the capture site to the MP must be of a length sufficient to enable the circumnavigation of the electrostatic repulsion region when the target has the same charge.

7.1.4. Separation and detection of *Escherichia coli*

The capture of *E. coli* from DW was achieved through functionalisation of MPs with a polyclonal antibody. Using the magnetophoretic observation chamber, the magnetic drift velocities of the captured bacteria were determined. The drift velocity decreased exponentially with increasing number of attached bacteria to a single MP. The magnetophoretic drift velocities of viable and non-viable bacteria were found to be significantly different. This may be attributed to the differences in morphology of the bacteria that had been treated with chlorine. It has been reported that disinfection techniques create wrinkles, holes in the cell wall and the cells lose integrity [68]. As *E. coli* are flagellates, motion induced by movement of their flagella may result in additional drag, thus slowing the MP-bacterial complex. Viability is therefore determined by the motility of viable bacteria. Further experimentation should be conducted to provide evidence for this; this is described in Section 7.1.4. As *E. coli* are flagellates, motion induced by movement of their flagella may result in additional drag, thus slowing the MP-bacterial complex.

7.2. Concluding remarks

A continuous microfluidic separation device has been developed that enables the concentration of dispersed MPs to be determined using microfluidics and magnetophoresis. Immuno-labelling of MPs allows the specific capture of a target, namely *E. coli* from a complex sample. After concentration, the MPs are separated via magnetophoresis and are categorised into unbound and bound MP-bacterial complexes by analysing their magnetically-induced drift velocities. The magnetic drift velocity ratio of the MP-bacterial complexes to single MPs was used to establish the difference between viable and non-viable *E. coli* cells. The detection time of capturing bacteria was reduced. Traditional plate counts commonly take more than 24 hours; this technique produced results between four and eight hours, which is a useful improvement. Captured bacteria were analysed at the single-cell level, and their viability was determined by differences in their magnetically induced drift velocities.

The research described in this thesis requires some further development before the biosensor can be used *in situ.* The research areas required to achieve this goal are described in this Chapter.

7.2.1. Towards a "Lab-on-a-Chip"

The application of the developed sensor is for use as a continuous monitoring system for pathogens in waterbodies. To enable this, the sensor requires some further development. There are three further key components of research and development required.

7.2.1.1. *MP-bacterial binding on-chip*

Spiral MFD channels have been described which encourage the immediate interaction between immuno-labelled microparticles with the targeted cells [232]. Channels that incorporate spirals would reduce the incubation duration of MPs and bacteria. There is the possibility of making the binding quasi-instantaneous, due to the fluid dynamics

forcing the interaction of bacteria with the MPs. The longer the period the antibody is kept at environmental temperatures (i.e. above 4 °C) the greater the chance of it denaturing and losing the specificity and selectivity of the biosensor. There are several targets on, or in bacteria, for a bacteria sensor to detect. Antibodies are expensive and time consuming to produce due to their complicated production [127]. To increase affinity and shelf-life of the sensor, aptamers can be designed specifically to the target required; they are comparatively inexpensive to produce with reversible binding, and as such seem useful for the biosensor design [100].

The removal of MPs from the bound bacteria is possible, by deploying an elution step. The elution process requires the pH of the sample to be reduced to acidic conditions (pH between 2 and 3) or the temperature elevated about 70 °C [412], thus denaturing the protein binding the MPs to the bacteria. In the proposed sensor there is no need for this elution step as the analysis of the captured bacteria will be conducted on-chip. Nonetheless this possibility should be noted. There are alternative applications that require the targeted cells to be recovered e.g. the separation of rare cell types from blood. As such, an elution step would be necessary.

7.2.1.2. *Continuous flow*

Waterbodies should be monitored continuously for a variety of contaminants, including indicator bacteria such as *E. coli*. The microfluidic and magnetophoretic device has the potential to enable such monitoring through automation of the sample inlets and buffer flows along with an on-chip mixing chamber (Section 7.1.1.). A characteristic of microfluidics, that would need to be carefully avoided, is the tendency for blockages and air bubbles to interfere with the sampling and analytical process. A filter would need to be applied to remove such debris before the sample entered the biosensor.

Multiple microfluidic chips could be used in parallel, and the sample flow directed between the chips. With the use of multiple-labels such an approach would enable the

detection of multiple targets enabling the detection of other indicators apart from *E. coli*. Clearly, the total volume of sample required for analysis would be increased.

The experimental setup as described within this thesis is of a relatively simple magnetophoretic separation and observation chamber, where the analysis of viable and non-viable cells is conducted. It would be relatively straightforward to write a Matlab code that recorded the MP-bacterial trajectories and calculated the magnetically induced drift velocities of each complex that traversed the FOV. Doing so would enable the automation of the analytical section of the proposed sensor and advance the sensor toward a total-analysis biosensor.

7.2.2. Increasing separation efficiency and through-put

The separation efficiency of the MFD described in Chapter 4 was determined to collect 80% of MPs. Increasing the magnetic mobility of the MP-bacterial complexes would increase the separation efficiency, and allow higher flow rates and therefore increase sample throughput. A method of doing so would be by use of MNPs. Many papers have described the use of MNP as capture and drug delivery bodies. There is an advantage of using immuno-labelled MNPs as capture technologies as each individual MNP can be small enough to be a particle with a single dipole. Labelling a cell with several or hundreds of MNPs will increase the magnetic mobility of the cell, to a far greater extent than that of labelling a cell with a magnetic microparticle comprised of only approximately five magnetic nanoparticles of a single dipole. The difficulty, quite obviously, in using MNPs is their size, and the limitations of conventional light microscopy. Labelling cells with exactly the same number of MNPs would prove challenging, given their size. A more sensitive method of analysing the magnetically-induced velocity would be required as this is dependent upon the magnetic-component of the labelled cells.

7.2.3. Viable and non-viable analysis

There is still a debate over the best method to determine the physiological status of cells. Due to the low-infective dose limits of some strains of pathogenic bacteria (e.g. *E. coli* 10 CFU/ ml) the method used in a biosensor must have a correlation with traditional plate counts and provide additional information of the state of cells.

7.2.3.1. *Chemotaxis and viability analysis*

Bacteria respond to changes in the chemical composition of the environment through a mechanism termed chemotaxis. Species of bacteria, such as *E. coli,* have flagellar which enable motility [59]. Signals received by receptors sense a change in the environment and modulate the rotation of the flagellar in order to approach attractants and to avoid repellents [60]. *E. coli* has been reported to swim through aqueous media at 1.76 m day^{-1} [413] It is hypothesised that the difference in the magnetically-induced drift velocity is, in part, due to the motility of bacteria. Viable bacteria, as determined by their motility, will migrate towards a nutrient source, whilst non-viable cells will remain stationary. If no nutrient source is apparent, the motile bacteria "tumble" in order to search for available nutrients. This motion, against the magnetic gradient, decreases the velocity through alteration of the trajectory. To enhance the migration, a repellent chemical may be used to encourage swimming away from the sample exit. The different magnetic-drift velocities as observed in Chapter 6, between viable and non-viable *E. coli* cells, is in part, attributed to the motility of the viable *E. coli* and the added drag force on the carrier MP. In order to test this theory, the same experiment should be repeated but with viable and non-viable cells of a non-motile species of bacteria such as *Stapholococcus aureus.*

7.2.3.2. *Raman spectroscopy*

Whilst motility is hypothesised as a mechanism for viability analysis at the single-cell level, RS offers a powerful tool to further enhance the sensitivity of the biosensor.

RS is the vibrational, inelastic spectrum of objects. It is caused by the Raman scattering of photons only; 1 in 10^6 photons are scattered in this manner. With recent advances in microscopy, video imaging and improved engineering of Raman spectroscopes and optical tweezers [183], it is now possible to use RS to analyse individual bacterial cells *in vitro*, with the potential for continuous monitoring. RS produces a "fingerprint" of bacterial cells, which is species specific and dependent upon not only the physiological state, but also the metabolism of the bacterial cells [176]. It is a powerful tool and would be ideal to use as the analytical part of a bacterial sensor. In addition, because of the unique fingerprint of each species of bacteria, there would be no need for immuno-magnetic labelling of MPs. Instead, a sample could be passed through the MFD, hydro-dynamically focussed into a region suitable for RS analysis, a fingerprint taken and an automated response given. As a proof of principle, RS analysis could be conducted upon the targets as captured by the biosensor described in this work, a profile of *E. coli* obtained and a correlation sought between viable and non-viable bacteria. One drawback of RS is that it is expensive and requires bulky instrumentation. However, advances have been made to reduce the size, and as RS is developed and recognised as a powerful tool, the cost involved would be reduced [414].

7.2.4. Scope of sensor – a broader perspective

There is a demand to manipulate particles at the micro-scale. Pathogens need to be monitored in hospitals [23], as biological warfare agents [415], and within environmental-, food- [24] and pharmaceutical-industries [106]. The detection of biomarkers in clinical applications has numerous uses including point-of-care diagnostics [416, 417], drug delivery [418] and screening [347], and in treatments [217].

To establish the use of the described biosensor as a separation device in clinical settings, the separation of tumour cells from serum should be tested. Using clinical samples, the use of a surface marker specific to the cancerous cell, could be used to isolate cells from

a patient who is irresponsive to treatment. Separation of the tumour cells could then be used in further experiments to screen potential drugs and their effect upon the cancerous cells. Collaboration with the John Radcliffe hospital, Department of Gynaecology and Obstetrics, has been established. The biosensor will be trialled in a clinical setting to isolate circulating tumour cells from blood.

8. References

[1] R. R. Converse, M. F. Piehler, and R. T. Noble, “Contrasts in concentrations and loads of conventional and alternative indicators of fecal contamination in coastal stormwater,” *Water Res.*, vol. 45, no. 16, pp. 5229–5240, 2011.

[2] C. S. Riesenfeld, P. D. Schloss, and J. Handelsman, “Metagenomics: genomic analysis of microbial communities,” *Annu. Rev. Genet.*, vol. 38, pp. 525–552, 2004.

[3] M. R. Barer and C. R. Harwood, “Bacterial Viability and Culturability,” *Adv. Microb. Physiol.*, vol. 41, pp. 93–137, 1999.

[4] C. W. P. Park, “Development of Rapid Assessment Method to Determine Bacterial Viability Based on Ultraviolet and Visible (UV-Vis) Spectroscopy Analysis Including Application to Bioaerosols,” *Aerosol Air Qual. Res.*, pp. 399–408, 2012.

[5] J. T. Walker, D. J. Bradshaw, M. Finney, M. R. Fulford, E. Frandsen, O. S. E, J. M. Ten Cate, W. R. Moorer, A. J. Schel, A. Mavridou, J. J. Kamma, G. Mandilara, L. Stosser, S. Kneist, R. Araujo, N. Contreras, P. Goroncy-Bermes, D. O’Mullane, F. Burke, A. Forde, M. O’Sullivan, and P. D. Marsh, “Microbiological evaluation of dental unit water systems in general dental practice in Europe,” *Eur J Oral Sci*, vol. 112, no. 5, pp. 412–418, 2004.

[6] W. L. Nicholson, N. Munakata, G. Horneck, H. J. Melosh, and P. Setlow, “Resistance of Bacillus endospores to extreme terrestrial and extraterrestrial environments,” *Microbiol. Mol. Biol. Rev.*, vol. 64, no. 3, pp. 548–572, 2000.

[7] A. Rompré, P. Servais, J. Baudart, M. R. De-Roubin, and P. Laurent, “Detection and enumeration of coliforms in drinking water: current methods and emerging approaches.,” *J. Microbiol. Methods*, vol. 49, no. 1, pp. 31–54, Mar. 2002.

[8] S. H. Na, K. Miyanaga, H. Unno, and Y. Tanji, “The survival response of Escherichia coli K12 in a natural environment,” *Appl. Microbiol. Biotechnol.*, vol. 72, no. 2, pp. 386–92, Sep. 2006.

[9] C. Davis, “Enumeration of probiotic strains: Review of culture-dependent and alternative techniques to quantify viable bacteria,” *J. Microbiol. Methods*, vol. 103, pp. 9–17, 2014.

[10] N. H. Keep, J. M. Ward, G. Robertson, M. Cohen-Gonsaud, and B. Henderson, “Bacterial resuscitation factors: Revival of viable but non-culturable bacteria,” *Cell. Mol. Life Sci.*, vol. 63, pp. 2555–2559, 2006.

[11] D. Pinto, V. Almeida, M. Almeida Santos, and L. M. M. Chambel, “Resuscitation of Escherichia coli VBNC cells depends on a variety of environmental or chemical stimuli,” *J. Appl. Microbiol.*, vol. 110, no. 6, pp. 1601–1611, 2011.

[12] M. Gengenbacher and S. H. E. Kaufmann, “*Mycobacterium tuberculosis* : success through dormancy,” *FEMS Microbiol. Rev.*, vol. 36, no. 3, pp. 514–532, 2012.

[13] J. A. Ho, H.-W. Hsu, and M.-R. Huang, “Liposome-based microcapillary immunosensor for detection of Escherichia coli O157:H7,” *Anal. Biochem.*, vol. 330, no. 2, pp. 342–9, Jul. 2004.

[14] D. Ivnitski, I. Abdel-Hamid, P. Atanasov, and E. Wilkins, “Biosensors for detection of pathogenic bacteria,” *Biosens. Bioelectron.*, vol. 14, no. 7, pp. 599–624, Oct. 1999.

[15] M. Zourob, N. Skivensen, R. Horvath, S. Mohr, M. B. McDonnel, and N. J. Goddard, “Integrated Deep-Probe Optical Waveguides for Label Free Bacteria

Detection," in *Principles of Bacterial Detection: Biosensors, Recognition Receptors and Microsystems*, 2008, pp. 139–168.

[16] H. Momtaz, F. S. Dehkordi, E. Rahimi, and A. Asgarifar, "Detection of Escherichia coli, Salmonella species, and Vibrio cholerae in tap water and bottled drinking water in Isfahan, Iran," *BMC Public Health*, vol. 13, no. 1, p. 556, Jan. 2013.

[17] N. Sanvicens, C. Pastells, N. Pascual, and M.-P. Marco, "Nanoparticle-based biosensors for detection of pathogenic bacteria," *TrAC Trends Anal. Chem.*, vol. 28, no. 11, pp. 1243–1252, Dec. 2009.

[18] G. A. Zelada-Guillén, J. Riu, A. Düzgün, and F. X. Rius, "Immediate detection of living bacteria at ultralow concentrations using a carbon nanotube based potentiometric aptasensor.," *Angew. Chem. Int. Ed. Engl.*, vol. 48, no. 40, pp. 7334–7, Jan. 2009.

[19] M. A. Hahn, J. S. Tabb, and T. D. Krauss, "Detection of single bacterial pathogens with semiconductor quantum dots," *Anal. Chem.*, vol. 77, no. 15, pp. 4861–9, Aug. 2005.

[20] S. Akter, M. Islam, K. S. Afreen, N. Azmuda, S. I. Khan, and N. K. Birkeland, "Prevalence and distribution of different diarrhoeagenic Escherichia coli virulotypes in major water bodies in Bangladesh," *Epidemiol. Infect.*, vol. 141, no. 12, pp. 2516–25, Dec. 2013.

[21] F. P. Brennan, J. Grant, C. H. Botting, V. O'Flaherty, K. G. Richards, and F. Abram, "Insights into the low-temperature adaptation and nutritional flexibility of a soil-persistent Escherichia coli," *FEMS Microbiol. Ecol.*, vol. 84, pp. 75–85, 2013.

[22] P. K. Pandey, P. H. Kass, M. L. Soupir, S. Biswas, and V. P. Singh, "Contamination of water resources by pathogenic bacteria," *AMB Express*, vol. 4, p. 51, Jan. 2014.

[23] J. Mairhofer, K. Roppert, and P. Ertl, "Microfluidic systems for pathogen sensing: a review," *Sensors (Basel).*, vol. 9, no. 6, pp. 4804–23, Jan. 2009.

[24] P. Arora, A. Sindhu, N. Dilbaghi, and A. Chaudhury, "Biosensors as innovative tools for the detection of food borne pathogens," *Biosens. Bioelectron.*, vol. 28, no. 1, pp. 1–12, Oct. 2011.

[25] D. Krewski, J. Balbus, D. Butler-Jones, C. Haas, J. Isaac-Renton, K. Roberts, and M. Sinclair, "Managing the microbiological risks of drinking water," *J. Toxicol. Environ. Health. A*, vol. 67, no. 20–22, pp. 1591–617, 2014.

[26] N. Schaffter and A. Parriaux, "Pathogenic-bacterial water contamination in mountainous catchments," *Water Res.*, vol. 36, no. 1, pp. 131–139, Jan. 2002.

[27] K. G. Field and M. Samadpour, "Fecal source tracking, the indicator paradigm, and managing water quality," *Water Res.*, vol. 41, no. 16, pp. 3517–38, Aug. 2007.

[28] A. Yousef, "Detection of Bacterial Pathogens in Different Matrices: Current Practices and Challenges," in *Principles of Bacterial Detection: Biosensors, Recognition Receptors and Microsystems*, M. Zourob, S. Elwary, and A. Turner, Eds. Springer, 2008, pp. 31–46.

[29] Ó. K. Vang, C. B. Corfitzen, C. Smith, and H. J. Albrechtsen, "Evaluation of ATP measurements to detect microbial ingress by wastewater and surface water in drinking water," *Water Res.*, vol. 64, pp. 309–320, 2014.

[30] WHO, “Guidelines for Drinking-water Quality.” World Health Organisation, 2011.

[31] P. I. Tarr, “Escherichia coli 0157 :17 Clinical, Diagnostic, and Epidemiological Aspects of Human Infection,” *Clin. Infect. Dis.*, vol. 20, pp. 1–10, 1995.

[32] F. B. Osei and A. A. Duker, “Spatial dependency of V. cholera prevalence on open space refuse dumps in Kumasi, Ghana: a spatial statistical modelling,” *Int. J. Health Geogr.*, vol. 7, p. 62, 2008.

[33] R. Subbaraman, S. Shitole, T. Shitole, K. Sawant, J. O’Brien, D. E. Bloom, and A. Patil-Deshmukh, “The social ecology of water in a Mumbai slum: failures in water quality, quantity, and reliability,” *BMC Public Health*, vol. 13, no. 1, p. 173, Jan. 2013.

[34] D. Y. Lee, H. Lee, J. T. Trevors, S. C. Weir, J. L. Thomas, and M. Habash, “Characterization of sources and loadings of fecal pollutants using microbial source tracking assays in urban and rural areas of the Grand River Watershed, Southwestern Ontario,” *Water Res.*, vol. 53, pp. 121–131, 2014.

[35] D. J. Wilson, E. Gabriel, A. J. H. Leatherbarrow, J. Cheesbrough, S. Gee, E. Bolton, A. Fox, P. Fearnhead, C. A. Hart, and P. J. Diggle, “Tracing the source of campylobacteriosis,” *PLoS Genet.*, vol. 4, no. 9, p. e1000203, Jan. 2008.

[36] B. L. Coleman, M. Louie, M. I. Salvadori, S. a McEwen, N. Neumann, K. Sibley, R. J. Irwin, F. B. Jamieson, D. Daignault, A. Majury, S. Braithwaite, B. Crago, and A. J. McGeer, “Contamination of Canadian private drinking water sources with antimicrobial resistant Escherichia coli,” *Water Res.*, vol. 47, no. 9, pp. 3026–36, Jun. 2013.

[37] S. K. Frey, E. Topp, T. Edge, C. Fall, V. Gannon, C. Jokinen, R. Marti, N. Neumann, N. Ruecker, G. Wilkes, and D. R. Lapen, “Using SWAT, Bacteroidales microbial source tracking markers, and fecal indicator bacteria to predict waterborne pathogen occurrence in an agricultural watershed,” *Water Res.*, vol. 47, no. 16, pp. 6326–6337, 2013.

[38] T. Wardlaw, P. Salama, C. Brocklehurst, M. Chopra, and E. Mason, *Diarrhoea: why children are still dying and what can be done*, vol. 375. New York: UNICEF, 2009.

[39] J.-Y. Jyoung, S. Hong, W. Lee, and J.-W. Choi, “Immunosensor for the detection of Vibrio cholerae O1 using surface plasmon resonance,” *Biosens. Bioelectron.*, vol. 21, no. 12, pp. 2315–9, Jun. 2006.

[40] P. M. Munro and R. R. Colwell, “Fate of Vibrio cholerae O1 in seawater microcosms,” *Water Res.*, vol. 30, no. 1, pp. 47–50, Jan. 1996.

[41] E. M. Fykse, T. Nilsen, A. D. Nielsen, I. Tryland, S. Delacroix, and J. M. Blatny, “Real-time PCR and NASBA for rapid and sensitive detection of Vibrio cholerae in ballast water,” *Mar. Pollut. Bull.*, vol. 64, no. 2, pp. 200–6, Feb. 2012.

[42] C.-S. Chin, J. Sorenson, J. B. Harris, W. P. Robins, R. C. Charles, R. R. Jean-Charles, J. Bullard, D. R. Webster, A. Kasarskis, P. Peluso, E. E. Paxinos, Y. Yamaichi, S. B. Calderwood, J. J. Mekalanos, E. E. Schadt, and M. K. Waldor, “The origin of the Haitian cholera outbreak strain,” *N. Engl. J. Med.*, vol. 364, no. 1, pp. 33–42, Jan. 2011.

[43] J. M. Drazen and M. S. Klempner, “Disaster, Water, Cholera, Vaccines, and Hope,” *N. Engl. J. Med.*, vol. 352, no. 8, p. 2015, 2015.

[44] R. McEgan, G. Mootian, L. D. Goodridge, D. W. Schaffner, and M. D. Danyluk,

"Predicting Salmonella populations from biological, chemical, and physical indicators in Florida surface waters," *Appl. Environ. Microbiol.*, vol. 79, no. 13, pp. 4094–4105, 2013.

[45] M. Pronk, N. Goldscheider, and J. Zopfi, "Particle-size distribution as indicator for fecal bacteria contamination of drinking water from karst springs," *Environ. Sci. Technol.*, vol. 41, no. 24, pp. 8400–8405, 2007.

[46] J. Bartram and S. Pedley, "Micrbiological analysis," in *Water quality - A practical guide to the design and implementation of freshwater quality studies and monitoring programmes*, UNEP/WHO, 1996.

[47] T.-T. Fong and K. Lipp, "Enteric viruses of humans and animals in aquatic environments: Health risks, detection, and potential water quality assessment tools," *Microbiol. Mol. Biol. Rev.*, vol. 69, no. 2, pp. 357–371, 2005.

[48] R. T. Noble, D. F. Moore, M. K. Leecaster, C. D. McGee, and S. B. Weisberg, "Comparison of total coliform, fecal coliform, and enterococcus bacterial indicator response for ocean recreational water quality testing," *Water Res.*, vol. 37, pp. 1637–1643, 2003.

[49] S. D. Leskinen, V. J. Harwood, and D. V Lim, "Rapid dead-end ultrafiltration concentration and biosensor detection of enterococci from beach waters of Southern California," *J. Water Health*, vol. 7, no. 4, pp. 674–84, Dec. 2009.

[50] D. M. Tritz, P. C. Iwen, and G. L. Woods, "Evaluation of MicroScan for identification of Enterococcus species," *J. Clin. Microbiol.*, vol. 28, no. 6, pp. 1477–8, Jun. 1990.

[51] H. C. Berg and L. Turner, "Cells of Escherichia coli swim either end forward," *Proc. Natl. Acad. Sci. U. S. A.*, vol. 92, no. 2, pp. 477–9, Jan. 1995.

[52] M. I. Zibaii, A. Kazemi, H. Latifi, M. K. Azar, S. M. Hosseini, and M. H. Ghezelaiagh, "Measuring bacterial growth by refractive index tapered fiber optic biosensor," *J. Photochem. Photobiol. B.*, vol. 101, no. 3, pp. 313–20, Dec. 2010.

[53] J. B. Kaper, J. P. Nataro, and H. L. Mobley, "Pathogenic Escherichia coli," *Nat. Rev. Microbiol.*, vol. 2, no. 2, pp. 123–40, Feb. 2004.

[54] P. Sule, S. M. Horne, C. M. Logue, and B. M. Prüss, "Regulation of cell division, biofilm formation, and virulence by FlhC in Escherichia coli O157:H7 grown on meat," *Appl. Environ. Microbiol.*, vol. 77, no. 11, pp. 3653–62, Jun. 2011.

[55] C. A. Phillips, "The epidemiology , detection and control of Escherichia coli O157," *J. Sci. Food Agric.*, vol. 79, pp. 1367–1381, 1999.

[56] F. Alhashash, V. Weston, M. Diggle, and A. McNally, "Multidrug-Resistant Escherichia coli Bacteremia," *Emerg. Infect. Dis.*, vol. 19, no. 10, pp. 19–21, 2013.

[57] M. E. Locking, K. G. J. Pollock, L. J. Allison, L. Rae, M. F. Hanson, and J. M. Cowden, "Escherichia coli O157 infection and secondary spread, Scotland, 1999-2008.," *Emerg. Infect. Dis.*, vol. 17, no. 3, pp. 524–7, Mar. 2011.

[58] C. Yang, H. Xie, Y. Li, J.-K. Zhang, and B.-L. Su, "Direct and rapid quantum dots labelling of Escherichia coli cells," *J. Colloid Interface Sci.*, vol. 393, pp. 438–44, Mar. 2013.

[59] A. Bren and M. Eisenbach, "How Signals Are Heard during Bacterial Chemotaxis : Protein-Protein Interactions in Sensory Signal Propagation," *J. Bacteriol.*, vol. 182, no. 24, 2000.

[60] R. Barak, W. N. Abouhamad, and M. Eisenbach, “Both Acetate Kinase and Acetyl Coenzyme A Synthetase Are Involved in Acetate-Stimulated Change in the Direction of Flagellar Rotation in Escherichia coli Both Acetate Kinase and Acetyl Coenzyme A Synthetase Are Involved in Acetate-Stimulated Change in the,” *J. Bacteriol.*, vol. 180, no. 4, pp. 985–988, 1998.

[61] Algonquin, “Anatomy and Physiology,” 2012. [Online]. Available: http://lyceum.algonquincollege.com/lts/onlineCourses/anatomy/content/module15-4.htm#. [Accessed: 17-Jan-2015].

[62] M. Berney, H.-U. Weilenmann, and T. Egli, “Flow-cytometric study of vital cellular functions in Escherichia coli during solar disinfection (SODIS),” *Microbiology*, vol. 152, no. Pt 6, pp. 1719–29, Jun. 2006.

[63] N. Parthuisot, P. Catala, P. Lebaron, D. Clermont, and C. Bizet, “A sensitive and rapid method to determine the viability of freeze-dried bacterial cells,” *Lett. Appl. Microbiol.*, vol. 36, no. 6, pp. 412–7, Jan. 2003.

[64] M. Letters, D. J. Grimes, and R. R. Colwell, “Viability and virulence of Escherichia coli suspended by membrane chamber in semitropical ocean water,” *FEMS Microbiol. Lett.*, vol. 34, pp. 161–165, 1986.

[65] A.-K. Kniggendorf and M. Meinhardt-Wollweber, “Of microparticles and bacteria identification--(resonance) Raman micro-spectroscopy as a tool for biofilm analysis.,” *Water Res.*, vol. 45, no. 15, pp. 4571–82, Oct. 2011.

[66] K. Zhu, A. S. Kaprelyants, E. G. Salina, and G. H. Markx, “Separation by dielectrophoresis of dormant and nondormant bacterial cells of Mycobacterium smegmatis.,” *Biomicrofluidics*, vol. 4, no. 2, Jan. 2010.

[67] G. V. Mukamolova, A. S. Kaprelyants, D. Kell, and M. Young, “Adoption of the transiently non-culturable state - A bacterial survival strategy?,” *Adv. Microb. Physiol.*, vol. 47, pp. 65–129, 2003.

[68] H. Liao, F. Zhang, X. Liao, X. Hu, Y. Chen, and L. Deng, “Analysis of Escherichia coli cell damage induced by HPCD using microscopies and fluorescent staining.,” *Int. J. Food Microbiol.*, vol. 144, no. 1, pp. 169–76, Nov. 2010.

[69] F. Joux and P. Lebaron, “Use of fluorescent probes to assess physiological functions of bacteria at single-cell level,” *Microbes Infect.*, vol. 2, no. 12, pp. 1523–35, Oct. 2000.

[70] G. Nebe-von-Caron, P. Stephens, C. Hewitt, J. Powell, and R. Badley, “Analysis of bacterial function by multi-colour fluorescence flow cytometry and single cell sorting,” *J. Microbiol. Methods*, vol. 42, no. 1, pp. 97–114, Sep. 2000.

[71] R. Sachidanandham and K. Gin, “A dormancy State in non-spore forming bacteria,” *Appl. Microbiol. Biotechnol.*, vol. 81, pp. 927–941, 2008.

[72] B. C. Okeke, M. S. Thomson, and E. M. Moss, “Occurrence, molecular characterization and antibiogram of water quality indicator bacteria in river water serving a water treatment plant,” *Sci. Total Environ.*, vol. 409, no. 23, pp. 4979–4985, 2011.

[73] F. Hammes, M. Berney, Y. Wang, M. Vital, O. Köster, and T. Egli, “Flow-cytometric total bacterial cell counts as a descriptive microbiological parameter for drinking water treatment processes,” *Water Res.*, vol. 42, no. 1–2, pp. 269–77, Jan. 2008.

[74] CIWP, “Indicators for Waterborne Pathogens,” in *Committee on Indicators for*

Waterborne Pathogens Board on Life Sciences Water Science and Technology Board Division on Earth and Life Studies, Board on L., N. R. C. of the Academies, Ed. Washington, D.C USA: National Academies Press, 2004.

[75] S. Sutton, "Accuracy of Plate Counts," *Microbiol. Top.*, vol. 17, no. 3, pp. 42–46, 2011.

[76] F. A. Skinner, P. C. T. Jones, and J. E. Mollison, "A Comparison of a direct- and a plate-counting technique for the quantitative estimation of soil micro-organisms," *J. Gen. Microbiol.*, vol. 6, pp. 261–271, 1952.

[77] R. N. Bushon, A. M. Brady, C. A. Likirdopulos, and J. V Cireddu, "Rapid detection of Escherichia coli and enterococci in recreational water using an immunomagnetic separation/adenosine triphosphate technique," *J. Appl. Microbiol.*, vol. 106, no. 2, pp. 432–41, Feb. 2009.

[78] S. J. Lee, J. S. Park, H. T. Im, and H. Jungi, "Microfluidic ATP-Bioluminescence Sensor for Detection of Airborne Microbes," in *Transducers. International Solid-State Sensors, Actuators and Microsystems Conference*, 2007, pp. 763–766.

[79] A. Vinelli, M. Onofri, and G. Zuccheri, "Biochemical and nanotechnological strategies for signal enhancement in the detection of nucleic acids with biosensors," in *Detection of Pathogens in Water Using Micro and Nano Technology2*, G. Zuccheri and N. Asproulis, Eds. London: IWA, 2012, p. 113.

[80] A. Taylor, J. Ladd, J. Homola, and S. Jiang, "Surface Plasmon Resonance (SPR) Sensors for the Detection of Bacterial Pathogens," in *Principles of Bacterial Detection: Biosensors, Recognition Receptors and Microsystems*, M. Zourob, S. Elwary, and A. Turner, Eds. Springer, 2008, pp. 83–104.

[81] V. Tsouti, C. Boutopoulos, I. Zergioti, and S. Chatzandroulis, "Capacitive microsystems for biological sensing," *Biosens. Bioelectron.*, vol. 27, no. 1, pp. 1–11, Sep. 2011.

[82] S. Melamed, L. Ceriotti, W. Weigel, F. Rossi, P. Colpo, and S. Belkin, "A printed nanolitre-scale bacterial sensor array," *Lab Chip*, vol. 11, no. 1, pp. 139–46, Jan. 2011.

[83] T. Love and B. Jones, "Introduction to Pathogenic Bacteria," in *Principles of Bacterial Detection: Biosensors, Recognition Receptors and Microsystems*, M. Zourob, S. Elwary, and A. Turner, Eds. Springer, 2008, pp. 2–12.

[84] J. R. Lakowicz, *Principles of Fluorescence Spectroscopy*, no. v. 1. Springer, 2006.

[85] K. Zhang, L. Fu, L. Zhang, Z.-Y. Cheng, and T.-S. Huang, "Magnetostrictive particle based biosensors for in situ and real-time detection of pathogens in water," *Biotechnol. Bioeng.*, vol. 111, no. 11, pp. 2229–38, Nov. 2014.

[86] F. C. Neidhardt, *Escherichia coli and Salmonella typhimurium : cellular and molecular biology*. Washington, D.C USA: American Society for Microbiology, 1987.

[87] B. Glynn, "Rapid nucleic acid-based detection methods for the detection of bacterial pathogens," in *Principles of Bacterial Detection*, M. Zourob, S. Elwary, and A. Turner, Eds. Springer, 2008, pp. 603–628.

[88] M. Gabig-Ciminska, A. Holmgren, H. Andresen, K. Bundvig Barken, M. Wümpelmann, J. Albers, R. Hintsche, A. Breitenstein, P. Neubauer, M. Los, A. Czyz, G. Wegrzyn, G. Silfversparre, B. Jürgen, T. Schweder, and S.-O. Enfors, "Electric chips for rapid detection and quantification of nucleic acids," *Biosens. Bioelectron.*, vol. 19, no. 6, pp. 537–546, Jan. 2004.

[89] S. Courtois, A. Cajon, A. Romey, F. Poyet, C. Mabilat, F. Payet, and MabilatClaude, “Multi-detection of waterborne pathogens in raw and treated water samples by using ultrafiltration concentration and DNA array technology,” in *Detection of Pathogens in Water Using Micro and Nano Technology*, G. Zuccheri and N. Asproulis, Eds. London: IWA, 2012, pp. 173–187.

[90] D. Li, S. Song, and C. Fan, “Target-responsive structural switching for nucleic acid-based sensors.,” *Acc. Chem. Res.*, vol. 43, no. 5, pp. 631–41, May 2010.

[91] V. Chizhikov, A. Rasooly, D. D. Levy, and K. Chumakov, “Microarray Analysis of Microbial Virulence Factors Microarray Analysis of Microbial Virulence Factors,” *Appl. Environ. Microbiol.*, vol. 67, no. 7, pp. 1–7, 2001.

[92] R.-F. Wang, M. L. Beggs, B. D. Erickson, and C. E. Cerniglia, “DNA microarray analysis of predominant human intestinal bacteria in fecal samples.,” *Mol. Cell. Probes*, vol. 18, no. 4, pp. 223–34, Aug. 2004.

[93] J. C. Liao, M. Mastali, V. Gau, M. A. Suchard, A. K. Møller, D. A. Bruckner, J. T. Babbitt, Y. Li, J. Gornbein, E. M. Landaw, E. R. B. Mccabe, B. M. Churchill, D. A. Haake, and J. C. L. I. N. M. Icrobiol, “Use of Electrochemical DNA Biosensors for Rapid Molecular Identification of Uropathogens in Clinical Urine Specimens,” *J. Clin. Microbiol.*, vol. 44, no. 2, pp. 561–570, 2006.

[94] C. Pohlmann, Y. Wang, M. Humenik, B. Heidenreich, M. Gareis, and M. Sprinzl, “Rapid, specific and sensitive electrochemical detection of foodborne bacteria,” *Biosens. Bioelectron.*, vol. 24, pp. 2766–2771, 2009.

[95] H.-M. So, D.-W. Park, E.-K. Jeon, Y.-H. Kim, B. S. Kim, C.-K. Lee, S. Y. Choi, S. C. Kim, H. Chang, and J.-O. Lee, “Detection and titer estimation of Escherichia coli using aptamer-functionalized single-walled carbon-nanotube field-effect transistors,” *Small*, vol. 4, no. 2, pp. 197–201, Feb. 2008.

[96] S. M. Shamah, J. M. Healy, and S. T. Cload, “Complex target SELEX,” *Acc. Chem. Res.*, vol. 41, no. 1, pp. 130–8, Jan. 2008.

[97] D. Ogasawara, N. S. Hachiya, K. Kaneko, K. Sode, and K. Ikebukuro, “Detection system based on the conformational change in an aptamer and its application to simple bound/free separation,” *Biosens. Bioelectron.*, vol. 24, no. 5, pp. 1372–6, Jan. 2009.

[98] Y. Xu, X. Yang, and E. Wang, “Review: Aptamers in microfluidic chips,” *Anal. Chim. Acta*, vol. 683, no. 1, pp. 12–20, Dec. 2010.

[99] A. Bogomolova and M. Aldissi, “Real-time aptamer quantum dot fluorescent flow sensor,” *Biosens. Bioelectron.*, vol. 26, no. 10, pp. 4099–103, Jun. 2011.

[100] C. C. Fowler, N. K. Navani, E. D. Brown, and L. Yingfu, “Aptamers and Their Potential as Recognition Elements for the Detection of Bacteria,” in *Principles of Bacterial Detection*, M. Zourob, S. Elwary, and A. Turner, Eds. Springer, 2008, pp. 689–714.

[101] P. S. Pendergrast, H. N. Marsh, D. Grate, J. M. Healy, and M. Stanton, “Nucleic Acid Aptamers for Target Validation and Therapeutic Application,” vol. 16, no. 3, pp. 224–234, 2005.

[102] K. Sefah, J. A. Phillips, X. Xiong, L. Meng, D. Van Simaeys, H. Chen, J. Martin, and W. Tan, “Nucleic acid aptamers for biosensors and bio-analytical applications,” *Analyst*, vol. 134, no. 9, pp. 1765–75, Sep. 2009.

[103] B. Hall, S. Cater, M. Levy, and A. D. Ellington, “Kinetic optimization of a protein-responsive aptamer beacon.,” *Biotechnol. Bioeng.*, vol. 103, no. 6, pp.

1049–59, Aug. 2009.

[104] R. Nutiu and Y. Li, “Aptamers with fluorescence-signaling properties,” *Methods*, vol. 37, no. 1, pp. 16–25, Sep. 2005.

[105] V. Nizet, “Antimicrobial peptide resistance mechanisms of human bacterial pathogens,” *Curr Issues Mol Biol*, vol. 8, pp. 11–26, 2006.

[106] M. S. Mannoor, S. Zhang, A. J. Link, and M. C. McAlpine, “Electrical detection of pathogenic bacteria via immobilized antimicrobial peptides,” *Proc. Natl. Acad. Sci. U. S. A.*, vol. 107, no. 45, pp. 19207–12, Nov. 2010.

[107] R. Yalow and S. Berson, “Assay of plasma insulin in human subjects by immunological methods,” *Nature*, vol. 184, pp. 1648–1649, 1959.

[108] C. Kaittanis, S. Santra, and J. M. Perez, “Emerging nanotechnology-based strategies for the identification of microbial pathogenesis,” *Adv. Drug Deliv. Rev.*, vol. 62, no. 4–5, pp. 408–23, Mar. 2010.

[109] M. Mujika, S. Arana, E. Castaño, M. Tijero, R. Vilares, J. M. Ruano-López, A. Cruz, L. Sainz, and J. Berganza, “Magnetoresistive immunosensor for the detection of Escherichia coli O157:H7 including a microfluidic network,” *Biosens. Bioelectron.*, vol. 24, no. 5, pp. 1253–8, Jan. 2009.

[110] A. K. Trilling, J. Beekwilder, and H. Zuilhof, “Antibody orientation on biosensor surfaces: a minireview,” *Analyst*, vol. 138, no. 6, pp. 1619–27, Mar. 2013.

[111] V. C. Martins, J. Germano, F. A. Cardoso, J. Loureiro, S. Cardoso, L. Sousa, M. Piedade, L. P. Fonseca, and P. P. Freitas, “Challenges and trends in the development of a magnetoresistive biochip portable platform,” *J. Magn. Magn. Mater.*, vol. 322, pp. 1655–1663, 2010.

[112] H. Wang, A. Mahdavi, D. A. Tirrell, and A. Hajimiri, “A magnetic cell-based sensor.,” *Lab Chip*, vol. 12, no. 21, pp. 4465–71, Nov. 2012.

[113] A. Rompré, P. Servais, J. Baudart, M. R. De-Roubin, and P. Laurent, “Detection and enumeration of coliforms in drinking water: current methods and emerging approaches,” *J. Microbiol. Methods*, vol. 49, no. 1, pp. 31–54, Mar. 2002.

[114] Y. Cheng, Y. Liu, J. Huang, K. Li, Y. Xian, W. Zhang, and L. Jin, “Amperometric tyrosinase biosensor based on Fe3O4 nanoparticles-coated carbon nanotubes nanocomposite for rapid detection of coliforms,” *Electrochim. Acta*, vol. 54, no. 9, pp. 2588–2594, Mar. 2009.

[115] T. C. Meredith, U. Mamat, Z. Kaczynski, B. Lindner, O. Holst, and R. W. Woodard, “Modification of lipopolysaccharide with colanic acid (M-antigen) repeats in Escherichia coli,” *J. Biol. Chem.*, vol. 282, no. 11, pp. 7790–8, Mar. 2007.

[116] G. Herrera, A. Martinez, M. Blanco, and J.-E. O’Connor, “Assessment of Escherichia coli B with enhanced permeability to fluorochromes for flow cytometric assays of bacterial cell function,” *Cytometry*, vol. 49, pp. 62–69, Oct. 2002.

[117] A. F. Maheux, L. Bissonnette, M. Boissinot, J.-L. T. Bernier, V. Huppé, E. Bérubé, D. K. Boudreau, F. J. Picard, A. Huletsky, and M. G. Bergeron, “Method for rapid and sensitive detection of Enterococcus sp. and Enterococcus faecalis/faecium cells in potable water samples,” *Water Res.*, vol. 45, no. 6, pp. 2342–54, Mar. 2011.

[118] M. M. Ngundi, C. R. Taitt, S. A. McMurry, D. Kahne, and F. S. Ligler, “Detection of bacterial toxins with monosaccharide arrays,” *Biosens. Bioelectron.*, vol. 21,

no. 7, pp. 1195–201, Jan. 2006.

[119] S. Viswanathan, L. Wu, M. Huang, and J. A. Ho, “Electrochemical Immunosensor for Cholera Toxin Using Liposomes and Poly (3 , 4-ethylenedioxythiophene) - Coated Carbon Nanotubes amplified detection of cholera toxin. The sensing interface,” *Anal. Chem.*, vol. 78, no. 4, pp. 1115–1121, 2006.

[120] M. Labib, M. Hedström, M. Amin, and B. Mattiasson, “A capacitive immunosensor for detection of cholera toxin,” *Anal. Chim. Acta*, vol. 634, no. 2, pp. 255–61, Feb. 2009.

[121] N. Bunyakul, K. A. Edwards, C. Promptmas, and A. J. Baeumner, “Cholera toxin subunit B detection in microfluidic devices,” *Anal. Bioanal. Chem.*, vol. 393, pp. 177–186, 2009.

[122] C. L. Schofield, R. A. Field, and D. A. Russell, “Glyconanoparticles for the colorimetric detection of cholera toxin,” *Anal. Chem.*, vol. 79, no. 4, pp. 1356–61, Feb. 2007.

[123] M. Pantastico-Caldas, K. E. Duncan, C. I. Istock, and J. A. Bell, “Population Dynamics of Bacteriophage and Bacillus Subtilis in Soil,” *Ecology*, vol. 73, no. 5, pp. 1888–1902, 2012.

[124] M. B. Mejri, A. Tlili, and A. Abdelghani, “Magnetic Nanoparticles Immobilization and Functionalization for Biosensor Applications,” *Int. J. Electrochem.*, vol. 2011, pp. 1–5, 2011.

[125] M. Namura, T. Hijikata, K. Miyanaga, and Y. Tanji, “Detection of Escherichia coli with fluorescent labeled phages that have a broad host range to E. coli in sewage water,” *Biotechnol. Prog.*, vol. 24, no. 2, pp. 481–6, 2008.

[126] C. Pereira, Y. J. Silva, A. L. Santos, A. Cunha, N. C. M. Gomes, and A. Almeida, “Bacteriophages with potential for inactivation of fish pathogenic bacteria: survival, host specificity and effect on bacterial community structure,” *Mar. Drugs*, vol. 9, no. 11, pp. 2236–55, Jan. 2011.

[127] S. K. Arya, A. Singh, R. Naidoo, P. Wu, M. T. McDermott, S. Evoy, T. Mcdermott, and S. Evoy, “Chemically immobilized T4-bacteriophage for specific Escherichia coli detection using surface plasmon resonance,” *Analyst*, vol. 136, no. 3, pp. 486–92, Feb. 2011.

[128] O. Lazcka, F. J. Del Campo, and F. X. Muñoz, “Pathogen detection: a perspective of traditional methods and biosensors.,” *Biosens. Bioelectron.*, vol. 22, no. 7, pp. 1205–17, Feb. 2007.

[129] J. Heo and S. Z. Hua, “An overview of recent strategies in pathogen sensing,” *Sensors (Basel).*, vol. 9, no. 6, pp. 4483–502, Jan. 2009.

[130] L. Su, W. Jia, C. Hou, and Y. Lei, “Microbial biosensors: a review,” *Biosens. Bioelectron.*, vol. 26, no. 5, pp. 1788–99, Jan. 2011.

[131] B. Van Dorst, J. Mehta, K. Bekaert, E. Rouah-Martin, W. De Coen, P. Dubruel, R. Blust, and J. Robbens, “Recent advances in recognition elements of food and environmental biosensors: a review,” *Biosens. Bioelectron.*, vol. 26, no. 4, pp. 1178–94, Dec. 2010.

[132] S. S. Iqbal, M. W. Mayo, J. G. Bruno, B. V. Bronk, C. A. Batt, and J. P. Chambers, “A review of molecular recognition technologies for detection of biological threat agents,” *Biosens. Bioelectron.*, vol. 15, pp. 549–578, 2000.

[133] O. Zielinski, J. A. Busch, A. D. Cembella, K. L. Daly, J. Engelbrektsson, A. K. Hannides, and H. Schmidt, “Detecting marine hazardous substances and

organisms: sensors for pollutants, toxins, and pathogens," *Ocean Sci. Discuss.*, vol. 6, no. 2, pp. 953–1005, May 2009.

[134] B.-K. Oh, W. Lee, W. H. Lee, and J.-W. Choi, "Nano-scale probe fabrication using self-assembly technique and application to detection of Escherichia coli O157:H7," *Biotechnol. bioprocess Eng.*, vol. 8, pp. 227–232, 2003.

[135] N. V Zaytseva, R. A. Montagna, and A. J. Baeumner, "Microfluidic biosensor for the serotype-specific detection of dengue virus RNA," *Anal. Chem.*, vol. 77, no. 23, pp. 7520–7, Dec. 2005.

[136] B. Elsholz, R. Wörl, L. Blohm, J. Albers, H. Feucht, T. Grunwald, B. Jürgen, T. Schweder, and R. Hintsche, "Automated detection and quantitation of bacterial RNA by using electrical microarrays," *Anal. Chem.*, vol. 78, no. 14, pp. 4794–802, Jul. 2006.

[137] H. M. Shapiro, H. Ave, and W. Newton, "Microbial analysis at the single-cell level : tasks and techniques," *J. Microbiol. Methods*, vol. 42, pp. 3–16, 2000.

[138] X. Xue, J. Pan, H. Xie, J. Wang, and S. Zhang, "Fluorescence detection of total count of Escherichia coli and Staphylococcus aureus on water-soluble CdSe quantum dots coupled with bacteria," *Talanta*, vol. 77, no. 5, pp. 1808–13, Mar. 2009.

[139] G. Zhuang, T. G. Jensen, and J. P. Kutter, "Detection of unlabeled particles in the low micrometer size range using light scattering and hydrodynamic 3D focusing in a microfluidic system," *Electrophoresis*, vol. 33, pp. 1715–1722, 2012.

[140] J. Nurmi, A. Ylikoski, T. Soukka, M. Karp, and T. Lövgren, "A new label technology for the detection of specific polymerase chain reaction products in a closed tube," *Nucleic Acids Res.*, vol. 28, no. 8, p. E28, 2000.

[141] S.-I. Tu, S. Reed, A. Gehring, Y. He, and G. Paoli, "Capture of Escherichia coli O157:H7 Using Immunomagnetic Beads of Different Size and Antibody Conjugating Chemistry.," *Sensors (Basel).*, vol. 9, no. 2, pp. 717–30, Jan. 2009.

[142] Z. Salamon, H. A. Macleo, and G. Tollin, "Surface plasmon resonance spectroscopy as a tool for investigating the biochemical and biophysical properties of membrane protein systems: Application to biological systems," *Biochim. Biophys. Acta*, vol. 1331, pp. 131–152, 1997.

[143] P. Pattnaik, "Surface plasmon resonance: applications in understanding receptor-ligand interaction," *Appl. Biochem. Biotechnol.*, vol. 126, no. 2, pp. 79–92, 2005.

[144] K. Sapsford and L. C. Shriver-Lake, "Bacterial Detection Using Evanescent Wave-Based Fluorescent Biosensors," in *Principles of Bacterial Detection: Biosensors, Recognition Receptors and Microsystems2*, M. Zourob, S. Elwary, and A. Turner, Eds. 6: Springer, 2008, pp. 109–120.

[145] K. Schmitt, B. Schirmer, C. Hoffmann, A. Brandenburg, and P. Meyrueis, "Interferometric biosensor based on planar optical waveguide sensor chips for label-free detection of surface bound bioreactions," *Biosens. Bioelectron.*, vol. 22, no. 11, pp. 2591–7, May 2007.

[146] S. K. Padigi, K. Asante, V. S. R. Kovvuri, R. K. K. Reddy, A. La Rosa, and S. Prasad, "Micro-photonic cylindrical waveguide based protein biosensor," *Nanotechnology*, vol. 17, no. 17, pp. 4384–4390, Sep. 2006.

[147] M. F. Kramer, G. Vesey, N. L. Look, B. R. Herbert, J. M. Simpson-Stroot, and D. V Lim, "Development of a Cryptosporidium oocyst assay using an automated fiber optic-based biosensor," *J. Biol. Eng.*, vol. 1, p. 3, Jan. 2007.

[148] M. Zourob, S. Mohr, B. J. Treves Brown, P. R. Fielden, M. B. McDonnell, and N. J. Goddard, "An integrated metal clad leaky waveguide sensor for detection of bacteria.," *Anal. Chem.*, vol. 77, no. 1, pp. 232–42, Jan. 2005.

[149] D. Bhatta, E. Stadden, E. Hashem, I. J. G. Sparrow, and G. D. Emmerson, "Multi-purpose optical biosensors for real-time detection of bacteria, viruses and toxins," *Sensors Actuators B Chem.*, vol. 149, no. 1, pp. 233–238, Aug. 2010.

[150] A. Brandenburg, R. Krauter, C. Künzel, M. Stefan, and H. Schulte, "Interferometric sensor for detection of surface-bound bioreactions," *Appl. Opt.*, vol. 39, no. 34, pp. 6396–6405, 2000.

[151] H. Latifi, M. I. Zibaii, S. M. Hosseini, and P. Jorge, "Nonadiabatic tapered optical fiber for biosensor applications," *Photonic Sensors*, vol. 2, no. 4, pp. 340–356, 2012.

[152] M. Zourob, S. Mohr, B. J. Treves Brown, P. R. Fielden, M. B. McDonnell, and N. J. Goddard, "Bacteria Detection using Disposable Optical Leaky Waveguide," *Biosens. Bioelectron.*, vol. 21, pp. 293–302, 2005.

[153] H. K. P. Mulder, A. Ymeti, V. Subramaniam, and J. S. Kanger, "Size-selective detection in integrated optical interferometric biosensors," *Opt. Express*, vol. 20, no. 19, p. 20934, 2012.

[154] A. Ferreira, M. Werneck, and R. Ribeiro, "Development of an evanescent-field fibre optic sensor for Escherichia coli O157:H7," *Biosens. Bioelectron.*, vol. 16, no. 6, pp. 399–408, Aug. 2001.

[155] D. A. Jackson, "Monomode optical fibre interferometers for precision measurement," *J. Phys. E.*, vol. 18, no. 12, pp. 981–1001, 2000.

[156] L. Yang and R. Bashir, "Electrical/electrochemical impedance for rapid detection of foodborne pathogenic bacteria," *Biotechnol. Adv.*, vol. 26, no. November, pp. 135–150, 2008.

[157] R. Pethig and G. H. Markx, "Applications of dielectrophoresis in biotechnology," *Trends Biotechnol.*, vol. 15, no. 10, pp. 426–432, 1997.

[158] P. Patel and G. H. Markx, "Dielectric measurement of cell death," *Enzyme Microb. Technol.*, vol. 43, no. 7, pp. 463–470, 2008.

[159] J. P. Carvell and J. E. Dowd, "On-line Measurements and Control of Viable Cell Density in Cell Culture Manufacturing Processes using Radio-frequency Impedance.," *Cytotechnology*, vol. 50, no. 1–3, pp. 35–48, 2006.

[160] R. Kargupta, S. Puttaswamy, A. L. Lee, T. E. Butler, Z. Li, and S. Sengupta, "Novel Electrical Impedance System for Rapid Detection of Mycobacteria," in *Annual conference of the Aiche*, 2015.

[161] G. H. Markx and C. L. Davey, "The dielectric properties of biological cells at radiofrequencies: applications in biotechnology," *Enzyme Microb. Technol.*, vol. 25, no. 3–50141–0229 English S0141–0229(99)00008–3 Elsevier Science Copyright (c) 1999 Elsevier Science Inc., pp. 161–171, 1999.

[162] E. L. Carstensen, "Passive Electrical Properties of Microorganisms," *Biophys. J.*, vol. 7, pp. 493–503, 1967.

[163] J. P. Carvell and J. E. Dowd, "On-line Measurements and Control of Viable Cell Density in Cell Culture Manufacturing Processes using Radio-frequency Impedance.," *Cytotechnology*, vol. 50, no. 1–3, pp. 35–48, 2006.

[164] K. Lei, "Review on Impedance Detection of Cellular Responses in Micro/Nano

Environment," *Micromachines*, vol. 5, no. 1, pp. 1–12, 2014.

[165] S. M. Radke and E. C. Alocilja, "Design and fabrication of a microimpedance biosensor for bacterial detection," *IEEE Sens. J.*, vol. 4, no. 4, pp. 434–440, 2004.

[166] J. H. Yeon and J.-K. Park, "Cytotoxicity test based on electrochemical impedance measurement of HepG2 cultured in microfabricated cell chip," *Anal. Biochem.*, vol. 341, no. 2, pp. 308–315, 2005.

[167] P. Cady and S. Dufour, "Electrical impedance measurements: rapid method for detecting and monitoring microorganisms.," *J. Clin. Microbiol.*, vol. 7, no. 3, pp. 265–272, 1978.

[168] S. Martínez, F. X. Muñoz, and E. Baldrich, "Inductive microcoils for the fast and simple detection of bacterial presence," *Sensors Actuators B Chem.*, vol. 147, no. 1, pp. 304–309, May 2010.

[169] O. Laczka, J.-M. Maesa, N. Godino, J. del Campo, M. Fougt-Hansen, J. P. Kutter, D. Snakenborg, F.-X. Muñoz-Pascual, and E. Baldrich, "Improved bacteria detection by coupling magneto-immunocapture and amperometry at flow-channel microband electrodes," *Biosens. Bioelectron.*, vol. 26, no. 8, pp. 3633–40, May 2011.

[170] G. A. Zelada-Guillen, S. V Bhosale, J. Riu, and F. X. Rius, "Real-Time Potentiometric Detection of Bacteria in Complex Samples," *Anal. Chem.*, vol. 82, pp. 9254–9260, 2010.

[171] R. Hernández, C. Vallés, A. M. Benito, W. K. Maser, F. X. Rius, and J. Riu, "Graphene-based potentiometric biosensor for the immediate detection of living bacteria," *Biosens. Bioelectron.*, vol. 54, pp. 553–7, Apr. 2014.

[172] S. Buchatip, C. Ananthanawat, P. Sithigorngul, P. Sangvanich, S. Rengpipat, and V. P. Hoven, "Detection of the shrimp pathogenic bacteria, Vibrio harveyi, by a quartz crystal microbalance-specific antibody based sensor," *Sensors Actuators B Chem.*, vol. 145, no. 1, pp. 259–264, Mar. 2010.

[173] M. A. Cooper, F. N. Dultsev, V. P. Ostanin, and D. Klenerman, "Separation and detection of bacteria using rupture event scanning," *Anal. Chim. Acta*, vol. 702, no. 2, pp. 233–8, Sep. 2011.

[174] X. Guo, C.-S. Lin, S.-H. Chen, R. Ye, and V. C. H. Wu, "A piezoelectric immunosensor for specific capture and enrichment of viable pathogens by quartz crystal microbalance sensor, followed by detection with antibody-functionalized gold nanoparticles.," *Biosens. Bioelectron.*, vol. 38, no. 1, pp. 177–83, 2012.

[175] R. Petry, M. Schmitt, and J. Popp, "Raman spectroscopy-a prospective tool in the life sciences," *Chemphyschem*, vol. 4, no. 1, pp. 14–30, Jan. 2003.

[176] R. M. Jarvis and R. Goodacre, "Discrimination of bacteria using surface-enhanced Raman spectroscopy," *Anal. Chem.*, vol. 76, no. 1, pp. 40–7, Jan. 2004.

[177] M. Veiseh, O. Veiseh, M. Martin, C. Bertozzi, and M. Zhange, "Single cell based sensors and synchrotron FTIR spectrscopy: a hybrid system towards bacterial detection," *Bionsensors Bioelectron.*, vol. 23, no. 2, pp. 253–260, 2007.

[178] O. Takeuchi, K. Hoshino, T. Kawai, H. Sanjo, H. Takada, T. Ogawa, K. Takeda, and S. Akira, "Differential roles of TLR2 and TLR4 in recognition of gram-negative and gram-positive bacterial cell wall components," *Immunity*, vol. 11, no. 4, pp. 443–51, Oct. 1999.

[179] H. Kim, K. M. Kosuda, R. P. Van Duyne, and P. C. Stair, "Resonance Raman and surface- and tip-enhanced Raman spectroscopy methods to study solid catalysts

and heterogeneous catalytic reactions," *Chem. Soc. Rev.*, vol. 39, pp. 4820–4844, 2010.

[180] P. Negri and R. A. Dluhy, "Ag Nanorod Based Surface-Enhanced Raman Spectroscopy Applied to Bioanalytical Sensing," *J. Biophotonics*, vol. 6, no. 1, pp. 20–35, 2013.

[181] A. Sengupta, M. Mujacic, and E. J. Davis, "Detection of bacteria by surface-enhanced Raman spectroscopy," *Anal. Bioanal. Chem.*, vol. 386, no. 5, pp. 1379–86, Nov. 2006.

[182] J. D. Driskell, R. J. Lipert, and M. D. Porter, "Labeled gold nanoparticles immobilized at smooth metallic substrates: systematic investigation of surface plasmon resonance and surface-enhanced Raman scattering," *J. Phys. Chem. B*, vol. 110, no. 35, pp. 17444–51, Sep. 2006.

[183] Y. Wang, Y. Ji, E. S. Wharfe, R. S. Meadows, P. March, R. Goodacre, J. Xu, and W. E. Huang, "Raman activated cell ejection for isolation of single cells," *Anal. Chem.*, vol. 85, pp. 10697–10701, 2013.

[184] E. Tourwé and A. Hubin, "Preparation of SERS-active electrodes via ex situ electrocrystallization of silver in a halide free electrolyte," *Vib. Spectrosc.*, vol. 41, no. 1, pp. 59–67, May 2006.

[185] R. Afshar, Y. Moser, T. Lehnert, and M. A. M. Gijs, "Magnetic particle dosing and size separation in a microfluidic channel," *Sensors Actuators B Chem.*, vol. 154, no. 1, pp. 73–80, May 2011.

[186] Miltenyi Biotec, "Protocol," 2008.

[187] N. Beyor, T. S. Seo, P. Liu, and R. A. Mathies, "Immunomagnetic bead-based cell concentration microdevice for dilute pathogen detection," *Biomed. Microdevices*, vol. 10, no. 6, pp. 909–17, Dec. 2008.

[188] P. Chen, Y.-Y. Huang, K. Hoshino, and X. Zhang, "Multiscale immunomagnetic enrichment of circulating tumor cells: from tubes to microchips.," *Lab Chip*, vol. 14, no. 3, pp. 446–58, 2014.

[189] D. Lukáš, K. Postava, O. Životský, and J. Pištora, "Optimization of electromagnet for high-field polar magneto-optical microscopy," *J. Magn. Magn. Mater.*, vol. 322, no. 9–12, pp. 1471–1474, May 2010.

[190] C. Hoffmann, M. Franzreb, and W. H. Holl, "A novel high-gradient magnetic separator (HGMS) design for biotech applications," *Ieee Trans. Appl. Supercond.*, vol. 12, no. 1, pp. 963–966, 2002.

[191] M. Cerff, A. Scholz, T. Käppler, K. E. Ottow, T. J. Hobley, and C. Posten, "Semi-continuous in situ magnetic separation for enhanced extracellular protease production-modeling and experimental validation.," *Biotechnol. Bioeng.*, vol. 110, no. 8, pp. 2161–72, 2013.

[192] J. Jung and K.-H. Han, "Lateral-driven continuous magnetophoretic separation of blood cells," *Appl. Phys. Lett.*, vol. 93, p. 223902, 2008.

[193] C. Fuh, "Development of magnetic split-flow thin fractionation for continuous particle separation," *Anal. Chim. Acta*, vol. 497, no. 1–2, pp. 115–122, 2003.

[194] M. Zborowski, L. P. Sun, L. R. Moore, P. S. Williams, and J. J. Chalmers, "Continuous cell separation using novel magnetic quadrupole flow sorter," *J. Magn. Magn. Mater.*, vol. 194, no. 1–3, pp. 224–230, 1999.

[195] A. N. Ghebremeskel and A. Bose, "A continuous, hybrid field-gradient device for

magnetic colloid-based separations," *J. Magn. Magn. Mater.*, vol. 261, no. 1–2, pp. 66–72, 2003.

[196] Q. Ramadan, L. Christophe, W. Teo, S. Li, and H. H. Feng, "Flow-through immunomagnetic separation system for waterborne pathogen isolation and detection: application to Giardia and Cryptosporidium cell isolation," *Anal. Chim. Acta*, vol. 673, no. 1, pp. 101–8, Jul. 2010.

[197] N. Pamme and A. Manz, "On-chip free-flow magnetophoresis: Continuous flow separation of magnetic particles and agglomerates," *Anal. Chem.*, vol. 76, no. 24, pp. 7250–7256, Dec. 2004.

[198] J. Kiely, R. Luxton, and P. Wraith, "Particle Facilitated Testing," US20100248345 A1, 2008.

[199] N. Pamme, "Magnetism and microfluidics," *Lab Chip*, vol. 6, no. 1, pp. 24–38, Jan. 2006.

[200] K. E. Sapsford and C. Shriver-Lake, "Bacterial Detection Using Evanescent Wave-Based Fluorescent Biosensor," in *Principles of Bacterial Detection*, A. Zourob, Mohammed ; Elwary, Souna ; Turner, Ed. Springer, 2008, pp. 109–120.

[201] D. P. Campbell, "Interferometric Biosensors," in *Principles of Bacterial Detection: Biosensors, Recognition Receptors and Microsystems*, 2008.

[202] A. Mehdinia, S. H. Kazemi, S. Z. Bathaie, A. Alizadeh, M. Shamsipur, and M. F. Mousavi, "Electrochemical DNA nano-biosensor for the study of spermidine-DNA interaction," *J. Pharm. Biomed. Anal.*, vol. 49, no. 3, pp. 587–93, Apr. 2009.

[203] E. Polo, S. Puertas, and P. R. Batalla, "Biosensors based on nanoparticles for elecrtochemical detection," in *Nanobiotechnology: Inorganic nanoparticles vs. organic nanoparticles*, Volume 4., de la F. J.M. and V. Grazu, Eds. Elsevier, 2012, pp. 247–261.

[204] L. Yang, X. Zhang, M. Ye, J. Jiang, R. Yang, T. Fu, Y. Chen, K. Wang, C. Liu, and W. Tan, "Aptamer-conjugated nanomaterials and their applications," *Adv. Drug Deliv. Rev.*, vol. 63, no. 14–15, pp. 1361–70, Nov. 2011.

[205] J. P. Devadhasan, S. Kim, and J. An, "Fish-on-a-chip: a sensitive detection microfluidic system for Alzheimer's disease," *J. Biomed. Sci.*, vol. 18, no. 1, p. 33, Jan. 2011.

[206] Y.-F. Young, H.-J. Lee, Y.-S. Shen, S.-H. Tseng, C.-Y. Lee, N.-H. Tai, and H.-Y. Chang, "Toxicity mechanism of carbon nanotubes on Escherichia coli," *Mater. Chem. Phys.*, vol. 134, no. 1, pp. 279–286, May 2012.

[207] R. L. Phillips, O. R. Miranda, C.-C. You, V. M. Rotello, and U. H. F. Bunz, "Rapid and efficient identification of bacteria using gold-nanoparticle-poly(para-phenyleneethynylene) constructs," *Angew. Chem. Int. Ed. Engl.*, vol. 47, no. 14, pp. 2590–2594, Jan. 2008.

[208] E. R. Goldman, A. R. Clapp, G. P. Anderson, H. T. Uyeda, J. M. Mauro, I. L. Medintz, and H. Mattoussi, "Multiplexed toxin analysis using four colors of quantum dot fluororeagents," *Anal. Chem.*, vol. 76, no. 3, pp. 684–8, Feb. 2004.

[209] A. Cusano, F. Arregui, M. Giordano, and A. Cutolo, "Multiplexed quantitation of four toxins using quantum dots," in *Optochemical Nanosensors*, Florida, USA, USA: CRC Press, 2013, pp. 485–486.

[210] R. Edgar, M. McKinstry, J. Hwang, A. B. Oppenheim, R. A. Fekete, G. Giulian, C. Merril, K. Nagashima, and S. Adhya, "High-sensitivity bacterial detection using biotin-tagged phage and quantum-dot nanocomplexes," *Proc. Natl. Acad.*

Sci. U. S. A., vol. 103, no. 13, pp. 4841–5, Mar. 2006.

[211] M. A. Hahn, P. C. Keng, and T. D. Krauss, "Flow cytometric analysis to detect pathogens in bacterial cell mixtures using semiconductor quantum dots," *Anal. Chem.*, vol. 80, no. 3, pp. 864–72, Feb. 2008.

[212] Y. Liu, R. Brandon, M. Cate, N. Llc, P. O. Box, and X. Peng, "Detection of Pathogens Using Luminescent CdSe / ZnS Dendron Nanocrystals and a Porous Membrane Immunofilter," *Anal. Chem.*, vol. 79, no. 22, pp. 8796–8802, 2007.

[213] L. Wang, H. Zheng, Y. Long, M. Gao, J. Hao, J. Du, X. Mao, and D. Zhou, "Rapid determination of the toxicity of quantum dots with luminous bacteria," *J. Hazard. Mater.*, vol. 177, no. 1–3, pp. 1134–7, May 2010.

[214] Q. Wang, T. Fang, P. Liu, X. Min, and X. Li, "Study of the bioeffects of CdTe quantum dots on Escherichia coli cells," *J. Colloid Interface Sci.*, vol. 363, no. 2, pp. 476–80, Nov. 2011.

[215] E. Verpoorte, "Beads and chips: new recipes for analysis," *Lab Chip*, vol. 3, p. 60N–68N, 2003.

[216] J. Andreassen, "One micron magnetic beads optimised for automated immunoassays," *Immunodiagnostics*, vol. 29, no. 22, 2005.

[217] M. Radisic, R. K. Iyer, and S. K. Murthy, "Micro- and nano-technology in cell separation," *Int. J. Nanomedicine*, vol. 1, no. 1, pp. 3–14, Jan. 2006.

[218] B. G. Nair, Y. Nagaoka, H. Morimoto, Y. Yoshida, T. Maekawa, and D. S. Kumar, "Aptamer conjugated magnetic nanoparticles as nanosurgeons," *Nanotechnology*, vol. 21, no. 45, p. 455102, Nov. 2010.

[219] C. Kaittanis, S. A. Naser, and J. M. Perez, "Bacterial Detection with Magnetic Relaxation," *Nano Lett.*, vol. 27, no. 2, pp. 380–383, 2007.

[220] Y. Liu and Y. Li, "Detection of Escherichia coli O157:H7 using immunomagnetic separation and absorbance measurement," *J. Microbiol. Methods*, vol. 51, no. 3, pp. 369–77, Nov. 2002.

[221] O. Rotariu, I. D. Ogden, M. MacRae, V. Bădescu, and N. J. C. Strachan, "An immunomagnetic separator for concentration of pathogenic micro-organisms from large volume samples," *J. Magn. Magn. Mater.*, vol. 293, no. 1, pp. 589–596, May 2005.

[222] P. Kinnunen, I. Sinn, B. H. McNaughton, D. W. Newton, M. A. Burns, and R. Kopelman, "Monitoring the growth and drug susceptibility of individual bacteria using asynchronous magnetic bead rotation sensors," *Biosens. Bioelectron.*, vol. 26, no. 5, pp. 2751–5, Jan. 2011.

[223] D. Day and H. Ringsdorf, "Polymerization of diacetylene carbonic acid monolayers at the gas-water interface," *J. Polym. Sci. Polym. Lett. Ed.*, vol. 16, no. 5, pp. 205–210, May 1978.

[224] M. R. West, T. W. Hanks, and R. T. Watson, "Polydiacetylene-Based Liposomes: An 'Optical Tongue' for Bacteria Detection and Identification," *J. Chem. Educ.*, vol. 86, no. 3, p. 373, Mar. 2009.

[225] L. E. Locascio, J. S. Hong, and M. Gaitan, "Liposomes as signal amplification reagents for bioassays in microfluidic channels," *Electrophoresis*, vol. 23, no. 5, pp. 799–804, Mar. 2002.

[226] Y. Amano and Q. Cheng, "Detection of influenza virus: traditional approaches and development of biosensors," *Anal. Bioanal. Chem.*, vol. 381, no. 1, pp. 156–

164, 2005.

[227] S. Park and R. A. Durst, “Immunoliposome sandwich assay for the detection of Escherichia coli O157:H7,” *Anal. Biochem.*, vol. 280, no. 1, pp. 151–8, Apr. 2000.

[228] H. J. Kim, H. P. Bennetto, M. A. Halablab, C. Choi, and S. Yoon, “Performance of an electrochemical sensor with different types of liposomal mediators for the detection of hemolytic bacteria,” *Sensors Actuators B Chem.*, vol. 119, no. 1, pp. 143–149, Nov. 2006.

[229] B. W. Peterson, P. K. Sharma, H. C. van der Mei, and H. J. Busscher, “Bacterial cell surface damage due to centrifugal compaction,” *Appl. Environ. Microbiol.*, vol. 78, no. 1, pp. 120–5, Jan. 2012.

[230] J. Judy, D. Maynes, and B. W. Webb, “Characterization of frictional pressure drop for liquid flows through microchannels,” *Int. J. Heat Mass Transf.*, vol. 45, no. 17, pp. 3477–3489, Aug. 2002.

[231] Y. Song, H. Zhang, C. H. Chon, S. Chen, X. Pan, and D. Li, “Counting bacteria on a microfluidic chip,” *Anal. Chim. Acta*, vol. 681, no. 1–2, pp. 82–6, Nov. 2010.

[232] A. A. S. Bhagat, S. S. Kuntaegowdanahalli, N. Kaval, C. J. Seliskar, and I. Papautsky, “Inertial microfluidics for sheath-less high-throughput flow cytometry,” *Biomed. Microdevices*, vol. 12, no. 2, pp. 187–95, Apr. 2010.

[233] M. Hill and N. R. Harris, “Ultrasonic Microsystems for Bacterial Cell Manipulation,” in *Principles of Bacterial Detection: Biosensors, Recognition Receptors and Microsystems2*, M. Zourob, S. Elwary, and A. Turner, Eds. 2008, pp. 909–924.

[234] M. Wiklund, S. Nilsson, and H. M. Hertz, “Ultrasonic trapping in capillaries for trace-amount biomedical analysis,” *J. Appl. Phys.*, vol. 90, no. 1, p. 421, 2001.

[235] R. Bosma, W. A. Van Spronsen, J. Tramper, and R. H. Wijffels, “Ultrasound , a new separation technique to harvest microalgae,” *J. Appl. Phycol.*, no. m, pp. 143–153, 2003.

[236] N. Harris and M. Hill, “Ultrasonic microsystems for bacterial cell manipulation,” in *Principles of Bacterial Detection: Biosensors, Recognition Receptors and Microsystems*, M. Zourob, S. Elwary, and A. Turner, Eds. , Springer., 2008.

[237] F. Petersson, A. Lena, A. Swa, and T. Laurell, “Free Flow Acoustophoresis : Microfluidic-Based Mode of Particle and Cell Separation,” *Anal. Chem.*, vol. 79, no. 14, pp. 5117–5123, 2007.

[238] J. J. Hawkes, M. S. Limaye, and W. T. Coakley, “Filtration of bacteria and yeast by ultrasound-enhanced sedimentation,” *J. Appl. Microbiol.*, vol. 82, no. 1, pp. 39–47, Jan. 1997.

[239] K.-H. Nam and D. T. Eddington, “Size-Based Separation of Microparticles in a Multilayered Microfluidic Device,” *J. Microelectromechanical Syst.*, vol. 19, no. 2, pp. 375–383, Apr. 2010.

[240] E. D. Pratt, C. Huang, B. G. Hawkins, J. P. Gleghorn, and B. J. Kirby, “Rare Cell Capture in Microfluidic Devices,” *Chem. Eng. Sci.*, vol. 66, no. 7, pp. 1508–1522, Apr. 2011.

[241] J. Bi, I. Rhebergen, M. Jura, and J. Martin, “Surface properties of suspended solids in stratified estuaries (Krka River estuary and Rhone River delta),” *Mar. Chem.*, vol. 32, pp. 235–252, 1991.

[242] Y. Suzuki, N. Hanagasaki, T. Furukawa, and T. Yoshida, “Removal of bacteria

from coastal seawater by foam separation using dispersed bubbles and surface-active substances," *J. Biosci. Bioeng.*, vol. 105, no. 4, pp. 383–8, Apr. 2008.

[243] R. B. Grieves and S. L. Wang, "Foam separation of Pseudomonas fluorescens and Bacillus subtilis var. niger," *Appl. Microbiol.*, vol. 15, no. 1, pp. 76–81, Jan. 1967.

[244] J. Haarhoff, "Dissolved air flotation: progress and prospects for drinking water treatment," *J. Water Supply Res. Technol.*, vol. 57, no. 8, pp. 555–56, 2008.

[245] J. C. Bourgeois, M. E. Walsh, and G. a Gagnon, "Treatment of drinking water residuals: comparing sedimentation and dissolved air flotation performance with optimal cation ratios," *Water Res.*, vol. 38, no. 5, pp. 1173–82, Mar. 2004.

[246] J. P. Brody and P. Yager, "Diffusion-based extraction in a microfabricated device," *Sensors Actuators A Phys.*, vol. 58, no. 1, pp. 13–18, Jan. 1997.

[247] D. Huh, J. H. Bahng, Y. Ling, H. Wei, O. D. Kripfgans, J. B. Fowlkes, J. B. Grotberg, and S. Takayama, "Gravity-Driven Microfluidic Particle Sorting Device with Hydrodynamic Separation Amplification," *Anal. Chem.*, vol. 79, pp. 1369–1376, 2007.

[248] S. Choi and J.-K. Park, "Continuous hydrophoretic separation and sizing of microparticles using slanted obstacles in a microchannel," *Lab Chip*, vol. 7, no. 7, pp. 890–7, Jul. 2007.

[249] Y. Bi, X. Pan, L. Chen, and Q.-H. Wan, "Field-flow fractionation of magnetic particles in a cyclic magnetic field," *J. Chromatogr. A*, vol. 1218, no. 25, pp. 3908–14, Jun. 2011.

[250] M. Yamada, M. Nakashima, and M. Seki, "Pinched flow fractionation: continuous size separation of particles utilizing a laminar flow profile in a pinched microchannel," *Anal. Chem.*, vol. 76, no. 18, pp. 5465–71, Sep. 2004.

[251] G. Chirica, J. Lachmann, and J. Chan, "Size exclusion chromatography of microliter volumes for on-line use in low-pressure microfluidic systems," *Anal. Chem.*, vol. 78, no. 15, pp. 5362–8, Aug. 2006.

[252] S. Qian, A. Wang, and J. K. Afonien, "Electrophoretic motion of a spherical particle in a converging-diverging nanotube.," *J. Colloid Interface Sci.*, vol. 303, no. 2, pp. 579–92, 2006.

[253] Y. Ai, S. W. Joo, Y. Jiang, X. Xuan, and S. Qian, "Transient electrophoretic motion of a charged particle through a converging-diverging microchannel: Effect of direct current-dielectrophoretic force," *Electrophoresis*, vol. 30, no. 14, pp. 2499–2506, 2009.

[254] T. Narahari, D. Dendukuri, and S. K. Murthy, "Tunable Electrophoretic Separations Using a Scalable, Fabric-Based Platform," *Anal. Chem.*, vol. 87, pp. 2480–2487, 2015.

[255] M. D. C. Jaramillo, E. Torrents, R. Martínez-Duarte, M. J. Madou, and A. Juárez, "On-line separation of bacterial cells by carbon-electrode dielectrophoresis," *Electrophoresis*, vol. 31, pp. 2921–2928, 2010.

[256] P. R. C. Gascoyne and S. Shim, "Isolation of circulating tumor cells by dielectrophoresis," *Cancers (Basel).*, vol. 6, no. 1, pp. 545–579, 2014.

[257] J. Newman, "Electric Energy and Potential," in *Physics of the Life Sciences*, 2008, pp. 373–400.

[258] R. Yusvana, D. J. Headon, and G. H. Markx, "Creation of arrays of cell aggregates in defined patterns for developmental biology studies using

dielectrophoresis," *Biotechnol. Bioeng.*, vol. 105, no. 5, pp. 945–954, 2010.

[259] T. Chen, S. Jiang, S. Xiong, M. Wang, D. Zhu, and H. Wei, "Application of denaturing gradient gel electrophoresis to microbial diversity analysis in Chinese Douchi," *Society*, no. February, pp. 2171–2176, 2012.

[260] K. D. Dorfan, S. B. King, D. W. Olson, J. D. P. Thomas, and D. R. Tree, "Beyond gel electrophoresis: Microfluidic separations, fluorescence burst analysis, and DNA stretching," *Chem. Rev.*, vol. 113, no. 4, pp. 2584–2667, 2013.

[261] M. J. Desai and D. W. Armstrong, "Characterization of Microorganisms by Capillary Electrophoresis Separation , Identification , and Characterization of Microorganisms by Capillary Electrophoresis," *Society*, vol. 67, no. 1, 2003.

[262] L. Kremser, D. Blaas, and E. Kenndler, "Capillary electrophoresis of biological particles: viruses, bacteria, and eukaryotic cells.," *Electrophoresis*, vol. 25, no. 14, pp. 2282–91, 2004.

[263] M. A. Rodriguez and D. W. Armstrong, "Separation and analysis of colloidal/nano-particles including microorganisms by capillary electrophoresis: a fundamental review," *J. Chromatogr. B*, vol. 800, no. 1–2, pp. 7–25, 2004.

[264] M. A. Resnick, R. D. Tippetts, and R. K. Mortimer, "Separation of spores from diploid cells of yeast by stable-flow free-boundary electrophoresis," *Science*, vol. 158, no. 802, pp. 803–4, 1967.

[265] R. C. Ebersole and R. M. McCormick, "Separation and isolation of viable bacteria by capillary zone electrophoresis," *Biotechnol. N.Y.*, vol. 11, no. 11, pp. 1278–82, 1993.

[266] M. Kaszuba, J. Corbett, F. M. Watson, and A. Jones, "High-concentration zeta potential measurements using light-scattering techniques," *Philos. Trans. A. Math. Phys. Eng. Sci.*, vol. 368, pp. 4439–4451, 2010.

[267] S. Vidojkovic, V. Rodriguez-Santiago, M. V. Fedkin, D. J. Wesolowski, and S. N. Lvov, "Electrophoretic mobility of magnetite particles in high temperature water," *Chem. Eng. Sci.*, vol. 66, no. 18, pp. 4029–4035, Sep. 2011.

[268] G. Giupponi and I. Pagonabarraga, "Determination of the zeta potential for highly charged colloidal suspensions," *Philos. Trans. R. Soc. A Math. Phys. Eng. Sci.*, vol. 369, no. 1945, pp. 2546–2554, 2011.

[269] M. L. Kovarik and S. C. Jacobson, "Integrated nanopore/nicrochannel devices for ac electroldnetic trapping of particles," *Anal. Chem.*, vol. 80, no. 3, pp. 657–664, 2008.

[270] H. A. Pohl, "The Motion and Precipitation of Suspensoids in Divergent Electric Fields," *J. Appl. Phys.*, vol. 22, no. 869, 1951.

[271] M. Elitas, R. Martinez-Duarte, N. Dhar, J. D. McKinney, and P. Renaud, "Dielectrophoresis-based purification of antibiotic-treated bacterial subpopulations.," *Lab Chip*, vol. 14, no. 11, pp. 1850–7, 2014.

[272] O. D. Velev, S. Gangwal, and D. N. Petsev, "Particle-localized AC and DC manipulation and electrokinetics," *Annu. Reports Sect. "C" (Physical Chem.*, vol. 105, p. 213, 2009.

[273] P. Zellner, T. Shake, Y. Hosseini, D. Nakidde, M. V Riquelme, A. Sahari, A. Pruden, B. Behkam, and M. Agah, "3D Insulator-based dielectrophoresis using DC-biased, AC electric fields for selective bacterial trapping.," *Electrophoresis*, vol. 36, no. 2, pp. 277–83, 2015.

[274] H. Watarai, “Continuous Separation Principles Using External Microaction Forces,” *Annu. Rev. Anal. Chem.*, vol. 6, no. 1, pp. 353–378, 2013.

[275] H. Li and R. Bashir, “Dielectrophoretic separation and manipulation of live and heat-treated cells of Listeria on microfabricated devices with interdigitated electrodes,” *Sensors Actuators B Chem.*, vol. 86, pp. 215–221, 2002.

[276] H. C. Tekin and M. A. M. Gijs, “Ultrasensitive protein detection: a case for microfluidic magnetic bead-based assays,” *Lab Chip*, vol. 13, no. 24, pp. 4711–39, Dec. 2013.

[277] H. Jeon, H. Lee, K. H. Kang, and G. Lim, “Ion concentration polarization-based continuous separation device using electrical repulsion in the depletion region.,” *Sci. Rep.*, vol. 3, p. 3483, Jan. 2013.

[278] J. Sangeetha and J. Philip, “The interaction, stability and response to an external stimulus of iron oxide nanoparticle–casein nanocomplexes,” *Colloids Surfaces A Physicochem. Eng. Asp.*, vol. 406, pp. 52–60, Jul. 2012.

[279] M. Zborowski, “Magnetic Formulary,” in *Laboratory Techniques in Biochemistry and Molecular Biology*, 32nd ed., M. Zborowski and J. J. Chalmers, Eds. Elsevier, 2008, pp. 29 – 57.

[280] W.-S. Chang, H. Shang, R. M. Perera, S.-M. Lok, D. Sedlak, R. J. Kuhn, and G. U. Lee, “Rapid detection of dengue virus in serum using magnetic separation and fluorescence detection,” *Analyst*, vol. 133, no. 2, pp. 233–40, Feb. 2008.

[281] J. D. Adams, P. Thévoz, H. Bruus, and H. T. Soh, “Integrated acoustic and magnetic separation in microfluidic channels,” *Appl. Phys. Lett.*, vol. 95, no. 25, p. 254103, Dec. 2009.

[282] I. Safarík and M. Safaríková, “Use of magnetic techniques for the isolation of cells,” *J. Chromatogr. B. Biomed. Sci. Appl.*, vol. 722, no. 1–2, pp. 33–53, Feb. 1999.

[283] C. Carr, M. Espy, P. Nath, S. L. Martin, and M. D. Ward, “Design, fabrication and demonstration of a magnetophoresis chamber with 25 output fractions,” *J. Magn. Magn. Mater.*, vol. 321, no. 10, pp. 1440–1445, 2010.

[284] M. Thompson and S. L. R. Ellison, “A review of interference effects and their correction in chemical analysis with special reference to uncertainty,” *Accredit. Qual. Assur.*, vol. 10, pp. 82–97, 2005.

[285] C. Carr, M. Espy, P. Nath, S. L. Martin, M. D. Ward, and J. Martin, “Design, fabrication and demonstration of a magnetophoresis chamber with 25 output fractions,” *J. Magn. Magn. Mater.*, vol. 321, no. 10, pp. 1440–1445, May 2009.

[286] C. Rivet, H. Lee, A. Hirsch, S. Hamilton, and H. Lu, “Microfluidics for medical diagnostics and biosensors,” *Chem. Eng. Sci.*, vol. 66, no. 7, pp. 1490–1507, Apr. 2011.

[287] C. Chen, J. Skog, C.-H. Hsu, R. T. Lessard, L. Balaj, T. Wurdinger, B. S. Carter, X. O. Breakefield, M. Toner, and D. Irimia, “Microfluidic isolation and transcriptome analysis of serum microvesicles,” *Lab Chip*, vol. 10, no. 4, pp. 505–11, Feb. 2010.

[288] G. Bogosian and E. V Bourneuf, “A matter of bacterial life and death,” *EMBO Rep.*, vol. 2, no. 9, pp. 770–4, Sep. 2001.

[289] N. Parthuisot, P. Catala, P. Lebaron, D. Clermont, and C. Bizet, “A sensitive and rapid method to determine the viability of freeze-dried bacterial cells,” *Lett. Appl. Microbiol.*, vol. 36, no. 6, pp. 412–7, Jan. 2003.

[290] M. Díaz, M. Herrero, L. A. García, and C. Quirós, “Application of flow cytometry to industrial microbial bioprocesses,” *Biochem. Eng. J.*, vol. 48, no. 3, pp. 385–407, Feb. 2010.

[291] C. W. Einholf and E. L. Carstensen, “Bacterial Conductivity in the Determination of Surface Charge by Microelectrophoresis,” *Biochim. Biophys. Acta*, vol. 148, pp. 506–516, 1967.

[292] E. Dziubakiewicz and B. Buszewski, “Capillary electrophoresis of microbial aggregates,” *Electrophoresis*, vol. 35, no. 8, pp. 1160–4, Apr. 2014.

[293] J. V Hankins, J. A. Madsen, D. K. Giles, J. S. Brodbelt, M. S. Trent, and E. Tor, “Amino acid addition to Vibrio cholerae LPS establishes a link between surface remodeling in Gram-positive and Gram-negative bacteria,” *Proc. Natl. Acad. Sci. U. S. A.*, vol. 109, no. 22, pp. 8722–8727, 2012.

[294] H. Wang, H. Cheng, D. Wei, and F. Wang, “Comparison of methods for measuring viable E. coli cells during cultivation: great differences in the early and late exponential growth phases,” *J. Microbiol. Methods*, vol. 84, no. 1, pp. 140–3, Jan. 2011.

[295] X. Liu, W. Xia, Q. Jiang, Y. Xu, and P. Yu, “Effect of kojic acid-grafted-chitosan oligosaccharides as a novel antibacterial agent on cell membrane of gram-positive and gram-negative bacteria,” *J. Biosci. Bioeng.*, vol. 120, no. 3, pp. 335–339, 2015.

[296] E. W. Stutz, G. Defago, and H. Kern, “Naturally occurring Pseudomonads involved in supression of black root rot of tobacco,” *Phytopathology*, vol. 76, pp. 181–185, 1986.

[297] C. J. Bunthof, K. Bloemen, P. Breeuwer, and F. M. Rombouts, “Flow Cytometric Assessment of Viability of Lactic Acid Bacteria,” *Appl. Environ. Microbiol.*, vol. 67, no. 5, pp. 2326–2335, 2001.

[298] J. Vives-Rego, P. Lebaron, and G. Nebe-von Caron, “Current and future applications of flow cytometry in aquatic microbiology,” *FEMS Microbiol. Rev.*, vol. 24, no. 4, pp. 429–48, Oct. 2000.

[299] C. J. H. G. Nebe-von-caron, “The Application of Multi-Parameter Flow Cytometry to Monitor Individual Microbial Cell Physiological State,” *Adv. Biochem. Eng. Biotechnol.*, pp. 197–223, 2004.

[300] S. Barbesti, S. Citterio, M. Labra, M. D. Baroni, M. G. Neri, and S. Sgorbati, “Two and three-color fluorescence flow cytometric analysis of immunoidentified viable bacteria,” *Cytometry*, vol. 40, no. 3, pp. 214–8, Jul. 2000.

[301] J. Comas and J. Vives-Rego, “Assessment of the effects of gramicidin, formaldehyde, and surfactants on Escherichia coli by flow cytometry using nucleic acid and membrane potential dyes,” *Cytometry*, vol. 29, no. 1, pp. 58–64, Sep. 1997.

[302] M. Kramer, N. Obermajer, B. Bogovic Matijasić, I. Rogelj, and V. Kmetec, “Quantification of live and dead probiotic bacteria in lyophilised product by real-time PCR and by flow cytometry,” *Appl. Microbiol. Biotechnol.*, vol. 84, no. 6, pp. 1137–47, Oct. 2009.

[303] F. Chau, A. Lefort, S. Benadda, V. Dubée, and B. Fantin, “Flow cytometry as a tool to determine the effects of cell wall-active antibiotics on vancomycin-susceptible and -resistant Enterococcus faecalis strains,” *Antimicrob. Agents Chemother.*, vol. 55, no. 1, pp. 395–8, Jan. 2011.

[304] M. Berney, F. Hammes, F. Bosshard, H.-U. Weilenmann, and T. Egli, “Assessment and interpretation of bacterial viability by using the LIVE/DEAD BacLight Kit in combination with flow cytometry.,” *Appl. Environ. Microbiol.*, vol. 73, no. 10, pp. 3283–90, May 2007.

[305] S. Langsrud and G. Sundheim, “Flow cytometry for rapid assessment of viability after exposure to a quaternary ammonium compound,” *J. Appl. Bacteriol.*, vol. 81, no. 4, pp. 411–8, Oct. 1996.

[306] H. C. Ansel, W. P. Norred, and I. L. Roth, “Antimicrobial activity of dimethyl sulfoxide against Escherichia coli, Pseudomonas aeruginosa, and Bacillus megaterium.,” *J. Pharm. Sci.*, vol. 58, no. 7, pp. 836–839, 1969.

[307] J. Feng, T. Wang, S. Zhang, W. Shi, and Y. Zhang, “An Optimized SYBR Green I/PI Assay for Rapid Viability Assessment and Antibiotic Susceptibility Testing for Borrelia burgdorferi,” *PLoS One*, vol. 9, no. 11, p. e111809, 2014.

[308] P. Lebaron, P. Catala, and N. Parthuisot, “Effectiveness of SYTOX Green stain for bacterial viability assessment,” *Appl. Environ. Microbiol.*, vol. 64, no. 7, pp. 2697–700, Jul. 1998.

[309] B. L. Roth, M. Poot, S. T. Yue, P. J. Millard, B. L. Roth, M. Poot, S. T. Yue, and P. J. Millard, “Bacterial viability and antibiotic susceptibility testing with SYTOX green nucleic acid stain . Bacterial Viability and Antibiotic Susceptibility Testing with SYTOX Green Nucleic Acid Stain,” *Appl. Environ. Microbiol.*, vol. 63, no. 6, pp. 2421–2431, 1997.

[310] K. Yoshioka, M. Saito, K. B. Oh, Y. Nemoto, H. Matsuoka, M. Natsume, and H. Abe, “Intracellular fate of 2-NBDG, a fluorescent probe for glucose uptake activity, in Escherichia coli Cells,” *Biosci. Biotechnol. Biochem.*, vol. 60, no. 11, pp. 1899–1901, 1996.

[311] Y. Wang, L. Claeys, D. van der Ha, W. Verstraete, and N. Boon, “Effects of chemically and electrochemically dosed chlorine on Escherichia coli and Legionella beliardensis assessed by flow cytometry,” *Appl. Microbiol. Biotechnol.*, vol. 87, no. 1, pp. 331–41, Jun. 2010.

[312] C. Laflamme, J. Ho, M. Veillette, M.-C. de Latrémoille, D. Verreault, A. Mériaux, and C. Duchaine, “Flow cytometry analysis of germinating Bacillus spores, using membrane potential dye,” *Arch. Microbiol.*, vol. 183, no. 2, pp. 107–12, Feb. 2005.

[313] S. B. Doherty, L. Wang, R. P. Ross, C. Stanton, G. F. Fitzgerald, and A. Brodkorb, “Use of viability staining in combination with flow cytometry for rapid viability assessment of Lactobacillus rhamnosus GG in complex protein matrices,” *J. Microbiol. Methods*, vol. 82, no. 3, pp. 301–10, Sep. 2010.

[314] K. Oh, D.-S. Shin, and K. Oh, “Effect of 2-NBDG , a Fluorescent Derivative of Glucose , on Microbial Cell Growth,” *J. Microbiol. Biotechnol.*, vol. 12, pp. 834–837, 2002.

[315] A. Natarajan and F. Srienc, “Dynamics of glucose uptake by single Escherichia coli cells.,” *Metab. Eng.*, vol. 1, no. 4, pp. 320–33, Oct. 1999.

[316] S. F. Bloomfield, G. S. A. B. Stewart, C. E. R. Dodd, I. R. Booth, and E. G. M. Power, “The viable but non-culturable phenomenon explained,” *Microbiology*, vol. 144, no. January, pp. 1–3, 1998.

[317] M. H. Phe, M. Dossot, H. Guilloteau, and J. C. Block, “Highly chlorinated Escherichia coli cannot be stained by propidium iodide,” *Can. J. Microbiol.*, vol. 53, no. 5, pp. 664–670, 2007.

[318] T. Tsuchido, N. Katsui, A. Takeuchi, M. Takano, and I. Shibasaki, “Destruction of the outer membrane permeability barrier of Escherichia coli by heat treatment.,” *Appl. Environ. Microbiol.*, vol. 50, no. 2, pp. 298–303, 1985.

[319] K. Myszka and K. Czaczyk, “Effect of starvation stress on morphological changes and production of adhesive exopolysaccharide (EPS) by Proteus vulgaris,” *Acta Sci. Pol. Technol. Aliment.*, vol. 10, no. 3, pp. 303–312, 2011.

[320] L. A. Bjergbaek and P. Roslev, “Formation of nonculturable Escherichia coli in drinking water,” *J. Appl. Microbiol.*, vol. 99, no. 5, pp. 1090–8, Jan. 2005.

[321] W. K. Jung, H. C. Koo, K. W. Kim, S. Shin, S. H. Kim, and Y. H. Park, “Antibacterial activity and mechanism of action of the silver ion in Staphylococcus aureus and Escherichia coli.,” *Appl. Environ. Microbiol.*, vol. 74, no. 7, pp. 2171–8, 2008.

[322] G. Nangmenyi, Z. Yue, S. Mehrabi, E. Mintz, and J. Economy, “Synthesis and characterization of silver-nanoparticle-impregnated fiberglass and utility in water disinfection,” *Nanotechnology*, vol. 20, no. 49, p. 495705, Dec. 2009.

[323] A. A. Miles, S. S. Misra, and J. O. Irwin, “The estimation of the bactericidal power of the blood,” *J. Hyg. (Lond).*, vol. 38, no. 6, pp. 732–49, Nov. 1938.

[324] R. L. Soon, R. L. Nation, S. Cockram, J. H. Moffatt, M. Harper, B. Adler, J. D. Boyce, I. Larson, and J. Li, “Different surface charge of colistin-susceptible and -resistant Acinetobacter baumannii cells measured with zeta potential as a function of growth phase and colistin treatment,” *J. Antimicrob. Chemother.*, vol. 66, no. 1, pp. 126–33, Jan. 2011.

[325] Malvern, “Zetasizer Nano Series User Manual,” 2004.

[326] S. Singh, K. C. Barick, and D. Bahadur, “Surface engineered magnetic nanoparticles for removal of toxic metal ions and bacterial pathogens,” *J. Hazard. Mater.*, vol. 192, no. 3, pp. 1539–47, Sep. 2011.

[327] E. Kłodzińska, M. Szumski, E. Dziubakiewicz, K. Hrynkiewicz, E. Skwarek, W. Janusz, and B. Buszewski, “Effect of zeta potential value on bacterial behavior during electrophoretic separation,” *Electrophoresis*, vol. 31, no. 9, pp. 1590–6, May 2010.

[328] K. A. Soni, A. K. Balasubramanian, A. Beskok, and S. D. Pillai, “Zeta potential of selected bacteria in drinking water when dead, starved, or exposed to minimal and rich culture media.,” *Curr. Microbiol.*, vol. 56, no. 1, pp. 93–7, Jan. 2008.

[329] M. H. Oo and S. L. Ong, “Implication of zeta potential at different salinities on boron removal by RO membranes,” *J. Memb. Sci.*, vol. 352, no. 1–2, pp. 1–6, Apr. 2010.

[330] G. N. Jarvis, M. W. Fields, D. A. Adamovich, C. E. Arthurs, and J. B. Russell, “The mechanism of carbonate killing of Escherichia coli,” *Lett. Appl. Microbiol.*, vol. 33, pp. 196–200, 2001.

[331] A. S. Whiteley, R. I. Griffiths, and M. J. Bailey, “Analysis of the microbial functional diversity within water-stressed soil communities by flow cytometric analysis and CTC+ cell sorting,” *J. Microbiol. Methods*, vol. 54, no. 2, pp. 257–267, Aug. 2003.

[332] T. S. Gunasekera, P. V. Attfield, and D. A. Veal, “A flow cytometry method for rapid detection and enumeration of fungal spores in the atmosphere,” *Appl. Environ. Microbiol.*, vol. 66, no. 3, pp. 1228–1232, 2000.

[333] S. Guyot, L. Pottier, E. Ferret, L. Gal, and P. Gervais, “Physiological responses of

Escherichia coli exposed to different heat-stress kinetics," *Arch. Microbiol.*, vol. 192, no. 8, pp. 651–61, Aug. 2010.

[334] Y. Hong and D. G. Brown, "Electrostatic Behavior of the Charge-Regulated Bacterial Cell Surface," *Langmuir*, vol. 24, no. 9, pp. 5003–5009, Mar. 2008.

[335] A. T. Poortinga, R. Bos, W. Norde, and H. J. Busscher, "Electric double layer interactions in bacterial adhesion to surfaces," *Surf. Sci. Rep.*, vol. 47, no. 1, pp. 1–32, Jun. 2002.

[336] R. M. Connatser, L. A. Riddle, and M. J. Sepaniak, "Metal-polymer nanocomposites for integrated microfluidic separations and surface enhanced Raman spectroscopic detection," *J. Sep. Sci.*, vol. 27, no. 17–18, pp. 1545–1550, Dec. 2004.

[337] Y. Li, Y. T. H. Cu, and D. Luo, "Multiplexed detection of pathogen DNA with DNA-based fluorescence nanobarcodes," *Nat. Biotechnol.*, vol. 23, no. 7, pp. 885–9, Jul. 2005.

[338] J. Nordgren and L. Svensson, "Detection of virus in the water environment," in *Detection of Pathogens in Water Using Micro and Nano-Technology*, G. Zuccheri and N. Asproulis, Eds. IWA Publishing, 2012, pp. 213–235.

[339] S. Courtois, A. Cajon, A. Romey, F. Poyet, and C. Mabilat, "Multi-detection of waterborne pathogens in raw and treated water samples by using ultrafiltration concentration and DNA array technology," in *Detection of Pthogens in Water Using Micro and Nano-Technology*, G. Zuccheri and N. Asproulis, Eds. London, 2012, pp. 173–187.

[340] M. W. Lechevallier, W. D. Norton, and R. G. Lee, "Giardia and Cryptosporidium spp. in filtered drining water supplies," *Appl. Environ. Microbiol.*, vol. 57, no. 9, p. 2617, 1991.

[341] T. Elad, R. Almog, S. Yagur-Kroll, K. Levkov, S. Melamed, Y. Shacham-Diamand, and S. Belkin, "Online monitoring of water toxicity by use of bioluminescent reporter bacterial biochips," *Environ. Sci. Technol.*, vol. 45, no. 19, pp. 8536–44, Oct. 2011.

[342] C. A. Stedmon, B. Seredyńska-Sobecka, R. Boe-Hansen, N. Le Tallec, C. K. Waul, and E. Arvin, "A potential approach for monitoring drinking water quality from groundwater systems using organic matter fluorescence as an early warning for contamination events," *Water Res.*, vol. 45, pp. 6030–6038, 2011.

[343] A. D. McLellan, G. C. Starling, and D. N. Hart, "Isolation of human blood dendritic cells by discontinuous Nycodenz gradient centrifugation," *J. Immunol. Methods*, vol. 184, no. 1, pp. 81–9, Jul. 1995.

[344] C. R. Mota, M. J. So, and F. L. de los Reyes, "Identification of Nitrite-Reducing Bacteria Using Sequential mRNA Fluorescence In Situ Hybridization and Fluorescence-Assisted Cell Sorting," *Microb. Ecol.*, vol. 64, pp. 256–267, 2012.

[345] B. J. Tauro, D. W. Greening, R. A. Mathias, H. Ji, S. Mathivanan, A. M. Scott, and R. J. Simpson, "Comparison of ultracentrifugation, density gradient separation, and immunoaffinity capture methods for isolating human colon cancer cell line LIM1863-derived exosomes," *Methods*, vol. 56, no. 2, pp. 293–304, Feb. 2012.

[346] J. Chen, X. Shi, A. G. Gehring, and G. C. Paoli, "Automated immunomagnetic separation for the detection of Escherichia coli O157:H7 from spinach," *Int. J. Food Microbiol.*, vol. 179, pp. 33–7, Jun. 2014.

[347] A. Bange, H. B. Halsall, and W. R. Heineman, “Microfluidic immunosensor systems.,” *Biosens. Bioelectron.*, vol. 20, no. 12, pp. 2488–503, Jun. 2005.

[348] D. R. Gossett, W. M. Weaver, A. J. Mach, S. C. Hur, H. T. K. Tse, W. Lee, H. Amini, and D. Di Carlo, “Label-free cell separation and sorting in microfluidic systems,” *Anal. Bioanal. Chem.*, vol. 397, no. 8, pp. 3249–67, Aug. 2010.

[349] J.-W. Choi, K. W. Oh, J. H. Thomas, W. R. Heineman, H. B. Halsall, J. H. Nevin, A. J. Helmicki, H. T. Henderson, and C. H. Ahn, “An integrated microfluidic biochemical detection system for protein analysis with magnetic bead-based sampling capabilities.,” *Lab Chip*, vol. 2, no. 1, pp. 27–30, Feb. 2002.

[350] N. Z. Danckwardt, M. Franzreb, A. E. Guber, and V. Saile, “Pump-free transport of magnetic particles in microfluidic channels,” *J. Magn. Magn. Mater.*, vol. 323, no. 22, pp. 2776–2781, Nov. 2011.

[351] Chemicell, “MSDS: ScreenMAG-Streptavidin,” 2007. [Online]. Available: http://www.chemicell.com/products/msds/docs/MSDS_2205_screenMAG-Streptavidin.pdf.

[352] M. J. Lovejoy, *Magnetic Particle Inspection: A Practical Guide*. Netherlands: Springer, 1993.

[353] M. Zborowski, L. R. Moore, P. S. Williams, and J. J. Chalmers, “Separations Based on Magnetophoretic Mobility,” *Sep. Sci. Technol.*, vol. 37, no. 16, pp. 3611–3633, Dec. 2002.

[354] X. Xiao, X. Yang, T. Liu, Z. Chen, L. Chen, H. Li, and L. Deng, “Preparing a highly specific inert immunomolecular-magnetic beads for rapid detection and separation of S. aureus and group G Streptococcus,” *Appl. Microbiol. Biotechnol.*, vol. 75, no. 5, pp. 1209–16, Jul. 2007.

[355] N. Pamme, “On-chip bioanalysis with magnetic particles,” *Curr. Opin. Chem. Biol.*, vol. 16, no. 3–4, pp. 436–43, Aug. 2012.

[356] F. Wittbracht, A. Weddemann, A. Auge, and A. Hütten, “Flow Guidance of Magnetic Particles by Dipolar Particle Interaction,” *2010 Fourth Int. Conf. Quantum, Nano Micro Technol.*, vol. 1, no. 2, pp. 102–106, Feb. 2010.

[357] E. M. Cherry and J. K. Eaton, “Simulation of Magnetic Particles in the Bloodstream for Magnetic Drug Targeting Applications,” in *8th International Conference on Multiphase Flow*, 2013.

[358] M. Hughes, K. A. Pericleous, and M. Cross, “The CFD analysis of simple parabolic and elliptic MHD flows,” *Appl. Math. Model.*, vol. 18, no. 3, pp. 150–155, 1994.

[359] T. Sakai, Y. Chen, and H. Ohashi, “Formation of micelle in the real-coded lattice gas,” *Comput. Phys. Commun.*, vol. 129, no. 1–3, pp. 75–81, Jul. 2000.

[360] S. R. Gorodkin, W. I. Kordonski, E. V. Medvedeva, Z. A. Novikova, A. B. Shorey, and S. D. Jacobs, “A method and device for measurement of a sedimentation constant of magnetorheological fluids,” *Rev. Sci. Instrum.*, vol. 71, no. 6, p. 2476, 2000.

[361] C. Kunstmann-Olsen, J. D. Hoyland, and H. G. Rubahn, “Influence of geometry on hydrodynamic focusing and long-range fluid behavior in PDMS microfluidic chips,” *Microfluid. Nanofluidics*, vol. 12, pp. 795–803, 2012.

[362] M. Zborowski, “Magnetic Cell Separation,” *Lab. Tech. Biochem. Mol. Biol.*, vol. 32, pp. 1–28, 2007.

[363] H. Lee, L. Xu, B. Ahn, K. Lee, and K. W. Oh, “Continuous-flow in-droplet magnetic particle separation in a droplet-based microfluidic platform,” *Microfluid. Nanofluidics*, vol. 13, no. 4, pp. 613–623, Apr. 2012.

[364] A. Weddemann, F. Wittbracht, A. Auge, and A. Hütten, “A hydrodynamic switch: Microfluidic separation system for magnetic beads,” *Appl. Phys. Lett.*, vol. 94, no. 17, p. 173501, 2009.

[365] G. M. Whitesides, “The origins and the future of microfluidics,” *Nature*, vol. 442, no. July, pp. 368–373, 2006.

[366] J. P. Golden, G. A. Justin, M. Nasir, and F. S. Ligler, “Hydrodynamic focusing-a versatile tool,” *Anal. Bioanal. Chem.*, vol. 402, pp. 325–335, 2012.

[367] E. M. Miller, A. H. C. Ng, U. Uddayasankar, and A. R. Wheeler, “A digital microfluidic approach to heterogeneous immunoassays,” *Anal. Bioanal. Chem.*, vol. 399, no. 1, pp. 337–45, Jan. 2011.

[368] L. Chen, A. Manz, and P. J. R. Day, “Total nucleic acid analysis integrated on microfluidic devices,” *Lab Chip*, vol. 7, no. 11, pp. 1413–23, Nov. 2007.

[369] N. Xia, T. P. Hunt, B. T. Mayers, E. Alsberg, G. M. Whitesides, R. M. Westervelt, and D. E. Ingber, “Combined microfluidic-micromagnetic separation of living cells in continuous flow,” *Biomed. Microdevices*, vol. 8, no. 4, pp. 299–308, 2006.

[370] C. Liu, T. Stakenborg, S. Peeters, and L. Lagae, “Cell manipulation with magnetic particles toward microfluidic cytometry,” *J. Appl. Phys.*, vol. 105, no. 10, p. 102014, 2009.

[371] M. Zborowski and J. J. Chalmers, “Rare cell separation and analysis by magnetic sorting,” *Anal. Chem.*, vol. 83, no. 21, pp. 8050–6, Nov. 2011.

[372] R. K. Mendes, S. Laschi, D. R. Stach-Machado, L. T. Kubota, and G. Marrazza, “A disposable voltammetric immunosensor based on magnetic beads for early diagnosis of soybean rust,” *Sensors Actuators B Chem.*, vol. 166–167, pp. 135–140, May 2012.

[373] W. M. Fedio, K. C. Jinneman, K. J. Yoshitomi, R. Zapata, C. N. Wendakoon, P. Browning, and S. D. Weagant, “Detection of E. coli O157:H7 in raw ground beef by Pathatrix™ immunomagnetic-separation, real-time PCR and cultural methods,” *Int. J. Food Microbiol.*, vol. 148, no. 2, pp. 87–92, Aug. 2011.

[374] J. P. Golden, J. Verbarg, P. B. Howell, L. C. Shriver-Lake, and F. S. Ligler, “Automated processing integrated with a microflow cytometer for pathogen detection in clinical matrices,” *Biosens. Bioelectron.*, vol. 40, no. 1, pp. 10–6, Feb. 2013.

[375] W. R. Rodriguez, N. Christodoulides, P. N. Floriano, S. Graham, S. Mohanty, M. Dixon, M. Hsiang, T. Peter, S. Zavahir, I. Thior, D. Romanovicz, B. Bernard, A. P. Goodey, B. D. Walker, and J. T. McDevitt, “A microchip CD4 counting method for HIV monitoring in resource-poor settings.,” *PLoS Med.*, vol. 2, no. 7, p. e182, Jul. 2005.

[376] Y.-N. Wang, Y. Kang, D. Xu, C. H. Chon, L. Barnett, S. a Kalams, D. Li, and D. Li, “On-chip counting the number and the percentage of CD4+ T lymphocytes,” *Lab Chip*, vol. 8, no. 2, pp. 309–15, Feb. 2008.

[377] Q. Ramadan, “Reversible assembly of magnetized particles: Application to water-borne pathogen enumeration,” *J. Appl. Phys.*, vol. 106, no. 12, p. 124701, 2009.

[378] S. F. Medeiros, A. M. Santos, H. Fessi, and A. Elaissari, “Stimuli-responsive magnetic particles for biomedical applications,” *Int. J. Pharm.*, vol. 403, no. 1–2,

pp. 139–61, Jan. 2011.

[379] B. C. Kim, J. Lee, W. Um, J. Kim, J. Joo, J. H. Lee, J. H. Kwak, J. H. Kim, C. Lee, H. Lee, R. S. Addleman, T. Hyeon, M. B. Gu, and J. Kim, "Magnetic mesoporous materials for removal of environmental wastes," *J. Hazard. Mater.*, vol. 192, no. 3, pp. 1140–7, Sep. 2011.

[380] G. Prochazkova, I. Safarik, and T. Branyik, "Harvesting microalgae with microwave synthesized magnetic microparticles," *Bioresour. Technol.*, vol. 130, pp. 472–7, Feb. 2013.

[381] Y. Jing, L. R. Moore, P. S. Williams, J. J. Chalmers, S. S. Farag, B. Bolwell, and M. Zborowski, "Blood Progenitor Cell Separation From Clinical Leukapheresis Product by Magnetic Nanoparticle Binding and Magnetophoresis," *Biotechnol. Bioeng.*, vol. 96, no. 6, pp. 1139–1154, 2007.

[382] M. D. Tarn, S. A. Peyman, D. Robert, A. Iles, C. Wilhelm, and N. Pamme, "The importance of particle type selection and temperature control for on-chip free-flow magnetophoresis," *J. Magn. Magn. Mater.*, vol. 321, no. 24, pp. 4115–4122, Dec. 2009.

[383] U. O. Häfeli, M. A. Lobedann, J. Steingroewer, L. R. Moore, and J. Riffle, "Optical method for measurement of magnetophoretic mobility of individual magnetic microspheres in defined magnetic field," *J. Magn. Magn. Mater.*, vol. 293, no. 1, pp. 224–239, May 2005.

[384] B. Issa, I. M. Obaidat, B. A. Albiss, and Y. Haik, "Magnetic nanoparticles: surface effects and properties related to biomedicine applications," *Int. J. Mol. Sci.*, vol. 14, no. 11, pp. 21266–305, Jan. 2013.

[385] M. Shinkai, "Functional magnetic particles for medical application," *J. Biosci. Bioeng.*, vol. 94, no. 6, pp. 606–613, Dec. 2002.

[386] M. González, L. A. Bagatolli, J. L. R. Arrondo, E. Carlos, C. R. Cantor, D. Gerardo, I. Echabe, C. E. Argaran, and G. D. Fidelio, "Protein Chemistry and Structure : Interaction of biotin with streptavidin : thermostability and conformational changes uppon binding," *J. Biol. Chem.*, vol. 272, pp. 11288–11294, 1997.

[387] L. M. Ahmad, B. Towe, A. Wolf, F. Mertens, and J. Lerchner, "Binding event measurement using a chip calorimeter coupled to magnetic beads," *Sensors Actuators B Chem.*, vol. 145, no. 1, pp. 239–245, Mar. 2010.

[388] E. Strachan, A. K. Mallia, J. M. Cox, B. Antharavally, S. Desai, L. Sykaluk, V. O'Sullivan, and P. A. Bell, "Solid-phase biotinylation of antibodies," *J. Mol. Recognit.*, vol. 17, no. 3, pp. 268–76, 2004.

[389] F. Thielbeer, K. Donaldson, and M. Bradley, "Zeta potential mediated reaction monitoring on nano and microparticles," *Bioconjug. Chem.*, vol. 22, no. 2, pp. 144–50, Feb. 2011.

[390] Invitrogen, "Dynabeads: The attraction is simply magnetic," 2010. [Online]. Available: http://tools.lifetechnologies.com/content/sfs/brochures/Dynabeads_Streptavidin_Products_and_Applications.pdf.

[391] R. M. Cooper, D. C. Leslie, K. Domansky, A. Jain, C. Yung, M. Cho, S. Workman, M. Super, and D. E. Ingber, "A microdevice for rapid optical detection of magnetically captured rare blood pathogens," *Lab Chip*, vol. 14, no. 1, pp. 182–8, Jan. 2014.

[392] F. Wittbracht, “Interaction of magnetic beads in microfluidic systems : fundamentals and applications,” Bielefeld University, 2012.

[393] G. Kasper, “Measurements of viscous drag on cyliders and chains of spheres with aspect ratios between 2 and 50,” *J. Aerosol Sci.*, vol. 16, no. 6, pp. 535 – 556, 1985.

[394] N. Wang, C. Hsu, L. Zhu, S. Tseng, and J.-P. Hsu, “Influence of metal oxide nanoparticles concentration on their zeta potential.,” *J. Colloid Interface Sci.*, vol. 407, pp. 22–8, Oct. 2013.

[395] M. Fitzpatrick, “Haemolytic uraemic syndrome and E. coli O157,” *Br. Med. J.*, vol. 318, no. March, pp. 684–685, 1999.

[396] X. Jiang, R. Wang, Y. Wang, X. Su, Y. Ying, J. Wang, and Y. Li, “Evaluation of different micro/nanobeads used as amplifiers in QCM immunosensor for more sensitive detection of E. coli O157:H7,” *Biosens. Bioelectron.*, vol. 29, no. 1, pp. 23–8, Nov. 2011.

[397] J. Soller, M. Embrey, L. Tuhela, A. Ichida, and J. Rosen, “Risk-based evaluation of Escherichia coli monitoring data from undisinfected drinking water,” *J. Environ. Manage.*, vol. 91, no. 11, pp. 2329–35, Nov. 2010.

[398] J. Luo, X. Liu, Q. Tian, W. Yue, J. Zeng, G. Chen, and X. Cai, “Disposable bioluminescence-based biosensor for detection of bacterial count in food,” *Anal. Biochem.*, vol. 394, no. 1, pp. 1–6, Nov. 2009.

[399] V. Duplan, E. Frost, and J. J. Dubowski, “A photoluminescence-based quantum semiconductor biosensor for rapid in situ detection of Escherichia coli,” *Sensors Actuators B Chem.*, vol. 160, no. 1, pp. 46–51, Dec. 2011.

[400] S. L. Miles, R. G. Sinclair, M. R. Riley, and I. L. Pepper, “Evaluation of select sensors for real-time monitoring of Escherichia coli in water distribution systems,” *Appl. Environ. Microbiol.*, vol. 77, no. 8, pp. 2813–6, Apr. 2011.

[401] A. M. Ibekwe, S. E. Murinda, A. K. Graves, A. M. Ibekwe, S. E. Murinda, and A. K. Graves, “Microbiological evaluation of water quality from urban watersheds for domestic water supply improvement,” *Int. J. Environ. Res. Public Health*, vol. 8, no. 12, pp. 4460–76, Dec. 2011.

[402] N. V. Kulagina, M. E. Lassman, F. S. Ligler, and C. R. Taitt, “Antimicrobial peptides for detection of bacteria in biosensor assays,” *Anal. Chem.*, vol. 77, no. 19, pp. 6504–8, Oct. 2005.

[403] M. Kawano and H. Watarai, “Brownian motion-magnetophoresis of nano/micro-particles,” *Analyst*, vol. 137, no. 18, pp. 4123–6, Sep. 2012.

[404] Y. Date, S. Terakado, K. Sasaki, A. Aota, N. Matsumoto, H. Shiku, K. Ino, Y. Watanabe, T. Matsue, and N. Ohmura, “Microfluidic heavy metal immunoassay based on absorbance measurement,” *Biosens. Bioelectron.*, vol. 33, no. 1, pp. 106–12, Mar. 2012.

[405] C. Zuchner, “Working with proteins : protein stability and storage - a brief guide Protein structure,” *UltraSensitive Protein Detection Unit*, 2009. [Online]. Available: http://www.uni-leipzig.de/uspdu/docs/Protein guide_Storage_Working.pdf.

[406] M. Berney, M. Vital, I. Hülshoff, H.-U. Weilenmann, T. Egli, and F. Hammes, “Rapid, cultivation-independent assessment of microbial viability in drinking water.,” *Water Res.*, vol. 42, no. 14, pp. 4010–8, Aug. 2008.

[407] M. Herrero, C. Quirós, L. A. García, and M. Díaz, “Use of flow cytometry to

follow the physiological states of microorganisms in cider fermentation processes.," *Appl. Environ. Microbiol.*, vol. 72, no. 10, pp. 6725–33, Oct. 2006.

[408] F. Bosshard, M. Berney, M. Scheifele, H.-U. Weilenmann, and T. Egli, "Solar disinfection (SODIS) and subsequent dark storage of Salmonella typhimurium and Shigella flexneri monitored by flow cytometry.," *Microbiology*, vol. 155, no. Pt 4, pp. 1310–7, Apr. 2009.

[409] C. Plank, O. Zelphati, and O. Mykhaylyk, "Magnetically enhanced nucleic acid delivery. Ten years of magnetofection-progress and prospects," *Adv. Drug Deliv. Rev.*, vol. 63, no. 14–15, pp. 1300–31, Nov. 2011.

[410] C.-Y. Huang, M.-F. Lai, T.-R. Ger, and Z.-H. Wei, "Cell culture arrays using micron-sized ferromagnetic ring-shaped thin films," *J. Appl. Phys.*, vol. 117, p. 17B309, 2015.

[411] E. Sharif, J. Kiely, and R. Luxton, "Novel immunoassay technique for rapid measurement of intracellular proteins using paramagnetic particles," *J. Immunol. Methods*, vol. 388, no. 1–2, pp. 78–85, Feb. 2013.

[412] A. W. Vermeer and W. Norde, "The thermal stability of immunoglobulin: unfolding and aggregation of a multi-domain protein.," *Biophys. J.*, vol. 78, no. January, pp. 394–404, 2000.

[413] P. D. Frymier, R. M. Ford, H. C. Bergo, and P. T. Cummingssii, "Three-dimensional tracking of motile bacteria near a solid planar surface," *Proc. Natl. Acad. Sci. U. S. A.*, vol. 92, no. June, pp. 6195–6199, 1995.

[414] C. Ricci, L. Nyadong, F. Yang, F. M. Fernandez, C. D. Brown, P. N. Newton, and S. G. Kazarian, "Assessment of hand-held Raman instrumentation for in situ screening for potentially counterfeit artesunate antimalarial tablets by FT-Raman spectroscopy and direct ionization mass spectrometry," *Anal. Chim. Acta*, vol. 623, pp. 178–186, 2008.

[415] D. V Lim, J. M. Simpson, E. A. Kearns, and M. F. Kramer, "Current and Developing Technologies for Monitoring Agents of Bioterrorism and Biowarfare Current and Developing Technologies for Monitoring Agents of Bioterrorism and Biowarfare," *Clin. Microbiol. Rev.*, vol. 18, no. 4, pp. 583–607, 2005.

[416] Y.-H. Lin, Y.-J. Chen, C.-S. Lai, Y.-T. Chen, C.-L. Chen, J.-S. Yu, and Y.-S. Chang, "A negative-pressure-driven microfluidic chip for the rapid detection of a bladder cancer biomarker in urine using bead-based enzyme-linked immunosorbent assay," *Biomicrofluidics*, vol. 7, no. 2, p. 24103, Jan. 2013.

[417] M. A. M. Gijs, F. Lacharme, and U. Lehmann, "Microfluidic Applications of Magnetic Particles for Biological Analysis and Catalysis," *Chem. Rev.*, vol. 110, no. 3, pp. 1518–1563, 2010.

[418] T. W. Prow, J. E. Grice, L. L. Lin, R. Faye, M. Butler, W. Becker, E. M. T. Wurm, C. Yoong, T. A. Robertson, H. P. Soyer, and M. S. Roberts, "Nanoparticles and microparticles for skin drug delivery," *Adv. Drug Deliv. Rev.*, vol. 63, no. 6, pp. 470–91, May 2011.